NASA Contractor Report 181808

Microcomputer Based Controller for the Langley 0.3-Meter Transonic Cryogenic Tunnel

S. Balakrishna, and W. Allen Kilgore

Vigyan Research Associates, Inc.
Hampton, VA 23665-1325

March 1989

National Aeronautics and
Space Administration

Langley Research Center
Hampton, Virginia 23665-5225

Chapter details:

1. Introduction
2. Review of 0.3-m TCT control problem
3. Modeling of the actuators and sensors
4. 0.3-m TCT control laws
5. Microcomputer based 0.3-m TCT controller
6. Flowchart for integrated control of 0.3-m TCT
7. Microcomputer system
8. Tunnel controller commissioning and tunnel performance
9. Operation of the microcomputer based 0.3-m TCT controller
10. Conclusions

Appendices:

A. Dynamics of LN_2 injection valve
B. Flowchart for 0.3-m TCT control
C. Details of the monitor display for tunnel control
D. Real time simulation for 0.3-m TCT
E. List of sensors, ranges and their names
F. Keyboard commands

List of figures:

13. 0.3-m TCT sensors and actuators for control.
14. 0.3-m TCT temperature control schematic.
15. 0.3-m TCT temperature loop feed forward logic.
16. Limit on LN_2 valve area as a function of metal to gas temperature difference.
17. 0.3-m TCT pressure/Reynolds number control schematic.
18. Tunnel trajectory in pressure-temperature plane.
19. 0.3-m TCT fan speed and Mach number control schematic.
20. Fan speed rate limit as a function of fan speed control loop error.
21. LN_2 storage and pressure control schematic.
22. Schematic for Motorola 6800 based P-T controller and SBC 80/20 based Mach number controller.
23. IBM PC/AT based temperature, pressure/Reynolds number, and Mach number controller.
24. IBM PC/AT based temperature, pressure/Reynolds number and Mach number controller.
25. Tunnel condition regulation under closed loop control during rake traverse. M=0.2, Re=4.0
26. Tunnel condition regulation under closed loop control during rake traverse. M=0.2, Re=3.0
27. Tunnel condition regulation under closed loop control during rake traverse. M=0.2, Re=6.0
28. Tunnel condition regulation under closed loop control during rake traverse. M=0.2, Re=2.0
29. Tunnel condition regulation under closed loop control during rake traverse. M=0.302, Re=6.0
30. Tunnel condition regulation under closed loop control during rake traverse. M=0.35, Re=8.0
31. Tunnel condition regulation under closed loop control during rake traverse. M=0.73, Re=4.0
32. Tunnel condition regulation under closed loop control during rake traverse. M=0.762, Re=20.0
33. Tunnel condition regulation under closed loop control during rake traverse. M=0.762, Re=20.0
34. Tunnel condition regulation under closed loop control during rake traverse. M=0.78, Re=20.0
35. Tunnel condition regulation under closed loop control during rake traverse. M=0.765, Re=21.36
36. Tunnel condition regulation under closed loop control during rake traverse. M=0.765, Re=21.36
37. Tunnel condition regulation under closed loop control during rake traverse. M=0.765, Re=21.36
38. Tunnel condition regulation under closed loop control during rake traverse. M=0.765, Re=20.0
39. Tunnel condition regulation under closed loop control during rake traverse. M=0.780, Re=20.0
40. 0.3-m TCT control schematic and intrusive disturbances during model data acquisition.
41. Wall shape 1 corresponding to streamline conditions along wall at α=0° and M=0.765.
42. Wall shape 2 corresponding to streamline conditions along wall at α=2° and M=0.765.
43. Tunnel responses while in closed loop control to set point command changes to temperature and disturbances caused by rake traverse. (M=0.760, P=68 psia, T=231/227/233 K)
44. Tunnel responses while in closed loop control to set point command changes to pressure and disturbances caused by rake traverse. (M=0.760, P=68/64/68 psia, T=230.6 K)
45. Tunnel responses while in closed loop control to set point command changes to Mach number and

disturbances caused by rake traverse. (M=0.7/0.73/0.76, P=68 psia, T=230.6 K)

46. Tunnel responses while in closed loop control to pulse Mach number set point command change and disturbances caused by rake traverse. (M=0.762/0.777/0.762, P=68 psia, T=230.6 K)
47. Tunnel responses while in closed loop control to pulse Mach number set point command change and disturbances caused by rake traverse. (M=0.76/0.73/0.76, T=230.6 K, Re=20 millon/chord)
48. Response to large set point changes during tunnel cooldown and warmup at constant Mach number condition.
49. Response to large setpoint changes during tunnel cooldown at constant fan speed.
50. Response to large set point changes during cooldown and the boundary layer system mass enthalpy disturbances.
51. Tunnel responses while in closed loop control to disturbances caused by rake traverse in the model wake. (M=0.767, P=68 psia, T=230.6 K, α=1.8°)
52. Tunnel responses while on closed loop control to disturbances caused by α changes and rake traverse. (M=0.700, P=68 psia, T=230.6 K, α=2°/0°)
53. Tunnel responses while on closed loop control to disturbances caused by pulse α changes and rake traverse. (M=0.760, P=68 psia, T=230.6 K, α=0°/2°/0°)
54. Tunnel responses while in closed loop control to disturbances caused by flex wall change from shape 2 to shape 1 and rake traverse. (M=0.700, P=68 psia, T=230.6 K, α=0°)
55. Tunnel responses while in closed loop control to disturbances caused by flex wall change from shape 1 to shape 2 and rake traverse. (M=0.700, P=68 psia, T=230.6 K, α=2°)
56. Tunnel responses while in closed loop control to disturbances caused by flex wall change from shape 2 to shape 1 and rake traverse. (M=0.760, P=68 psia, T=231 K, α=0°)
57. Tunnel responses while in closed loop control to disturbances caused by flex wall change from shape 1 to shape 2 and rake traverse. (M=0.762, P=68 psia, T=233 K, α=0°)
58. Display format for the controller monitor.
59. Typical tunnel control display on the monitor.
60. Schematic for performance test on LN_2 injection valve.

SYMBOLS

Nomenclature:

A	test section area, m^2
A_G	GN_2 exhaust valve area normalized to full open area
A_{Gv1}	GN_2 primary valve 1 area normalized to full open area
A_{Gv2}	GN_2 secondary valve 2 area normalized to full open area
A_L	LN_2 injection valve area normalized to full open area
A_{LN}	LN_2 back pressure valve area normalized to full open area
A_t	test section area or the throat area of the nozzle system, m^2
$\bar{c}$	model mean aerodynamic chord, m
C_{gv}	flow coefficient of GN_2 exhaust valve
C_{Lqv}	flow coefficient for LN_2 injection valve
C_m	specific heat of metal wall material, KJ/kg/K
C_p	specific heat at constant pressure, KJ/kg/K
C_v	specific heat at constant volume, KJ/kg/K
D	dimension
e	exponentiation
e_l	error in LN_2 pressure control loop error, atm
e_n	error in fan speed control loop, rpm
E	thermocouple output votage, VDC
h_G	enthalpy of GN_2, KJ/kg
h_L	enthalpy of LN_2, KJ/kg
k	constant
K_{dl}	LN_2 pressure control loop derivative gain
K_f	fan power constant
K_G	gas exhaust valve constant
K_{il}	LN_2 pressure control loop integral gain
K_{im}	Mach number control loop integral gain
K_{in}	fan speed control loop integral gain
K_{ip}	pressure control loop integral gain
K_{it}	temperature control loop integral gain
K_m	Mach number control loop gain
K_{pl}	LN_2 pressure control loop proportional gain
K_{pm}	Mach number control loop proportional gain

K_{pn}	fan speed control loop proportional gain
K_{pp}	pressure control loop proportional gain
K_{pt}	temperature control loop proportional gain
K_{re}	Reynolds number estimation constant
k_t	test section constant
M	Mach number
$\dot{m}_{T.S.}$	test section mass flow, kg/s
$\dot{m}_G$	GN_2 exhaust mass flow, kg/s
$\dot{m}_L$	LN_2 injected mass flow, kg/s
M_{set}	Mach number control loop set point
N	fan speed, rpm
N_{set}	fan speed control loop set point, rpm
p	momentum
P	tunnel gas pressure, atm
P_G	pressure of gas, atm
P_L	pressure of liquid, atm
P_{Lq}	LN_2 pressure, atm
P_{Lset}	LN_2 pressure control loop set point, atm
P_{set}	tunnel pressure control loop set point, atm
P_{static}	tunnel static pressure, atm
P_{total}	tunnel total pressure, atm
Q	heat, KJ
$\dot{Q}_F$	rate of fan heat, approximately the fan power, KJ/s
$\dot{Q}_m$	rate of heat release from metal walls in the tunnel, KJ/s
$\Re$	universal gas constant
Re	Reynolds number of tunnel flow per chord
S	Lapalce operator
t	time
t_1	first order time lag
t_c	tunnel circuit time, s
t_m	lumped tunnel metal heat release/absorption time constant, s
t_p	plenum time constant, s
t_r	rheostat servo time constant, s
T	tunnel gas temperature, K
T_m	tunnel average metal temperature, K
T_s	tunnel gas static temperature, K

T_{set}	temperature control loop set point, K
Tuse	the temperature set pont with in constraints obtain the temperature set point, K
ΔT	metal temperature to gas temperature difference, K
u	specific internal energy, J
U	internal energy, KJ/kg
U_G	internal energy of exhausting GN_2, KJ/kg
U_L	internal energy of incoming LN_2, KJ/kg
v	one dimensional velocity of gas in the tunnel, m/s
V	volume of the tunnel, m^3
V_G	volume of gas, m^3
V_L	volume of liquid, m^3
W_G	mass of gas in the tunnel, kg
W_t	mass of the tunnel walls, kg
y	lumped wall heat transfer coefficient, KJ/K/s
Z	Z-transform
α	angle of attack, deg
γ	ratio of specific heats
μ	viscosity
ρ	density, kg/m^3
θ_{rh}	position of rheostat normalized to 100%
$\dot{\theta}_{rh}$	rate of change of position of rheostat
ϕ	phase of electrical power
τ_G	transport delay in effect of GN_2 discharge on temperature, s
τ_L	transport delay in effect of LN_2 injection on the tunnel gas temperature, s
τ_F	transport delay in effect of fan speed on temperature, s
Δ, Δt	sampling time, s

Subscripts:

max	maximun value
∞	free-stream condition

Units:

atm	atmosphere
deg, °	degree

gpm	gallons per minute
Hz	Hertz, cycles/s
inch	inch
J	joule
K	kelvin
kg	kilogram
KJ	kilojoule
KW	kilowatt
liter	liter
m	meter
mA	milliampere
micron	one thousandth of a millimeter
mole	mole, gram molecular weight
ms	milliseconds
min	minute
mV	millivolt
μV	microvolts
psia	pounds per square inch
psid	pounds per square inch, differential
psig	pounds per square inch, gage
rad	radian
rms	root mean square
rpm	revolution per minute
V	volts
VDC	volts, direct current
s	second

Abbreviations:

DAC	Digital to Analog Converter
ADC	Analog to Digital Converter
A/D	Analog to Digital
D/A	Digital to Analog
EPROM	Erasable Programmable Read Only Memory
RAM	Random Access Memory
DOS	Disk Operating System

CPU	Central Processing Unit of the microcomputer
ASCII	keyboard code
HSNLF	High Speed Natural Laminar Flow

INTRODUCTION

The Langley 0.3-m Transonic Cryogenic Tunnel (TCT) is a major U.S. research tunnel capable of testing relatively small airfoil models at full scale flight equivalent Reynolds numbers. The 0.3-m TCT has been operational since 1973. (ref. 1) It is a closed circuit fan driven pressure tunnel in which the heat generated by the fan operation is cancelled by injection of liquid nitrogen (LN_2) into the tunnel. The injected liquid evaporates into the tunnel test gas and cools the tunnel resident gas mass. Therefore, 0.3-m TCT uses gaseous nitrogen (GN_2) as the test gas. The gaseous mass buildup and pressure variation caused by LN_2 injection is corrected by controlled discharge of warmer tunnel gases at a different point in the tunnel. The tunnel gas temperature, the tunnel pressure and the flow Mach number can be controlled by adjusting the LN_2 mass flow into the tunnel and the GN_2 discharge from tunnel for a given fan speed.

The viscosity of GN_2 is directly related to the temperature and its density is inversely related to temperature. The tunnel flow Reynolds number ($\frac{\rho v \bar{c}}{\mu}$) is related directly to density and inversely to viscosity. Hence, Reynolds number is a strong function of the tunnel gas temperature. Thus, in a cryogenic tunnel, the three flow parameters Reynolds number, Mach number, and dynamic pressure are uniquely related and can be controlled by adjusting the three tunnel variables viz., temperature, test section mass flow rate, and the tunnel pressure.

The dynamics of the tunnel pressure, gas temperature and the Mach number are dictated by the interaction of the tunnel resident gas mass with mass-enthalpy control inputs from injected LN_2, GN_2 discharge and the fan speed which controls the pressure ratio across the fan. The physical laws governing the thermodynamic behavior of the tunnel gas are complex, non-linear, and highly coupled. For a full understanding of the tunnel control problem and control law analysis, a representative dynamic model of the tunnel thermodynamic process is essential. A lumped multivariable model of a cryogenic fan drvien pressure tunnel has been postulated and verified in 1979. (ref. 2, 3, 4, 5) Based on this mathematical model, control laws for closed loop control of the 0.3-m TCT pressure, gas temperature, and test section Mach number have been generated and used for the past 10 years.

A Motorola 6800 microprocessor based pressure/temperature controller for the 0.3-m TCT was commissioned in 1979. This controller maintained the tunnel gas temperature to ± 0.2 K and pressure to ± 0.1 psia of the set values. However, the controller could not safely cool the tunnel structure or handle large temperature set point changes. The controller inadvertantly imposed large thermal stresses on the tunnel structure if unsupervised. In 1982, the test section Mach number control loop was commissioned using the original control law design realized on an Intel SBC 80/20 microprocessor

based custom built system. This controller could update the Mach number loop at a rate of 250 ms. The sampling speed was inadequate for good control, since the design called for an update rate of 100 ms. The performance of the Mach number loop was not satisfactory. The loop could not be used in an automatic Mach number control mode during data acquisition because of disturbances caused by the drag rake traverse.

The 0.3-m TCT has undergone many research changes during the mid 1980's significantly modifying the contraction and the test section which effect the tunnel Mach number response. These changes consist of modification to the test section, from 8 x 24 inch to 13 x 13 inch with associated modifications to the contraction. The top and bottom walls have also been changed from the original slotted construction to flexible solid walls. (ref. 6) Problems with the LN_2 injection actuators resulted in a change of the original digital valves to signalled electropneumatic plug valves. A boundary layer control system has also been added. (ref. 7) The boundary layer control system removes test section mass flow near the walls either by passive discharge to the atmosphere or by recirculation of the removed mass back to the tunnel. Such a boundary layer treatment system naturally imposes mass enthalpy disturbances on the tunnel control. All these changes have resulted in considerable modifications to the tunnel dynamics affecting the control laws originally developed in 1979. A review and redesign of the tunnel control system became necessary.

The microprocessor based controllers designed at the end of 1970s are based on 8 bit capability. The software was developed on an external system where an executable version was generated. This was then transferred to the controller as a burnt-in EPROM device. Such controllers cannot accommodate easy modifications to the control laws, since no operating system with editing and compiling features are available on the controller. The clock speeds of 8 bit devices used on the original systems are typically 5-10 times slower compared to the 16 bit microcomputer systems available now. The software for the original 8 bit microprocrssor based tunnel controllers were written in either assembly language or in machine code. Such codes are difficult to edit, debug, or change.

With continuing geometrical and engineering modifications to the 0.3-m TCT configuration, which is an evolutionary activity, a need for a tunnel controller flexiable enough to accommodate easy and iterative changes to the control laws has been keenly felt. Development of a new microcomputer based tunnel controller with software written in a higher level and easy to understand language was taken up in late 1987. A major requirement of this system is that with continually changing computer hardware, the software should not become obsolete. Further, the aim is to use only commercially available and popular microcomputer systems, either the 16 bit or 32 bit architecture with compatible real time devices. Emphasis is on avoiding custom built hardware anywhere in the controller.

This paper gives a review of the 0.3-m TCT control system and describes development of a microcomputer based integrated tunnel controller designed around generic Personal Computer (PC) architecture of the AT class. The details include a review of the tunnel control problem, new solutions to large set point change, nonlinear control laws, microcomputer system hardware/software development, and the commissioning and performance of the new microcomputer based controller.

REVIEW OF 0.3-M TCT CONTROL PROBLEM

Description of 0.3-m TCT:

Figure 1 shows a schematic of Langley's 0.3-m TCT. The 0.3-m TCT is an external insulted pressure tunnel with an Al-6061 aluminum pressure shell of about 3200 kg mass. Operation pressures range from 1 to 6 atm and gas temperatures from 78 to 340 K. The tunnel consists of a settling chamber with a contraction leading to the tunnel test section followed by a diffuser, a motor driven fan and a return leg leading to the settling chamber. The tunnel was originally commissioned with an octagonal test section, but was changed to an 8 x 24 inch slotted wall 2-D test section during late 1970s. Today the tunnel has a 13 x 13 inch test section with solid flexible walls. LN_2 is injected into the tunnel at the down stream diffuser segment through four nozzles. The tunnel fan has fixed pitch/fixed inlet guide vane configuration and is located in the return leg of the tunnel. The pressure ratio of the fan is controlled by a variable speed motor. Tunnel gas is discharged to the atmosphere through a variable area valve. The discharge valve is located at the big end of the tunnel near the settling chamber. The tunnel has provision for boundary-layer mass flow removal from the sidewalls of the test section.

Review of the tunnel dynamic modeling:

A generic lumped multivariable model of a closed circuit fan driven cryogenic pressure tunnel has been synthesised and reported in reference 3. This basic modeling is now reviewed with a view to improve the tunnel control performance.

A fan driven closed circuit cryogenic wind tunnel can be looked upon as a thermodynamical system where the tunnel resident gas mass, while in motion through the streamlined walls of the tunnel geometry, thermally interacts with the metal walls, the control inputs viz., LN_2 injection in to the tunnel, GN_2 discharge from a relatively warmer segment of the tunnel and the fan induced compression/wall friction heating. This thermodynamic interaction occurs both spatially and temporally. The tunnel modeling can be analysed graphically to obtain an understanding of the

pressure-temperature coupling.

The internal energy associated with a unit volume and mass of stationary gas at an uniform temperature T is the total molecular energy associated with the gas, and is a function of the gas temperature as predicted by first law of thermodynamics. At absolute zero temperature, the internal energy and gas specific heat tend to zero. This can be expressed as:

$$u = \int_0^T C_v \, dT$$

where $C_v = \frac{dQ}{dT}$ at constant volume

The density of nitrogen differs slightly from an ideal gas, based on data from Jacobsen, and for a finite volume of V, m^3 pressure of P, atm and a temperature of T, K, the mass can be expressed as: (ref. 3)

$$W_G = 338.9 \frac{PV}{T}\left\{1 + 250 \frac{P}{T^2}\right\}$$

The internal energy associated with a volume V of the gas is:

$$U = W_G u = W_G \int_0^T C_v \, dT$$

Assuming that C_v is linear with temperature, at least in the range of temperature in the gaseous state we have: (ref. 3)

$$\int_0^T C_v \, dT = C_v T$$

and $$C_v = 20.8 \left(1 + 250 \frac{P^{0.7}}{T^2}\right)$$

and $$U = 253.5 \, P \left(1 + 250 \frac{P}{T^2}\right)\left(1 + 250 \frac{P^{0.7}}{T^2}\right)$$

The 0.3-m TCT quasisteady control problem can be graphically illustrated using an energy state diagram shown in figure 2. A plot of the mass of gas as a function of internal energy is shown for pressures varying from 1 to 6 atm, and temperature from 100 to 350 K, representing 14.1 m^3 volume of the 0.3-m TCT. The three control inputs viz., LN_2 injection, GN_2 discharge, and fan operation represent rate vectors of mass energy components. The effect of the control inputs is to add mass/energy components to the tunnel internal energy. From any initial condition, the trajectory of the tunnel state can be determined on the energy state plot for given control inputs. For example, fan

operation adds only energy to the system and hence is a vertical locus. It increases the temperature of the gas and increases the pressure in the tunnel. Addition of LN_2 (and assuming ideal evaporation and isothermal mixing) results in mass addition with coupled energy reduction, thereby reducing both the temperature and pressure. The magnitude of temperature decrease is relatively large and pressure decrease is relatively small. Discharge of GN_2 from the tunnel results in decrease of mass and energy resulting in a drop in pressure as well as temperature. The degree of cooling is much smaller and pressure decrease is relatively large. Inclusion of tunnel metal wall stored heat, which is in equilibrium with gas temperature, modifies the energy state diagram. Figure 3 shows a new energy state diagram which includes the heat stored in the metal wall. Again, in this case, a fan operation results in increase of tunnel temperature and pressure. Injection of LN_2 results in an increase of tunnel pressure and decrease of tunnel temperature. Discharge of GN_2 results in decrease of pressure and a small decrease in temperature.

The quasisteady tunnel control problem is therefore the strategy of using these three mass energy control vector magnitudes to either maintain mass energy equlibrium at any given point or to move the tunnel state from any one point to other.

Modeling of temperature dynamics:

The closed circuit cryogenic tunnel duct can be considered as a thermally autonomous pressure vessel which is ideally isolated from the ambient temperature environment. This system is assumed to be open to a LN_2 supply source and open to ambient for purposes of discharging GN_2. These inputs carry mass and energy into and out of the system. Assuming uniform evaporation and mixing, ignoring the work done within, and by invoking the first law of thermodynamics we have, the following expressions for enthalpy of the LN_2 and GN_2:

$$h_L = U_L + P_L V_L \qquad\qquad h_G = U_G + P_G V_G$$

Then,

$$-\dot{Q}_m + \dot{Q}_F + \dot{m}_L h_L = \dot{m}_G h_G + \frac{d}{dt}(W_G C_v T) = \dot{m}_G h_G + C_v T \frac{d}{dt}(\dot{m}_L - \dot{m}_G) + W_G C_v \frac{dT}{dt}$$

This can be simplified to

$$\dot{m}_L(h_L - C_v T) - \dot{m}_G(C_p - C_v)T - \dot{Q}_m + \dot{Q}_F = W_G C_v \frac{dT}{dt} \qquad (1)$$

This basic thermodynamic model describes the gas temperature dynamics of the cryogenic wind tunnel.

Similar cryogenic wind tunnel dynamic modelling efforts have also been reported for the DFVLR's KKK cryogenic tunnel. (ref. 8, 9) A comparison of the basic modelling concepts in references 8 and 9 with the modelling work for 0.3-m TCT show some important differences in postulates for the thermodynamics of mass-enthalpy mixing. In the work at the 0.3-m TCT, the evaporation of LN_2 into the tunnel resident mass, the wall heat release to the tunnel resident gas, and gas discharge are considered to be isothermal phenomena where as the fan induced compression alone is considered adiabatic. In references 8 and 9 all mass/energy interaction is assumed to be adiabatic, as is evident from use of C_{PG} (specific heat at constant pressure) in the following equations drawn from these references.

Thermodynamic equation 12 (page 6) from reference 8 is,

$$(C_T m_T + m_G C_{PG})\frac{dT_G}{d\theta} = - \dot{m}_L[r_{N_2} + C_{PG}(T_G - T_S)] + \ldots + \ldots$$

Thermodynamic equation 1 (page 29) from reference 9 is,

$$C_{PG} m_G(t)\frac{dT(t)}{dt} = - \dot{m}_L(t - \tau_1)\left\{r_{N_2} + C_{PG}[T(t) - T_s]\right\} + \ldots + \ldots$$

$$+ C_{PG}[T_+ - T(t)]\ \dot{m}_{G_+}(t - \tau_2)$$

where m_G corresponds to tunnel resident gas mass, $\dot{m}_{G_+}$ corresponds to gas charge into the tunnel. For the case of gas discharge $\dot{m}_{G_-}$ out of the tunnel, this equation is modified to

$$C_{PG} m_G(t)\frac{dT(t)}{dt} = - \dot{m}_L(t - \tau_1)\{r_{N_2} + C_{PG}[T(t) - T_s]\} + \ldots + \ldots$$

$$- C_{PG}[T(t) - T(t)]\ \ \dot{m}_{G_-}(t-\tau_2)$$

which cancels out the effect of gas discharge on the energy term. The gas discharge energy term does not occur in either of these energy equations because of the adiabatic assumption. One consequence of this assumption is that for gas discharge out of the tunnel, there is no energy loss in the system at all, suggesting that gas temperature is unaffected.

Experimental evidence from open loop impulse response test for 0.3-m TCT is shown in figure 4. (ref 3) This figure clearly demonstrates that an impulse gas discharge pulse during an equilibrium condition operation results in tunnel gas temperature cooling. This supports the physical law assumptions of an

isothermal like situation in the mass enthalpy mixing in cryogenic tunnels as far as gas discharge is concerned. More support of this feature will be evident in the pressure response tests in figure 44 to be discussed in a subsequent section.

Metal wall heat release model:

The 0.3-m TCT is an externally insulated pressure vessel and the tunnel gas is directly exposed to the internal wall of the pressure vessel. The gas and metal exchange their internal energy to seek equilibrium in their temperatures because of heat transfer. Representation of the heat transfer between the tunnel metal and the gas is complex and can be represented by another dynamic model. The heat transfer from the tunnel shell to the gas occurs at the internal surface of the 0.3-m TCT totalling about 60 m^2. The heat exchange is through convection heat transfer due to moving gas along the internal surface. Heat transfer is rapid at the test section where the flow velocity is high. In reference 3, this problem of generating a simple heat transfer model has been addressed and a model has been developed.

$$\int_{\text{surface}} \dot{Q}_m = \frac{W_t C_m T\, S}{1+t_m\, S} \qquad (2)$$

where t_m is a simplified time constant which describes a lumped rate of heat release/absorbtion from the metal shell to gas. The heat release rate is a function of the local flow velocity which varies spatially around the tunnel. The time constant has been estimated for the 0.3-m TCT as:

$$t_m = \frac{943}{T^{0.12}(P\,M)^{0.8}} \qquad (2a)$$

$$\int \dot{Q}_m = \frac{W_t C_m T\, S}{1+t_m\, S} = (T - T_m)\, y \qquad (2b)$$

Equations (2a) and (2b) suggest that heat transfer rate is poor at low Mach numbers and low pressures, and heat transfer rate is very good at high Mach numbers and high pressures. The time constant of heat transfer t_m has been estimated by treating the tunnel as a set of 15 cylindrical segments of various sizes, each with a fixed local pressure, temperature, and Mach number for any given equilibrium flow condition. (ref. 3) A number of such estimates covering the full tunnel operating envelope yield a set of time constants. These time constants have been function fitted to arrive at an approximate time constant model of equation (2a). The model in equation (2) is further simplified to yield an average metal temperature T_m and a heat transfer coefficient y. The coefficient y is an equivalent heat transfer coefficient which provides an approximate heat exchange rate given an

average tunnel metal temperature and gas temperature.

Modeling of pressure dynamics:

Consider the pressure of an ideal gas as a function of temperature and mass representing the gas mass resident in the cryogenic tunnel. We have:

$$P = kW_G T \qquad kW_G = \frac{P}{T} \qquad kT = \frac{P}{W_G}$$

Differentiating with respect to time

$$\frac{dP}{dt} = kW_G \frac{dT}{dt} + kT \frac{dW_G}{dt}$$

for cryogenic tunnels $\frac{dW_G}{dt} = \dot{m}_L - \dot{m}_G$

Hence $$\frac{dP}{dt} = \frac{P}{T} \frac{dT}{dt} + \frac{P}{W_G} (\dot{m}_L - \dot{m}_G) \qquad (3)$$

This simple model describes the pressure dynamics. It assumes uniform mixing of LN_2 with the tunnel resident gas, and that no work is done by the system. The mass enthalpy interaction is assumed to be isothermal.

Mach number control of the 0.3-m TCT:

The operation of the tunnel fan creates a pressure rise across the fan which results in flow of tunnel resident gas around the tunnel circuit. Under equilibrium flow conditions, the pressure rise and the total tunnel circuit pressure loss cancel each other. Circuit pressure loss is a function of the mass flow and hence Mach number at any given point. The circuit losses increase with increasing mass flow and dynamic pressure. The circuit geometry in 0.3-m TCT is such that the bulk of the circuit losses occur in the test section and the down stream diffuser. Ideally, the test section has an uniform cross section and its Mach number is determined by the mass flow and the area of cross section. Assuming steady one dimensional isentropic flow in the convergent nozzle ending in a uniform area test section without a model. The continuity equation can be stated as,

$$\dot{m}_{T.S.} = k_t \frac{P}{\sqrt{T}} A_t \frac{M_\infty}{(1+0.2\, M_\infty^2)^3} \qquad (4)$$

In a test section with varying geometry, the effect of area change A_t on the flow can be studied using

an one dimensional approximation. The differential momentum equation for isentropic flow can be expressed as:

$$\frac{dp}{\rho v^2} = -\frac{dv}{v} \qquad \text{The continuity equation is } \rho VA = \text{constant}$$

By taking a natural logarithm of the continuity equation, equation (4) and differentiating it we have:

$$\frac{dA_t}{A_t} = -\frac{dv}{v} - \frac{d\rho}{\rho} = -\frac{dM}{M}\left(1 - M^2\right) \qquad (4a)$$

This simple model describes, in a one dimensional sense, acceleration of flow over the convergent divergent nozzle system created by the airfoil with its changing angle of attack, changing wall contours, and the traversing rake. The effect of the contour change can be looked upon as an equivalent cross sectional area change dA. Figure 5 shows a plot of $\frac{dM}{M}/\frac{dA}{A}$ as a function of M. It illustrates the effect of area change on Mach number. The Mach number sensitivity to area change is always higher than 1, and as the flow Mach number approaches Mach 1, the sensitivity increases asymptotically. When the local flow reaches Mach 1, the flow is sonic and the flow chokes. Tunnel flow choking results in loss of monotonicity of mass flow with fan speed.

When an airfoil is mounted in the 0.3-m TCT for two dimensional testing, it typically spans the whole width of the test section and creates two passages for the tunnel test section flow, shown in figure 6. Each passage can be looked upon as a complex convergent divergent type nozzle system. The airfoil shape, its attitude, and the test section top and bottom wall contours together decide the geometry of these nozzle shapes. The Mach number distribution along the test section is a function of local test section area as detailed in equations (4) and (4a). The flow on the top segment of any typical airfoil accelerates due to its lifting nature and can be expected to reach supersonic Mach number for high entry Mach number, M_∞. Figure 7 illustrates the actual distribution of local surface Mach number on a typical two dimensional airfoil for an entry Mach number of $M_\infty = 0.765$ in the 0.3-m TCT. The Mach number on the upper surface of the airfoil reachs a local maximum of M = 1.31 and on the lower side a maximum of M = 0.82. A normal shock occurs on the airfoil at about 62% chord location. This suggests a partially choked flow in the upper segment. If the normal shock extends up to the wall, the top segment of the flow path chokes. The airfoil bottom surface Mach number distribution clearly shows an unchoked flow. For high entry Mach number both the top and bottom passage can choke making Mach number control using fan speed control impossible.

Drag polar data on an airfoil is usually obtained by traversing a drag rake with a set of pitot tubes in the wake of the model. The rake traverse mechanism for the 0.3-m TCT consists of a 6.5 inch span

wedge of root thickness of 0.625 inch, a tip thickness of 0.375 inch and it carries a set eight of pressure probes. The wedge has a root chord of about 2 inch and a tip chord of 1 inch. The traverse takes place in the wake of the full span 2-D model. This nearly 4% thick rake having an average chord of 1.5 inches behaves like another airfoil. It modifies the geometry of the flow paths as it traverses across the model wake and can affect the Mach number distribution.

The flexible top and bottom walls provide ability to adapt to the model and avoid wall interference by seeking a natural streamline shape. (ref. 10) Twenty one pairs of actuators provide this streamlining ability through computer control. In arriving at streamline conditions, an algorithm iteratively adjusts the wall shapes which leads to geometrical disturbances in the test section during the process of wall adaptation.

Therefore the 0.3-m TCT flow Mach number, under transonic flow conditions, is strongly affected by angle of attack changes of the model, rake traverse in the wake of the model, and the flexible wall contouring mechanism. All of these changes which cause geometrical disturbances that occur in the critical test section of the tunnel cause disturbances to the Mach number. The automatic Mach number control loop is required to nullify the effect of these geometrical disturbances and hold the test section entry Mach number constant.

Fan speed model:

The fan performance map for the 0.3-m TCT can be summarised as a function of the tunnel pressure, temperature, and test section Mach number as:

$$N = K_m \, M\sqrt{T} \, (1 - 0.3 \, M) \, P^{-0.035} \qquad (5)$$

where K_m = a function of test section geometry

Equation (5) describes the combined effects of pressure ratio across the fan and the tunnel circuit loss factor combined into one steady state model for unchoked flow around the tunnel. It has been obtained experimentally. The gain of the test section Mach number for incremental fan speed change can be evaluated from equation (5) as:

$$\frac{dM}{dN} = \frac{1}{(1 - 0.6 \, M)} \, \frac{P^{0.035}}{K_m\sqrt{T}} \qquad (5a)$$

This is a nonlinear quasisteady state expression which describes sensitivity of fan speed on Mach number. The sensitivity changes by about a factor of 2 when the Mach number is changed from 0.15

to 0.9. This sensitivity function is the logical gain schedule for the automatic Mach number control loop. The constant K_m has been found to be a function of the tunnel geometry. It has changed from about 600 for the 8 x 24 inch slotted test section with its contraction, down to 521 when the test section area was changed to 13 x 13 inch with its contraction and solid walls. K_m is also affected by angle of attack of the model and the wall contouring strategy to some extent.

The dynamics of the tunnel flow for fan speed change is dictated by the pressure rise characteristics of fan, the motor and its drive with varying tunnel flow loads. It is also affected by the plenum pressure dynamics. In the 0.3-m TCT, the fan is required to change the kinetic energy of tunnel resident gas mass with varying fan speeds. With its solid wall configured test section, plenum time effects do not exist in the present configuration of 0.3-m TCT, except when boundary layer treatment is operational. The fan dynamics involved in accelerating or decelerating the flow can be approximated to a simple time constant which varies with tunnel conditions. Instead of modeling this time constant analytically, it is embedded in the fan speed model obtained experimentally and is discussed elsewhere. (ref. 11)

MODELING OF THE ACTUATORS AND SENSORS

The 0.3-m TCT is controlled by three basic actuator systems. The tunnel states are sensed by six basic transducers for control purposes. The dynamics of these sensors and actuators constitute a part of the overall control loop. They affect the accuracy and stability of the tunnel closed loop control. The following sections describe the modeling of these actuators and sensors and associated ancilliary systems.

LN_2 storage system:

The LN_2 storage system has two 106,000 liter vacuum dewar vessels with an air exchanger for building up the desired pressure in the system. The LN_2 pump suction can be connected to either storage vessels. The pump output is carried in an insulted pipe to the tunnel area and returns back to the tank through a back pressure valve. This back pressure valve can be manually or automatically adjusted to control the pump LN_2 pressure output. A ten gallon accumulator is provided near the tunnel injection point to allow steady pressure from the LN_2 source. The accumulator is made of an aluminium upright dead end tube connected at one end to the LN_2 pressure line. The LN_2 rises in the uninsulated tube and encounters GN_2 which it compresses. Since the tube is not insulated, the gas above the liquid remains in a gaseous state and provides a stable source pressure.

The impeller driven LN_2 pump pressure is a function of the LN_2 mass flow. Since the tunnel mass flow varies considerably, the LN_2 pressure is kept constant with a pressure relief route.

LN_2 injection valve dynamics:

The LN_2 injection into the 0.3-m TCT requires a proportional flow control valve capable of providing mass flow control from about 6 kg/s down to 0.02 kg/s with the tunnel back pressure varying from 1 to 6 atm. The present configuration uses a 300 psig rated electro-pneumatically actuated diaphragm driven control valve. This control valve has good rangeability and a response of better than 0.7 s for full stroke. Two valves are used to inject LN_2 into the 0.3-m TCT. The electro-pneumatic coil accepts 4-20 mA proportional command to drive a flapper-nozzle system which generates a 3-15 psia pneumatic signal. This signal is power boosted and fed to the spring loaded diaphragm actuator which proportionally drives air into the valve from full close to full open.

Before adapting this valve to the 0.3-m TCT in 1987, a set of binary weighted digital valves were used. Digital valves are ideal for static operation and for mass flow calibration. But the digital valves could not accept command rates of 10 Hz from the tunnel controller for long periods because of damages to the valve seats, fouling, scouring, and stuck elements.

Performance tests have been made on the electro-pneumatic valve to determine the dynamics and are presented in Appendix A. Figure 8 shows the Bode plots of the frequency response tests. Figure 9 shows response of the LN_2 valve to a step command and shows existence of transport delay in response. Figure 10 shows the static calibration of the LN_2 valve for commands shows some nonlinearity and an insignificant hysteresis. The electro-pneumatic injection valve has good repeatability, is nonlinear for command to stroke, has a transport lag of about 100 ms and a first order time constant of about 0.23 s. The valve response bandwidth of about 4-5 rad/s is adequate for LN_2 flow control. The valve dynamic model is nonlinear with amplitude. A best fit linear model for commands up to 25% peak to peak, and for smaller perturbation is

$$\frac{e^{-0.103\ S}}{(1+\ 0.23\ S)} \qquad \text{velocity limit of about } 130\%/s$$

GN_2 discharge valve:

Two 4 inch cryogenic high pressure valves have been converted for electrohydraulic actuation to provide high bandwidth response. These GN_2 discharge valves are required to remove mass flow from the tunnel by passive release to the atmosphere. This work only when tunnel pressure is above

atmospheric pressure. For sizing the valve, the lowest tunnel pressure considered is 16 psia. With small differential pressure to atmosphere, the area command rate for mass flow control is about 50%/s at high mass flow conditions corresponding to high Mach numbers. Therefore a response speed of 0.25 s for full area control is desired and is realized only by electrohydraulic actuation. The valves have a 3 inch stroke requirement for full control. Hydraulic jacks of stroke 3 inches, bore of 1.5 inches with a rod of 0.75 inches are used to actuate the valves. Each hydraulic jack is connected to ports A and B of a series 102 Moog valve capable of 0-5 gpm flow control for signals of 0-5 mA. The hydraulic oil supply is from a finely filtered (to better than 5 microns) hydraulic pump working at 3000 psig which is water cooled. The valve stroke is measured by a linear potentiometer connected to provide 1 VDC at full close and 5 VDC at full open. The valve is operated in closed loop for position. An analog amplifier which compares the command and the position potentiometer drives the servo coil in negative feedback.

A schematic diagram of the valve drive system is shown in figure 11. The volume of the actuator is about 5 $inch^3$ and at an oil flowrate of 0-5 gpm the maximum response is about 0.3 s for full stroke. The frequency response is flat up to 5 Hz, because of the short volume between the hydraulic servo valve and the actuator. An oil accumulator stabilizes the small perturbation response without starving the line for oil during rapid commands. The dynamic model of the valve for small perturbation of 5% is

$$\frac{760}{S^2 + 42\,S + 760}$$ with a velocity limit of about 300%/s

A transport lag of a few milliseconds exists and can be ignored. This position response is for zero gas flow loads and zero mechanical load on the stem and is slightly underdamped. With flow loads, the performance mildly degrades, but it has not been quantified. The valve has a power failure block to take care of safe close creep bias in case of electrical failure. Two such valves have been converted and provide a higher resolution for gas discharge. One valve opens to nearly 90% before the other valve starts opening. This opening schedule is realized as a part of the control law. A third pneumatically operated valve of the same size is used as a remotely operated, manually supervised emergency valve, which has a response time of 4-5 s. The pneumatic valve cannot be used in closed loop control because of its very sluggish response.

Fan drive system:

The 0.3-m TCT fan drive is a fixed pitch twelve bladed rotor with a seven blade fixed inlet guide vane optimised for the pressure ratio envelope of the tunnel operation. The tunnel Mach number is

controlled by fan speed variation ranging from about 600 to 5600 rpm. The fan speed control is obtained by use of a 2 pole water cooled 2000 KW induction motor excited from a variable frequency generator with the frequency of supply varying from 10 to 95 Hz. Another requirement of the variable frequency supply is that the ratio of supply voltage to frequency be below 35 Vrms per Hz.

The variable frequency generator control scheme is shown in figure 12. A 4600 V, 3ϕ, 60 Hz 4 pole synchronous motor drives a separately excited direct current (DC) generator. The DC generator can provide variable voltage of $\pm$0-600 VDC whose magnitude and polarity is controlled by variable field excitation obtained from a field DC amplifier. A set point rheostat generated command drives the field amplifier. The DC generator provides power up to 2000 KW. This DC variable voltage source is used to drive the armature winding of a shunt excited 600 KW DC motor which can run at variable speeds of $\pm$0-1200 rpm depending upon the DC supply voltage. The DC motor shaft drives the rotor of a 6 pole alternating current (AC) machine rotor. The rotor winding of this AC machine is excited by 4600 V, 3ϕ, 60 Hz supply through slip rings and creats a 60 Hz rotating field. The stator of this AC machine, which is wound for 3ϕ, sees in its rotor an electrical rotating field of 60 Hz and is mechanically rotated at $\pm$0-1200 rpm. If the electrical rotating field is mechanically moved in an opposing direction to rotor rotating field, the net stator frequency is their difference and vice versa. The stator generates a frequency of 60 Hz $\pm$motor speed/20. At zero DC motor speed the output is at 60 Hz. At +600 rpm the output is 90 Hz and at -900 rpm the output is 15 Hz. The output power of the AC machine at its stator is the sum of mechanical energy from the DC motor shaft and the rotor to stator AC power transfer. The machine is rated for an output of 1000 KW at variable frequency. Thus the DC motor speed controls the output frequency on the AC machine stator winding. The DC motor speed is controlled by DC generator supply voltage which in turn is controlled by field control of the DC generator.

In the case of 0.3-m TCT, the two rotating systems are required to provide full 2000 KW through a single rotating DC source with its remotely controlled field. The DC source can excite both the DC motors and the variable frequency generators. The DC generator field control is by a rheostat which forms an arm of a DC bridge whose unbalance voltage drives the field amplifier. The rheostat is a 40 turn potentiometer driven by a DC servo drive whose position is signalled from the tunnel controller.

A fan speed of 3600 rpm calls for zero speed on the variable frequency generator, and the AC power transfer has to be derived from the AC machine by a pure transformer action through the machine air gap. This creates considerable thermal problems and can result in damaged windings if used for long periods. To overcome this, it is necessary to avoid operating the fan at speeds between 3550-3650 rpm. Even at speeds as low as 10 rpm on the AC machine shaft, the power transfer is good with adequate

shaft fan cooling and AC machine has no thermal problems.

The dynamic modeling of the fan speed control system should adequately describe all the elements of the speed control chain, viz., the position rhoestat servo which is a second order system having a velocity limit, the field amplifier for the DC generator driving the field with its time constant, the two rotating alternators driven by the DC motors with their inertial/electrical charecteristics, and the inertial/electrical modeling of the fan drive induction motor with varying fan load. This is a complex chain, and hence an inverse approach of using parameter identification for modeling has been used. The total system is modeled for small perturbation using the actual fan speed command and response time histories. (ref. 11) This results in the following approximate model which covers most of the tunnel operating envelope.

$$\frac{N}{N_{set}} = \frac{5}{S^2 + 2.8\,S + 5} \quad \text{with a speed rate limit of 300 rpm/s}$$

The dynamics fan speed command to fan pressure ratio involves generation or dissipation of the extra kinetic energy to create new equilibrium mass flow. This dynamics is partially embedded in the above model, since the response of the system has been actually measured. The test section dynamics is very fast since the tunnel has no plenum and hence no storage problems. When the tunnel plenum is open to the test section through some ports, another first order time constant describes the transport time delays. Presently, for the solid wall test section, the fan speed to Mach number dynamics is represented by a simple time constant.

To close the Mach number control loop it is necessary to sense the total and static pressures in the test section which are used to estimate the Mach number using the following isentropic relation.

$$M = \sqrt{5\left(\frac{P_{total}}{P_{static}}\right)^{3.5} - 5} \qquad (6)$$

The pressure sensors which are used to measure these pressures have a response time constant which is a major factor in the Mach number measurement. Two such time constants are used in the model representing the sensors in the Mach number control loop.

Tunnel temperature measurement:

Accurate and fast measurement of tunnel gas temperature is necessary for control purposes. The choice of either thermocouples or platinum resistance device exists. The response time constant of the sensing device in a gas is a function of the heat transfer rate, which is related to the density and velocity of the

gas. In the 0.3-m TCT, the temperature is required at the settling chamber where the velocity is the lowest around the tunnel. Platinum resistance device usually have higher mass and hence copper-constantan thermocouples have been used. The output of a copper-constantan themocouple is nonlinear with temperature and linearisation is necessary. The range of the thermocouples in the 0.3-m TCT are between 74.15 and 342.15 K which corresponds to an output voltage of -5.587 to 2.864 mV, with the reference junction kept at ice point. Because of the large range of temperature spanned, two polynomials have been fitted for temperature as a function of output voltage assuming an amplification of the output by about 592 and a datum shift of -3.306 V. This amplification and datum shifting provides a 0-5 VDC signal for the 74 to 342 K temperature range. The polynomials are given in terms of the output E of the zero shifted amplifier:

$$T = 74.1826 + 105.3\,E - 40.66\,E^2 + 20.54\,E^3 - 5.21\,E^4$$
$$\text{for } 0 \leq E < 1.191 \text{ VDC}$$

$$T = 80.678 + 84.52\,E - 12.717\,E^2 + 1.805\,E^3 - 0.1102\,E^4 \qquad (7)$$
$$\text{for } 1.191 \leq E \leq 5 \text{ VDC}$$

Two such thermocouples are used in the 0.3-m TCT to measure the gas temperature and the metal wall temperature. The response time of the tunnel gas temperature sensor varies with the tunnel conditions. The slowest response time of 3 s occurs at 80 K, 1 atm and a Mach number of 0.2. Quicker responses occur at 6 atm, Mach 0.8 and a temperature of 300 K with the response time constant being about 0.5 s or lower. These response time constants have been estimated using a heat transfer model similar to the convection modeling in reference 3. The size of the thermocouple wires used for gas temperature measurement are 0.028 inches. Efforts to reduce the size of the thermocouple wires to improve response results in weakening the strength of the wires to withstand the flow loads. Another problem of thin thermocouple wires is thermal stresses caused under rapid cooldown conditions when impinged by droplets of LN_2.

The metal wall temperature is sensed at the third corner of the tunnel, with the sensor located on the external face, but is insulted from the ambient. The contact mechanism dictates the fidelity of temperature transfer from metal to thermocouple. This metal temperature is monitored to keep the tunnel structural cooldown or warmup within safe limits.

Tunnel pressure measurements:

Measurement of total and static pressures in the settling chamber and test section are essential for estimating tunnel flow Mach number. The stability, repeatability, and accuracy of measurement are very critical in estimation of Mach number as low as M=0.200, to 0.001 resolution. This call for accuracy in pressure measurement typically of the order of 0.003 psia in 30 psia corresponding to 0.01%. An error of 0.01 psia creates an undesirable Mach number uncertainty of 0.002 to 0.003. The transducer accuracy and stability should be adequate for measuring Mach number to 0.001 or better. This static performance should be accompanied by quick response time. A quick response can be realised by a low volume transducer with short tubing.

Amongst the presently available class of high accuracy transducers, one of the best is the quartz bourdon type pressure transducer. This device is associated with very slow response. A study in reference 12 indicates the unsuitability of quartz bourdon devices for Mach number evaluation in control. The study points to very sluggish response for very small increments to pressure, equivalent first order time constant as high as 1 s. For large pressure fluctuations, the response is good and improves to an equivalent first order time constant of about 0.15 seconds.

Perhaps the next best class of pressure transducers is the temperature controlled capacitance type transducer with a carrier excitation similar to the Barocell made by Datametrics of USA. These have a specified stability of the order of 0.01% and an accuracy only mildly inferior to the quartz burdon type pressure transducer. The Datametrics Barocell is a differential capacitance type pressure tranducer which is kept at a uniform temperature to avoid zero shifts. It is usually referenced to vacuum on one side to measure absolute pressures. The measurement port is connected to the tunnel pitot tube for sensing the total and static pressures. The length of the connecting pipe line is a few meters and does introduce response time delays. Response test for step inputs, with the connecting pipe included, indicates a first order equivalent time constant of better than 0.2 s for small increments. The total pressure is measured at a pressure ring mounted within the settling chamber. The static pressure is measured at the test section entry using a pitot static tube.

The Datametrics has a standard signal conditioning unit for the Barocell which consists of a carrier excitation to the capacitance bridge, bridge null circuitry for inphase and quadrature unbalances, amplifier and demodulator. The system provides 0-5 VDC output for the full range of 6 atm. One each is used for the tunnel static pressure and total pressure. Provision also exists for autoranging amplification, and analog to digital conversion. However, for the purposes of control, the transducers are operated in a fixed range mode.

The LN_2 pressure is sensed on the LN_2 supply line. The requirements of this sensor are very nominal. Since the LN_2 is an incompressible liquid, the frequency response of coupling is very good. Accuracy sought in pressure measurement is of the industrial type with 0.2 to 0.5% accuracy. A bonded strain gauge type stainless steel sensor compatible to LN_2 is used. The signal is preamplified to provide 0-5 VDC for the full supply range of 0-176 psia. This signal is used for evaluating the LN_2 mass flow and as a part of the control law mechanization.

Fan speed sensor:

The tunnel fan speed is controlled from the tunnel integrated control station. Hence it is essential to measure accurately the fan speed. The choices for fan speed sensors are DC tachogenerator, AC tachogenerator, or pulse counter. In the 0.3-m TCT, an optical pulse counter is used to measure the fan speed. An optical beam is modulated by a multiple line encoder mounted on the fan shaft, and the pulse rate is sensed by a photosensor. This sensor output is differentiated through a rate network to generate the speed. Its accuracy is very good and the differentiation network provides a 0-5 VDC signal output for 0-7200 rpm range.

Figure 13 provides a schematic diagram of the locations of the various tunnel sensors, tunnel control actuators, and the schematic layout of the flexible wall system with rake and angle of attack systems.

0.3-m TCT CONTROL LAWS

Four inner control loops are proposed for the control of 0.3-m TCT. These are for the tunnel gas temperature, the tunnel total pressure, the tunnel fan speed, and the LN_2 pressure control. Further, two of these four inner loops are brought into two outer loops to control test section Mach number and Reynolds number. As the tunnel dynamic response model equations indicate, the control problem associated with cryogenic tunnel, in a global sense, is the dominance of the non-linearity and coupled nature of the process. For small perturbation, stability and control, laws have been postulated in reference 3 for the 0.3-m TCT. These remain valid qualitatively even with the tunnel modifications. The larger control problem is tunnel trajectory control involving large set point changes. New nonlinear control strategies are proposed for each of these loops.

Tunnel temperature control loop:

Figure 14 shows a schematic of the tunnel temperature control loop. The tunnel gas temperature is sensed by a copper constantan thermocouple referred to an ice point, its output is linearised and is compared with set temperature. The error is used in a porportional integral derivative (PID) control law with a fan feedforward. Its output commands the LN_2 mass flow. The small perturbation control law is:

$$\dot{m}_L = \frac{N\sqrt{P}}{T}\left\{K_{it}\int(T - T_{set}) + K_{pt}(T - T_{set}) + \frac{d}{dt}(T - T_{set})\right\} + K_f\frac{P}{\sqrt{T}}\left(\frac{N}{1000}\right)^{2.26} \quad (8)$$

and $$\dot{m}_L = 0.8676\, C_{Lqv}\sqrt{(P_{Lq} - P)}\, A_L$$

Constraints on this law are that each of the integral component and the output command are limited to 0-100 % range of the LN_2 flow by minimax clipping. This control law has worked well near the set point on the Motorola controller since 1980.

The tunnel temperature control loop has a gain schedule of $\frac{N\sqrt{P}}{T}$ to cover the full tunnel envelope and is operational for all $T \geq T_{set}$. The control law also works for small differences in temperature for $T_{set} > T$ ranging up to maximum LN_2 flow dictated by fan feedforward at the tunnel conditions. The loop performs its control function for even large differences of $T_{set} > T$, by totally stopping the LN_2 flow and waiting for the fan heat to bring the temperature near the set point. But for a general metal warmup, it is energy efficient to switch the fan feedforward term of the LN_2 flow control off. A hysterisis type non-linear switching logic is introduced to account for the direction of the tunnel temperature traverse and to switch the fan power feed forward *on* or *off*. This non-linear hysterisis logic is shown in figure 15. This logic is:

$$\begin{aligned} &\text{IF } T - T_{set} < -5 \quad \text{Feed forward } \textit{off} \\ &\text{IF } T - T_{set} > 0 \quad \text{Feed forward } \textit{on} \end{aligned} \quad (9)$$

The temperature control law of equation (8), totally ignores information on the tunnel metal temperature in its control strategy. A study of the simple heat release model in equation (2b) indicates that metal cooling rate is a function of difference between average metal temperature and gas temperature. Even with very large LN_2 injection, the metal cooling rate cannot be accelerated, unless the heat transfer rate from the metal mass equals the LN_2 cooling capability. At low fan speeds and

low tunnel pressures, the metal cooling rate is very low because of poor heat transfer. Since the heat transfer rate is dictated by tunnel pressure and fan speed, use of excess LN_2 is likely to result in accumalation of LN_2 at the lower point in the tunnel without major contributions to metal cooling rate. Accumalation of unevaporated liquid in the tunnel is highly undesirable and is considered a safety hazard. It is therfore necessary to use the average metal temperature and gas temperature to limit the LN_2 mass flow in to the tunnel based on heat transfer rate. A non-linear empirical function based on the temperature difference is used to limit the maximum mass flow into the tunnel. The law is:

$$\dot{m}_{Lmax} = 100\% \quad \text{for } (T_m - T) \leq \frac{\Delta T_{max}}{2}$$

$$\dot{m}_{Lmax} = 100\left\{1 - \left(T_m - T - \frac{\Delta T_{max}}{2}\right) \frac{2}{\Delta T_{max}}\right\}\% \quad \text{for } (T_m - T) > \frac{\Delta T_{max}}{2}$$

$$\dot{m}_{Lmax} = 0 \quad \text{for } (T_m - T) > \Delta T_{max} \qquad (10)$$

where ΔT_{max} corresponds to maximum safe temperature difference allowed between the average metal temperature and the gas temperature. This maximum safe temperature difference is based on structural integrity. These constraint laws are superimposed on the control law indicated in equation (5). Metal temperature measurement is essential for mechanizing the control law. Local external metal temperature around the tunnel varies considerably under transient conditions. Metal temperature near the settling chamber where the response is relatively slow is a representative point for sensing the metal temperature.

The metal temperature based LN_2 mass flow limiting control logic is illustrated in figure 16. A typical number used for ΔT_{max} is 50 K. This choice indicates that up to a difference of between 0 - 25 K in gas to metal temperature, there is no limit on maximum LN_2 flow except as limited by the valve and the LN_2 pressure. However, when the metal to gas temperature difference is between 25 - 50 K, the maximum allowed LN_2 flow is linearly brought down from 100% at 25 K to 0% at 50 K error. Beyond 50 K difference, the LN_2 flow is totally stopped. For the case of metal temperature being lower than gas temperature, the control law of equation (10) is not relevant. The intent of this law is to avoid thermal stresses on the structure by very fast cooling or leading to situations where the LN_2 is likely to accumulate in the tunnel. The rate of cooling now is dictated by convection heat transfer rate. For high rates of cooling, the fan speed has to be increased or the tunnel pressure increased to create conditions for higher convection heat transfer.

Tunnel total pressure and Reynolds number control loops:

Figure 17 shows a schematic for the 0.3-m TCT total pressure and Reynolds number control loop. The tunnel pressure is controlled by varying the discharge of tunnel gas. The pressure build up occurs when the valve is fully closed while injection of LN_2 continues into the tunnel with simultaneous the fan operation, which generates heat. The tunnel total pressure is sensed by a capcitance type differential transducer and is compared with the tunnel pressure set point. The error is used to modulate a PID control law which in turn drives the GN_2 discharge valve area. The mass flow control law is:

$$\dot{m}_G = \frac{1}{T}\left\{K_{ip}\int(P - P_{set}) + K_{pp}(P - P_{set}) + \frac{d}{dt}(P - P_{set})\right\} \qquad (11)$$

and $\dot{m}_G = K_G A_{Gv1} \frac{P}{\sqrt{T}}$ for choked flow out of the valve to atmosphere.

This control law has a gain schedule of the type $\frac{1}{T}$ in mass flow which translates to $\frac{1}{P\sqrt{T}}$ in area. The integral term and the output are clipped to a range of 0-100%. This control law has been derived using the analysis in reference 4, and has performed well for nearly 8 years of operation in the older version of the tunnel controller.

A second GN_2 discharge valve is also available for pressure control. At low tunnel pressures (near atmospheric) and high Mach numbers, the control law is likely to demand area larger than 100% for valve 1. A second valve is used in tandem, which works on the following logic:

$$A_{Gv2} = \int 0.1 \qquad \text{when } A_{Gv1} > 0.90$$

$$A_{Gv2} = \int -0.1 \qquad \text{when } A_{Gv1} < 0.70 \quad \text{and} \quad 0 < A_{Gv2} < 1 \qquad (12)$$

This logic has valve 2 opening or closeing at a rate of 10% depending on the demand area of valve 1.

The 0.3-m TCT is used frequently for controlling the tunnel Reynolds number directly while holding the Mach number. The estimation of the precise tunnel pressure or temperature manually by the operator to hold the Reynolds number is quite involved. Reynolds number of the flow in 0.3-m TCT can be estimated as follows:

$$\rho = 338.9 \frac{P_s}{T_s}$$

$$u = \sqrt{\frac{\Re\gamma}{mole}}\, M\sqrt{T_s} = 20.38\, M\sqrt{T_s}, \text{ for } \Re = 8.31, \text{ mole} = 0.028$$

$$\mu = 1.082\ T_s^{0.9}\ x10^{-7}$$

Using the isentropic relation between total and static variables we have

$$Re = \frac{\rho\ u\ \bar{c}}{\mu} = K_{re}\ \frac{\bar{c}\ M\ P}{T^{1.4}(1 + 0.2\ M^2)^{2.1}}$$

where K_{re} is a constant (K_{re}=63714) and $\bar{c}$ is the model reference chord in meters.

For a given Mach number either the tunnel gas temperature or the tunnel pressure can be varied to realize the desired Reynolds number. The energy efficient method is to keep the tunnel pressure as low as possible and to adjust the tunnel temperature (ref. 13), to control the Reynolds number. However, in a tunnel dominated by metal mass, rapid variation of tunnel temperature is not possible due to the long settling times involved in the metal cooling. Gas temperature can be varied rapidly, but it will not be in equilibrium with metal wall temperature. A preferable procedure is to bring the tunnel gas temperature down initially to an energy efficient region. At that fixed temperature, the tunnel pressure can be modulated to control the Reynolds number in a limited range. The pressure modulation control law for a fixed tunnel gas temperature and tunnel Mach number is:

$$P_{set} = \frac{Re\ T^{1.4}\ (1+0.2\ M^2)^{2.1}}{\bar{c}\ M\ K_{re}} \qquad (13)$$

This mode is equivalent to generating a pressure set point for the tunnel pressure loop based on the required Reynolds number. The mode is useful when a Mach number scan test is done under constant Reynolds number conditions.

If the route of varying the tunnel temperature is to be used to control Reynolds number, then the set point for temperature loop can be evaluated using the expression:

$$T_{set} = \left\{ \frac{P\ \bar{c}\ M\ K_{re}}{Re\ (1 + 0.2\ M^2)^{2.1}} \right\}^{-1.4}$$

This mode of control provides an energy efficient method of varying Reynolds number and can be used effectively if the temperature control loop has good band width and stability, without the loop slow down problems caused by of metal heat transfer rates. In the case of 0.3-m TCT, the wall plays a dominant role and slows the steady state response of metal temperature. Temperature control loop band width is very low. Therefore, the pressure modulation route of controlling the flow Reynolds number has been used.

Tunnel P-T trajectory control:

In order to take the tunnel pressure/temperature from one state to another, tunnel set points have to be changed. Control of this locus is the tunnel trajectory control problem. At a given fan speed or test section Mach number, the tunnel trajectory can be studied on a P-T plot, as illustrated in figure 18. Consider the tunnel presently operating at a starting P_1-T_1 located on lines of constant gas mass in the tunnel. To take the tunnel to any other arbitarary and final point P_2-T_2, four terminal zones can be identified on the P-T plane in which P_2-T_2 can be located. Zone 1 and 2 are zones where the final tunnel gas mass is equal to or lower than the starting mass. Zone 3 and 4 are areas where the final tunnel gas mass will be higher than the existing gas mass. Zones 2 and 3 are areas where the final temperature is lower than starting temperature, implying a cooldown and hence mass addition through LN_2 injection. Zones 1 and 4 are areas where final temperature is higher than starting temperature, with only fan heat being demanded. It can be noted that in zone 4, though additional gas mass is required to reach the point, the temperature control law cannot provide additional mass in the form of LN_2.

In other words, for set point commands where the final conditions ask for a higher tunnel pressure and higher temperature simultaneously, simple closed loop control laws just shut the LN_2 valve and shut the GN_2 valve. In theory, with the tunnel fan operation the gas temperature should slowly rise. Once the temperature has been achieved, the LN_2 valves injects some cooling LN_2 mass which will then build the tunnel pressure. This will take considerable time.

Under simple closed loop control laws zone 4 cannot be reached quickly. It is therefore necessary to conceive of a trajectory control algorithm such that the final state is automatically and quickly reached. The following logic algorithm has been proposed to take care of tunnel state movement into zone 4, where P_1-T_1 is the initial state of the tunnel and P_2-T_2 is considered as the final set point. T_{use} is the set point actually used in the temperature control loop.

$$\text{If} \quad \frac{P_2}{T_2} \geq \frac{P_1}{T_1} \quad \text{and} \quad \text{if} \quad T_2 > T_1 \quad \text{then} \quad T_{use} = T_1 - 0.1 \quad \text{else} \quad T_{use} = T_2 \qquad (14)$$

This simple algorithm identifies the terminal point of the trajectory relative to current tunnel state. If the final point is in zone 4, then temporarily the temperature set point is pushed to cool conditions so that tunnel gas mass can build while demanding the new tunnel pressure. Once adequate tunnel gas mass buildup occurs, the temperature set point is changed to the final set point T_2. In actual implementation a small dead band is created around this logic, so that this logic is invoked only for

fairly strong excursion to zone 4. Once the tunnel state reaches any other zone 1, 2 or 3, the tunnel control for pressure and temperature described in equations (8), (10) and (11) can work adequately with the desired set points. These control laws can accommodate large set point changes covering the full range of operational envelope in pressure and temperature.

This logic adequately creates a safe trajectory from any point P_1-T_1 to any other point P_2-T_2 within the P-T plane of the tunnel operating envelope. The quickness of reaching the final point is decided by the fan energy chosen, which decides $\dot{m}_L$ and the fan heat. The tunnel Mach number or the tunnel fan speed does not directly affect the logic except that the rate of cooldown or warmup and the tunnel pressure buildup rate will be decided by the fan energy used.

Fan speed and Mach number control law:

Figure 19 shows a schematic of the control loops used for the tunnel fan speed control and Mach number control. Details of the variable frequency generator system and the electronic remote control of the frequency, necessary for fan speed control, have already been presented in figure 12. The schematic shows an inner fan speed control loop and an outer loop for the tunnel test section Mach number control. The following control law provides the rheostat position θ_{rh} for the inner loop:

$$\theta_{rh} = \frac{1}{7500}\left[K_{in}\int(e_n) + K_{pn}(N_{set} - N)\right] \qquad (15)$$

$$e_n = N_{set} - N \quad \text{with}$$

$$-e_{nmax1} < e_n < e_{nmax1} \text{ for } |N_{set} - N| \leq 100$$

$$-e_{nmax2} < e_n < e_{nmax2} \text{ for } |N_{set} - N| > 100$$

$$-\dot{\theta}_{max} < \dot{\theta}_{rh} < \dot{\theta}_{max} \qquad (15a)$$

Integral term authority is 100% of the full rheostat range.

Two step saturation type non-linearity has been invoked for the proportional integral (PI) fan speed control law. The proportional control law uses the full fan speed loop error without any saturation, and assists in stability and quick response. The fan speed error is faithfully used for the integral control law till the fan speed error grows to e_{nmax1}. Then the integral error term is saturated at e_{nmax1} till the fan speed error grows to 100 rpm. After the fan speed error exceeds 100 rpm, the

integral error is switched to e_{nmax2}. This dual saturation limits the rate of fan speed command from an integral control point of view. The integral term with the saturation provides steady state accuracy of a high order without creating any stability problems. Hence the fan speed control law is a simple PI law for small errors, but is a nonlinear PI control law for large speed errors. Another feature of the control law is the limitation on the maximum rheostat position command rate of 50 rpm/s. The non-linear saturation characteristics to the fan speed inner loop are presented in figure 20. The fan speed control law has been synthesised based on a study of the various elements of the fan speed control system detailed previously. In this design, the shortcomings in the control laws generated in reference 4 and the performance of the Intel SBC 80/20 based controller were taken into account. The control law proposed, (ref. 4) could not provide desired accuracy in speed control. In the control law proposed in equation (15), the integral control law has been slowed down considerably and made non-linear for the sake of fan speed stability and response shown in equation (15a).

The external Mach number control loop generates speed command necessary for realizing the desired Mach number. This control law is again a PI control law with a very weak integration term of low authority. The control law is:

$$N_{set} = N + K_m \frac{\sqrt{T}(1\text{-}0.6\ M)}{P^{0.035}} \left\{ K_{pm}(M_{set}\text{-}\ M) + K_{im} \int (M_{set}\text{-}\ M) \right\} \tag{16}$$

$$-100 < K_{im} \int (M_{set}\text{-}\ M) < 100$$

The Mach loop provides an incremental command to the fan speed loop to move towards the correct Mach number. The control has a gain schedule embedded in it which is a function of the tunnel gas temperature $\sqrt{T}(1\text{-}0.6M)$. The small perturbation gain schedule is based on the analysis of the Mach loop detailed in reference 4. The Mach control loop generates the N_{set}, where as in fan speed control mode N_{set} is chosen manually. The stability of the Mach number control loop is dictated by the response time constants of the total and static pressure sensors and their accuracy, the dynamics of the speed control system with its long chain of devices viz., rheostat position servo, the field amplifier response, the DC field time constant, the variable frequency generator mass/electrical characteristics, and finally the tunnel fan motor dynamics with its varying fan load. The Mach number is a function of the two pressures. Any noise in the pressure measurements, particularly at low Mach numbers like 0.200, can create an uncertainty in sensed Mach number. A noise of 0.01 psi in 18 psia creates an error of 0.002 in Mach number. This uncertainty results in poor Mach number control.

LN_2 pressure control loop:

The LN_2 pumping system pressure control schematic is shown in figure 21. The pump inlet is from the pressurized storage tank and the outlet is taken to a back pressure valve which acts as a pressure relief valve. The relieved mass flow is returned to the LN_2 storage tank. The liquid pressure upstream of the back pressure valve is controlled by a PID controller. The mass flow of LN_2 relieved back to the tank is controlled by the valve area A_{LN}, where:

$$A_{LN} = K_{il}\int(e_l) + K_{pl}(e_l) + K_{dl}\frac{d}{dt}(e_l) \qquad (17)$$

where $e_l = P_{Lset} - P_L$

and $-e_{lmax} < e_l < e_{lmax}$

The LN_2 pumping system pressure is a non-linear function of the back pressure valve area and the LN_2 mass flow demand from the tunnel. The pump pressure volume performance curve shows a minimum pressure of about 100 psig even with the back pressure valve fully open. Depending upon the tunnel mass flow demand, the tunnel pressure can be controlled in the range of 100-150 psig. The pressure gain for unit area varies highly nonlinearly with mean valve area. Under some conditions, valve area has no effect at all on the LN_2 pressure. The back pressure valve controls the liquid pressure only between 60-80% opening. For valve areas out of this range, no control exists. This is due to the pump pressure volume characteristics. The LN_2 pressure response to area control is slow. Hence, the control law could not be designed fully apriori. It needs to be tuned at site with only a gross estimation of the proportional and integral gain terms available.

MICROCOMPUTER BASED 0.3-m TCT CONTROLLER

Hitherto, the modeling of the 0.3-m TCT, the control laws, the various actuators and sensors have been discussed. An appropriate controller to mechanise the closed loop control laws for the 0.3-m TCT needs to be identified. A review is now made of the tunnel controllers that were used during the period 1979-1987 for controlling the 0.3-m TCT. A schematic diagram of the Motorola 6800 based Pressure-Temperature controller and the Intel SBC 80/20 microprocessor based Mach number controller is shown in figure 22.

The Motorola 6800 based system consists of a six channel analog to digital converter, (ADC) with a multiplexer having 16 bit resolution, and a range of 0-5 VDC. This feeds to an 8 bit microprocessor

based system with EPROM burnt in control laws. The controller generates the pressure-temperature control laws and commands for the valves. The commands are available as two 4-20 mA outputs through 12 bit digital to analog converter, (DAC) for pressure control actuators. The temperature control signals are available as pure binary drives of 11 bit resolution. The binary drives feed two digital LN_2 valves having a resolution of 11 bits as 12 elements. The temperature control output is also available as an analog 4-20 mA drive. The control law is simple and the system cannot handle large set point changes safely. The computational speed is 10 Hz for the two loops.

The Intel SBC 80/20 system has a 4 channel ADC with multiplexer having a resolution of 12 bits and a range of 0-5 VDC. This feeds to the microprocessor with burnt-in assembly language Mach number and fan speed control laws. The system generates an analog output which signals the rheostat position drive servo. The update speed of this system was only 4 Hz, leading to inferior Mach number control performance.

The two controllers functioned in isolation and the Mach number controller was rarely used during tunnel operation. Mach number controller performance was not satisfactory, and could not be tuned adequately with the available tuning freedom. This resulted in poor tunnel control performance and two operators were needed to run the Mach loop, P-T loops and the LN_2 system on almost a manual mode. The software on both these controllers were not transparent. They could not be easily modified. Machine language/assembly language codes were available, and the systems were custom configured with specialised operator interfaces. Modification of these control laws was not cost effective because the development systems for the microprocessor systems were not easily accessible.

The concept of having a development/operating system divorced from the controller perhaps is an economical idea for bulk manufactured microprocessor based systems with no need for modifications, and where the software is made inaccessible for commercial reasons. For custom built dedicated research facilities like the controller for 0.3-m TCT, this concept is not valid. Over the decade of 1980's the cost of microcomputer systems with versatile operating system have come down enormously. Reliability of microcomputer systems in terms of mean time between failure has increased greatly. There are standard and well proven real time hardware packages which complement the microcomputer systems providing multichannel analog to digital and digital to analog conversion, and resoultions up to 16 bits are available. These devices integrate well into the microcomputers, and are addressable at software level with minimum time overheads.

It is proposed to build a new microcomputer based 0.3-m TCT controller with following requirements.

* A standard commercial microcomputer system with a built-in operating system and real time interface cards should be used as the tunnel controller.
* The operator interface to the tunnel controller should be through an enhanced graphics monitor for operator display and a keyboard for operator input.
* The display/keyboard combination should be safe for wrong and inadvertent single key stroke commands and provide simple display of all relevant tunnel information either graphically or through alpha numeric text on the monitor.
* The display/keyboard combination should provide menu type information to the operator for controlling the tunnel.
* The software should consist of a display module, keyboard command module, ADC module, DAC module, control law module and a tunnel safety/integration modules to run in an endless loop.
* The software should not get numerically or functionally locked up, and should not cease to function for any fault other than total power failure or an electronic hardware failure. No combination of keyboard commands or electronic input signals should stop the execution of the control laws in the endless loop.
* Software should be written in a higher level compilable language, so that the executable code is opaque for modifications.
* Software should not be rendered obsolete because of iterative advances that occur in hardware. The software should be easily transportable to microcomputers of similar class working on DOS without any changes.
* Hardware chosen to be such that absolutely no custom built devices are used. The system must use well proven and standard real time cards of high reliability and of industrial quality.
* The system should integrate all the tunnel control burden into a single software with emphasis on ease of modifications. A computational cycle time of better than 100 ms for all the control loops, display and command is essential.
* The integration of tunnel control laws must globally cover the tunnel operating envelope.
* The display should show windows corresponding to each control loop, and indicate the tunnel process variable, the command and the set point in appropriate windows. Operator inputs to be displayed on a buffer area in the window so that it can be loaded on to the loop or deleted after appropriate operator inspection and monitoring.
* Operator commands to be serviced one at a time in each cycle so that the computation cycle is never stopped. Operator commands should not take more than a millisecond to be serviced.
* Emergency commands should run the tunnel down to zero fan speed, shut the LN_2 off and discharge all the tunnel gas. The controller system should identify sensor failures and take the

tunnel control system on an emergency shutdown.

* The tunnel temperature control should restrict the gas cooling rate to 20 K/min, so that the fine protruding devices like thermocouples, probes and turning vanes are not exposed to thermal shocks which can reduce their life. This is to allow adequate time for the LN_2 to evaporate into the tunnel stream.
* The tunnel average metal cooling rate should be restricted to a maximum of 10 K/min. The maximum temperature difference between metal wall and gas should not exceed 50 K.
* The tunnel test section Mach number control loop should be able to maintain Mach number for disturbances caused by angle of attack change, flexible wall movements, and the drag rake traverse by automatically adjusting the fan speed through the Mach number loop control law.
* An automatic Reynolds number control loop should be available. Given the model chord, the Reynolds number loop should modulate the set value of tunnel total pressure to hold the tunnel Reynolds number.
* Tunnel condition regulation required is ± 0.3 K in total temperature, ± 0.07 psia in total pressure, ± 3 rpm in fan speed, ± 0.002 in test section Mach number and ± 0.2 % in flow Reynolds number per chord.
* The tunnel controller should be capable of identifying the onset of tunnel choking and revert from Mach number loop to fan speed loop to avoid fan speed runaway.
* The tunnel control loop gain scheduling must be totally internal with no demands on operator to keep tuning the system for different tunnel operating conditions.

Choice of microcomputer system for tunnel control:

The 1980s have seen a revolution in the availability of well proven and reliable microcomputer systems with considerable software at low cost. An IBM PC/AT type machine or any of its clones working on DOS operating system is typical of such microcomputer systems. It has become an industrial standard and is well accepted. It is a 16 bit microcomputer working on clock speeds of 12 MHz and beyond, and has been interfaced with host of devices. Many vendors have designed high performance real time data acquisition and control packages like 16 bit resolution ADC, 12 bit DAC, and digital I/Os for this class of IBM PC/XT/AT microcomputers. These real time devices are software addressable with very little time overheads.

A PC/AT class of microcomputer has been chosen for the new 0.3-m TCT controller. The configuration requires 512K RAM memory with hardware BIOS, 10/12 MHz clock, DOS operating system, enhanced graphics color monitor with its interface card, a hard disk, a diskette drive and a 5060 type keyboard with the whole system working on an uninterrupted electrical supply. This is

complimented by real time 8 channel ADC and an 8 channel DAC. Figure 23 shows a schematic of the new PC/AT based controller for temperature, pressure/Reynolds number and Mach number control of 0.3-m TCT.

Analog to digital converter:

Data Translation DT2801/5716 8 channel analog to digital converter is a PC/AT architecture compatible real time card. This has been chosen for taking the analog inputs into the microcomputer. The ADC changes an analog electrical voltage in to a digital variable with 16 bit resolution, in the range of 0-65535. The eight channel multiplexer in the ADC card chooses any one of the eight inputs, and amplifies the input signal. A sample and hold circuit acquires the signal from the multiplexer and keeps it constant during the analog to digital conversion period. Once the analog to digital conversion is complete, the multiplexer is ready to switch the next channel. All the supervision of analog to digital conversion, channel selection and, error detection functions are carried out by an 8 bit microprocessor (with its own firmware) within the analog to digital converter card. The important specifications of the device are,

1. Number of channels = 8 floating inputs
2. Input range = bipolar 0-5 VDC or 0-10 VDC
3. Resolution = 16 bit (1 in 65536)
4. A/D response in software = 7500/s
5. Noise and drift = less than 5 μV (< 1 bit)

The DT2801/5716 A device directly plugs into the standard 62 pin system mother board of the PC/AT at base address &H2EC. The A/D converter can be addressed as a port using BASIC language software. Software can address any required channel randomly, perform an A/D conversion and bring the digitized information back to the main CPU in a period of less than 0.5 ms per channel. The analog inputs are connected to the ADC through a screw terminal with ribbon cable connector which plugs into the ADC card.

Digital to analog conversion:

The Data Translation DT2815 is an eight channel digital to analog converter compatible to IBM PC/AT and has been chosen for the 0.3-m TCT controller. The DAC can convert any digital number in the range 0-4095 from the CPU and appropriately scale it to analog electrical output of either 0-5 VDC or 4-20 mA. It consists of a Universal pereferal driver which provides the interface between the

microcomputer and the DAC. Though the device is an 8 bit converter, it accepts the 16 bit information from the microcomputer in two bytes of each eight bits. The two bytes contains not only the 12 bit data to be converted but also information on the channel number, and the type of output (current or voltage) in the other 4 bits. A multiplexer reads the 4 bit channel information and the 12 bit digital data from the CPU. The digital data is converted to an analog signal. This voltage or current is taken to a sample and hold circuit which provides a continuous analog output until the channel is readdressed. Some important specifications of the DAC are,

1. Number of channels = 8
2. Output ranges = 0-5 VDC or 4-20 mA, selectable on the card for each channel
3. Resolution = 12 bits or 1/4096
4. Dynamic response = 3300 Hz per channel
5. Drift = 10 μV (< 1 bit)
6. Short circuit/open circuit/reverse polarity protected
7. Output impedance = 20 mA resistive load for current and 5 mA for voltage

The DAC plugs into the 62 pin connector on the IBM PC architecture compatible system board. The base address for the device is &H1224. It also uses &H1225. The DAC process is software controlled and can be performed channel by channel in about 0.6 ms by BASIC software.

0.3-m TCT controller configuration:

A diagram of the IBM PC/AT based temperature, pressure/Reynolds number, fan speed/Mach number controller for the 0.3-m TCT with details of the interconnection between various modules is shown in figure 24. The microcomputer with its 512K RAM has an enhanced color graphics monitor, 20 MB disk drive, a 12 MHz clock, a $5\frac{1}{4}$ inch diskette drive, and a 5060 keyboard is the central computer. High resolution analog signals from the various tunnel sensors are connected to the eight channel A/D converter through a screw terminal board. These are, the two 78-342 K range signals from tunnel gas and metal temperature thermocouple sensors, the two 0-88 psia signals from the tunnel total pressure and static pressure Barocell sensors, 0-6400 rpm signal from fan speed sensor, 0-176 psia LN_2 pressure sensor and 0-5 psia signal from screen pressure drop sensor, all ranged precisely to 0-5 VDC.

The outputs of the D/A converter are connected to the various tunnel actuators. Channels 1 to 3 have current outputs of 4-20 mA to drive electropneumatic coils for the two LN_2 injection valves and the LN_2 pumping system back pressure valve. Channels 4 to 7 are in voltage output mode ranged such that channels 4 and 5 provide 1-5 VDC for the two gas discharge valve system set points. Channels 6

and 7 provides 0-5 VDC for the rheostat drive servo and 5 VDC fixed for the reference voltage to the rheostat drive bridge supply.

With all the analog tunnel sensors and the actuator drives connected, the microcomputer can close the loop and control the tunnel in an integrated manner based on the tunnel software. The software requirements are discussed in the following section.

0.3-m TCT control software:

The tunnel control software can be written in any of the higher level languages which makes the code easy to understand and modify. BASIC has some distinct advantages over other languages like FORTRAN, PASCAL or C in the present context because of the choice of an IBM PC/AT. The graphics modes for operator display are easy to manage in this language on the DOS. The real time cards, chosen, from Data Translation Inc, are configured to accept and respond to BASIC language commands directly with minimal time oveheads. Hence BASIC has been chosen as the language for the control law mechanization for 0.3-m TCT.

The software for integrated tunnel control is required to perform following modular functions.

i) Initialisation of the various real time devices, numerical alogorithms requiring previous history at the startup, tunnel system engineering constants and multicolor window generation with fixed text.
ii) ADC of the seven input signals, input range safety check and engineering unit conversion.
iii) Keyboard command reading, if any command exists.
iv) Set point supervision and calculation of flow Mach number and Reynolds number.
v) Control law realisation for temperature, pressure, Reynolds number, fan speed, Mach number, LN_2 pressure, and generation of control commands.
vi) Display of tunnel variables.
vii) Tunnel safety monitoring.
viii) DAC of the seven control commands to the drive actuators.
ix) Repeat of steps ii) to viii) in an endless loop.

In the following chapter details of the software flow charts and some of the issues relating to reliable operation of the tunnel controller are also presented.

FLOWCHART FOR INTEGRATED CONTROL OF 0.3-m TCT

The software for the integrated control of the 0.3-m TCT is to be realised in the least amount of code so that the cycle time for one iteration is less than 100 ms for all the functions. The detailed flowcharts for realising all the control functions are shown in Appendix B. Though the software has been written as a set of contiguous statements, following functional modules can be identified.

Initialisation:

This segment of the software routine starting with clearing the screen is executed only once, at a restart, after a power failure, or a forced aborting of the programme. The intialisation involves following functions.

1. Define the base addresses for the real time ADC and DAC. ADC initialisation involves defining the constants for write, read, clear, wait and stop commands to be loaded into the status, command and data out high/low registers. The DAC initialisation proceeds by resetting the status register and checking the status of the register after a finite time delay. If the DAC reset status is not proper the program stops execution declaring a DAC problem. The firmware which selects the unipolar output ranges with mixed current voltage outputs, and the number of channels is loaded in to the data register. These are custom configured for the sensor/actuator configuration in the 0.3-m TCT.

2. A number of numerical constants essential for closed loop control are read in next. These are, tunnel control loop gain settings for the control laws of the tunnel temperature, pressure, fan speed, Mach number, LN_2 source pressure, transducer calibration constants to convert ADC output to engineering units, LN_2 and GN_2 discharge valve area coefficients, previous cycle data intialisation, and maximum metal to gas temperature difference allowed.

3. Fixed screen presentation using graphic statements consisting of commands for five color windows. Four windows show fixed texts for LN_2 pump control loop, gas and metal temperature loop, pressure/Reynolds number loop, and fan speed/ Mach number control loop. The fifth window block defines the horizantal row information in respect of the four loops corresponding to SET POINT, PROCESS, COMMAND, keyboard INPUT and STATUS area. Fixed text defines the control loop text, engineering units used, modes displays viz., AUTO, MANUAL, AUTORE/AUTOP for concerned loops. In the INPUT area, the menu for set point commands to LN_2 pressure (B), temperature loop (Temp), area of LN_2 valve (ALQ%), pressure loop (Pres), Reynolds number loop (Ryno), area of GN_2 valve (AGv), model chord (Chrd), Mach (Mach) and fan speed (Nrpm) are shown with the menu

prompt in a high lighted letter corresponding to the input. The STATUS band provides certain data text for wall temperature time gradient (GRAD), free stream saturation temperature (SAT), model mean aerodynamic chord (CHORD), screen pressure drop to indicate icing (Del P) and the test section static pressure (P st).

ADC with engineering unit conversion:

This software subroutine performs ADC for the seven chosen channels in a loop. In each cycle of the loop, the ADC is reset with a stop command, the internal amplifier gain and the channel number are read. After initiating a data conversion command and an appropriate wait period, the low byte and the high byte of the converted signal are read from the data register. The high byte is multiplied by 256 and added to the low byte. The result is normalized to 65536, corresponding to 16 bit range of the AD converter, to scale the data for full range of 0-10 VDC. Any fault in ADC is identified by reading the status. If a fault exists, the ADC is reset and the whole chain of conversion is restarted. The seven channel output data is stored and checked whether the data is within safe range. If the signal is out of range, a sensor failure situation exists, which initiates a shut down of the tunnel on an emergency mode. The output from the ADC is engineering unit converted using the calibration constants already defined.

Keyboard commands:

In this software routine, using an INKEY$ command of DOS, the keyboard buffer is searched for operator commands. At a time only one command is serviced. If no commands exist, the subroutine returns to main program. Only specific alphanumeric ASCII character code commands viz., decimal point, 0 to 9, B, C, D, G, L, M, N, P, R, T and <Enter> (or carriage return) are declared to be legitimate. Any other command from keyboard is ignored, and the subroutine is bypassed. The program can read any one of the 22 legitimate commands in any cycle of computation, if such a command is already issued by the operator. The letter commands B, C, G, L, M, N, P, R, and T choose one of the nine possible data input modes, which will allow subsequent numeric inputs into a buffer. Appendix F gives a full explination of all the letter keyboard commands. Any legitimate character command after the first mode command is considered to be only a numeric input. If letter inputs are given, it will be treated as a zero. The next five numerical commands from keyboard are stored in the buffer and these provides set point commands to the concerned control loop already chosen by the mode command. In any chosen input mode, the location of the decimal point is predecided based on the variable concerned. The buffer data is displayed in flashing black numbers on the monitor in the appropriate window as it is loaded one at a time in to the buffer from the keyboard.

The input cannot be transferred to the main control loop till the buffer is fully loaded.

The letter command D can reset the chosen mode and it clears all the numerical commands stored in the input buffer. Once the buffer is full, the operator is expected to check the numbers. If not satisfied, the whole input can be reset to clear by D command. New inputs have to start with a legitimate letter command. If the data in the input area is proper, the data can be transferrd only to the concerned control loop by the enter command. This command automatically clears the buffer for a subsequent input. Even after the transfer of data, the quantity is checked against the allowed range of numbers for the concerned variable. If the number read in is out of that range, the nearest safe number is assumed to have been commanded and will be used for control purposes.

Thus the keyboard subroutine only accepts legitimate alphanumeric commands. Commands cannot be transfered to the loop unless meaningful data is created on the buffer. The keyboard commands are well protected from wrong or inadvertent inputs from operators.

Estimation of the flow parameters and set point supervision:

In this software module several control loop scheduling variables, which vary continuously, are calculated. The ratio of total pressure to static pressure is used to estimate the test section flow Mach number using equation (6). A function of Mach number $MF=(1+0.2\ M^2)$ is required a number of times during the control law mechanisation and is estimated and stored. Using the model chord, a parameter frequently required in estimation of Reynolds number is estimated.

$$KRE = \frac{K_{re}\ \bar{c}\ M}{T^{1.4}\ MF^{2.1}}$$

Another function which provides the free stream saturation temperature is estimated using expression

$$SAT1 = MF\left(50 + 27.34\ P_s^{0.286}\right)$$

This expression has been derived from study of properties of GN_2, and is based on data from Jacobsen. (ref. 14) The fan feed forward is estimated using another function fit which relates the fan speed, tunnel pressure and temperature to fan power. This expression for the 0.3-m TCT in its present configuration of 13 x 13 inch test section is,

$$FKW = 110\ P\left(\frac{N}{1000}\right)^{2.26}\frac{1}{\sqrt{T}} \qquad (13)$$

The full open area LN_2 mass flow is estimated using the valve coefficient and the pressure across the LN_2 valve.

The tunnel trajectory in the P-T plane is estimated by evaluating the present state and the final state. The direction control law described in equation (14) is mechanised. A dead band of 2 K is used around the existing tunnel conditions to avoid limit cycles. This software uses equation (14) as a series of logic steps to decide the tunnel actual temperature set point to be used. The law works effectively for situations when the final destination is in the zone 4.

Control law realization:

1. Temperature control loop: The equations (8), (9) and (10) constitute the metal/gas temperature control law and these equations are converted into control software in this module. The integral term RIT is estimated first and is limited in amplitude to the range (-FBF) to (1-FBF) where FBF corresponds to fan feedforward. The fan feedforward is enabled or disabled as instructed by the logic in equation (9). The software estimates ALQ corresponding to LN_2 valve area. This estimation uses the loop error ET, the sampling time DEL and the loop gain terms. The logic in equation (10) limits the LN_2 mass flow to LMT and hence the rate of cooling as well as the maximum metal to gas temperature difference. Under manual mode, the LN_2 valve area is directly taken from the keyboard command, LCMDS. Even under manual control, the LN_2 valve area is limited to have thermal control of the tunnel structure. The temperature loop error is diplayed on the monitor as a flag as long as it is less than ± 0.3 K and the gas to wall temperature difference is less than 24 K. Two duplicate outputs of ALQ are created as outputs DAC(1) and DAC(2) to drive the two LN_2 injection valves. Emergency command IE, when enabled, drives the valve area to zero area.

2. Pressure/Reynolds number control loop: The equation (11) details the pressure control law, which is mechanised into software. In AUTOP mode, the PID control law generates the valve area command AGV1 using the pressure loop error EP, the sampling time DEL and the loop gain terms. The integral control term RIP is ranged to stay within a minimax limit of 0-100%. If the output drive AGV1 generated by the control law exceeds 90%, a second valve AGV2 is opened at the rate of 1% valve area per computational cycle. Integration continues till the control law commands AGV1 to a value less than 90%. For values of AGV1 less than 90% but more than 70%, the AGV2 valve area integration stops at its previous value and stays constant. At values of AGV1 lower than 70%, the valve area AGV2 goes down to zero at a rate of 1% per cycle. Magnitude of AGV2 is also limited to 0-100%. The two outputs AGV1 and AGV2 are setup as outputs DAC(4) and DAC(5) for DAC in the range of 1 to 5 VDC. The valve area AGV1 is limited to a rate of 50% opening per second.

In the case of closed loop control of Reynolds number corresponding to mode AUTORE, the identity in equation (13) generates the tunnel total pressure setpoint required to hold the Reynolds number. The pressure set point is calculated every cycle for the current values of Mach number and temperature.

The tunnel pressure loop error is used to signal a flag when the error is less than ± 0.07 psia. The pressure loop can be taken to manual control for the valve AGV1, with a keyboard commanded GCMDS in percent valve area position. During an emergency condition, the tunnel pressure is discharged to atmosphere automatically by opening the valve AGV1 to 100%.

3. Fan speed and Mach number control: Equation (14) provides the basic fan speed control strategy, and has been mechanised into appropriate software. In the manual mode the set point NCMDS for the fan speed loop is derived from the keyboard. NCMDS1 corresponds to modified speed set point based on safety and other integration requirements. NCMDS1 is the used set point for the fan speed and Mach number loops. The fan speed control rheostat zero corresponds to a minimum fan speed of 600 rpm. For set point commands less than 580, the set point reverts to zero. Fan speed error EN is used for proportional control without any modifications. Fan speed error is faithfully used for the integral control law till the fan speed error grows to about 5 rpm. Then the integral error term is saturated at 5 rpm, till the fan speed error grows to 100 rpm. After the fan speed error exceeds 100 rpm, the integral error is switched to 50 rpm. The fan rheostat position is estimated as SNRPM using the EN, sampling time DEL and the PI loop gain constants. Another feature of the fan speed control law is the limitation on the maximum rheostat position command rate which is limited to 50 rpm/s. Individually, the authority of the both P and I elements of control law is 100%, restriction that together they cannot exceed 100%. The fan speed rheostat command SNRPM is normalized to unity for full range of 7200, and setup as an output for the DA conversion routine, as DAC(6). This output represents rheostat position driving the Ward-Leonard speed control variable frequency generation system described previously. A simultaneous command of 5 VDC is generated to feed the rheostat drive bridge excitation, as DAC(7). Without this reference, the rheostat servo cannot function. A trap has been built for identifying the speed band of 3550 to 3650 which is a singularity of the variable frequency generator system. The control algorithm displays this status as an audio-visual cue to the operator.

The Mach number control loop is the AUTOM mode addressable from keyboard. This outer loop generates a speed control set point NCMDS1 based on the Mach loop error EM, sampling time DEL and the PI loop constants. The control strategy used is detailed in equation (6), and is mechanised only as a simple PI law using Mach number loop error EM. The Mach number loop gain schedule

involves the tunnel gas temperature and the Mach number. As the Mach number is increased the loop gain drops as in the function (1-0.6M). The Mach error integral magnitude RIM is limited to an authority of 100 rpm only, but is added to existing fan speed, which virtually provides 100% authority. A logic flag has been created to indicate an error in test section Mach number of ± 0.002, and is displayed whenever the error is less than this band.

If the true fan speed has not come up to 580 rpm, the Mach number loop cannot be enabled and will revert to fan speed mode automatically. Secondly, while on AUTOM mode, if the demand on ALQ touches 99%, the temperature loop cannot accommodate the fan induced energy due to lack of flow injection and cooling capability. Therefore, the software is designed such that the Mach number loop reverts to fan speed control mode with a set point drop of about 500 rpm. An emergency command of IE=1 takes the fan speed down to zero speed at a rate of 50 rpm/s.

4. LN_2 pumping system: Equation (17) provides the algorithm that has been used for the LN_2 pressure control. Since the pumping system is highly non-linear and sluggish, the error magnitude ELP is clipped to a very small value of 0.15 atm. The PI control law is mechanised using this error ELP and the sampling time DEL with the loop gain constants. The integration rate is very slow, and is compatible with the sluggish system with its long time delays. The integral amplitude RIL is limited to 100% authority which extends to valve proportional command also. The control drive for LN_2 back pressure valve ALN is derived from the loop error ELP, sampling time DEL and the other loop constants. The relief valve drive command is set up as DAC(3) for output. For an error of less than ± 2.0 psia in the LN_2 pressure control loop, the software creates a flag to indicate that the control loop is holding the desired pressure.

Display of tunnel variables:

The following tunnel variables are displayed on the monitor. These quantities are,

Set Points:
- LN_2 pressure
- tunnel gas temperature
- tunnel total pressure
- fan speed
- test section Mach number
- Reynolds number
- model chord
- temperature set point actually used

Process variables:	LN_2 pressure
	tunnel total pressure
	tunnel static pressure
	tunnel gas temperature
	tunnel metal wall temperature
	fan speed
	test section Mach number
	free stream saturation temperature
	screen pressure loss
	tunnel metal temperature time rate
Actuator commands:	LN_2 back pressure valve area
	LN_2 injection valve areas
	GN_2 discharge control main valve command
	auxiliary valve command
	fan rhoestat position
Flags:	LN_2 pressure loop error $\leq$ 2.0 psia
	temperature loop error $\leq$ 0.3 K
	tunnel pressure error $\leq$ 0.07 psia
	Mach number error $\leq$ 0.002
Message displays:	Speed Band
	Emergency Stop
	Sensor Failure
Modes:	Auto (LN_2 loop)
	Auto/Manual (temperature loop)
	AutoP/AutoRe/Manual (pressure loop, Reynolds number control loop)
	Auto/Manual (Mach number control or fan speed)
Input modes:	B (LN_2 pressure)
	C (chord)
	D (delete command)
	G (GN_2 valve area)

L (LN_2 valve area)

M (Mach number)

N (fan speed)

P (pressure)

R (Reynolds number)

T (temp)

Tunnel safety monitoring:

The tunnel metal temperature rate of cooling or heating is estimated by integrating the temperature difference (TMWL-TMWL1) from one cycle to the next over 40 cycles. Noisy data will average itself out to zero, and a steady cooling or a warmup is estimated by extrapolating this 4 s data to a minute.

The cryogenic tunnel initially starts with ambient air and associated moisture (because of partial pressure of water due to humidity), particularly when an entry has been made into the tunnel to change models. If the tunnel operation is started with a cooldown, this moisture is likely to condense into ice and settle on the screen, choking the flow path. Hence a process of purge of moisture is necessary before the tunnel cooldown to temperatures below 273 K. The tunnel purging process consists of operating the tunnel at a warm temperature with both LN_2 injection and gas discharge while the fan is generating adequate heat. This process is carried out for a reasonable length of time to assure a slow reduction in the moisture in the tunnel. The water removal process is monitored by comparing the screen pressure drop to an ideal circuit pressure drop across the same screen under same tunnel conditions with known loss coefficient. If the pressure drop exceeds the ideal, the screen is icing. Software has been written to estimate the settling chamber flow Mach number and then evaluating the safe pressure drop allowed, DLPC. This is compared to measured pressure drop DLP. In the event icing has occurred the screen displayed pressure drop DLP starts flashing with an audio alarm.

Total power failure results in zero electrical commands for LN_2 injection valve, gas discharge valve and fan command. The LN_2 valve is an air to open and electrical current to open type valve. The gas discharge valve hydraulics takes the valve to close position on electrical supply loss using the oil accumulator stored energy. Power loss to fan runs the fan down to zero speed. This situation is safe, except that the tunnel gas mass is held steady.

DAC:

The seven outputs DAC(1) to DAC(7) are now available as commands in the range of 0 to 1. They are converted into electrical drives in the DAC software. The first three channels DAC(1) to DAC(3) need to be translated to 4-20 mA signals and the rest to 0-5 VDC. The software converts these numerical commands to electrical voltages sequentially.

The DAC requires a 16 bit command as two bytes of eight bit each called the low and high bytes. Bit 1 of the low byte sets the output mode as voltage or current. Bits 2, 3 and 4 of the low byte corresponds to one of the eight DAC channel numbers. Bits 5, 6, 7 and 8 of low byte correspond to 1, 2, 3 and 4th bits of the 12 bit DAC data. Bits 1, 2 to 8th bits of the high byte correspond to 5, 6 to 12th bit of DAC data.

Each numerical output is first normalized to 0 to 4095 range corresponding to 12 bit resolution of the DAC hardware. The numerical output is divided by 16 and the integer of the result corresponds to the full high byte. (Maximum integer in the division of 4096/16 corresponds to 256 which is an 8 bit binary number). The reminder is multiplied by 16 to generate 1, 2, 3 and 4th bit of DAC data corresponding to 5, 6, 7 and 8th bit of the low byte. The first bit of the low byte sets the current or voltage output mode, and the channel number is selected by the 2, 3 and 4th bits of the low byte. Thus between the high and the low bytes, the digital to analog converter receives full data signal, channel number and the electrical output mode. Then the two low and high bytes are loaded to the output port at &H224. The execution of the seven channel DAC is completed in a set of simple BASIC statements.

Repetition of the control law in an endless loop:

The software is written to return to ADC routine after executing all the modules described above, and repeat the computations endlessly. It bypasses the initialisation, which is called for only on a planned shutdown involving loss of power to the microcomputer. The software is written so that it does not stop because of any software uncertainties like divide by zero situations, or because of peculiar combination of inputs. The keyboard DOS functions like Print Screen, Pause/Break, Cntrl-Alt-Del which are valid commands for DOS are disabled. (the <Cntrl-Alt-Del> command could be kept for maintenance shut down, but the tunnel operators need to be informed about it and taught not to use these commands). Electronic hardware failure or power failure alone can stop the program execution.

MICROCOMPUTER SYSTEM

An IBM PC/AT clone system with a 12 MHz clock, 512K RAM, 20 MB hard disk, $5\frac{1}{4}$ and $3\frac{1}{2}$ inch flexible disk drives, a 13 inch enhanced graphics monitor, and a 5060 modified keyboard is used as the tunnel controller. Two real time cards DT2801/5716A and a DT2815 are plugged into the system mother board expansion slots. The real time software modules were checked independently with two separate subroutines for ADC and DAC. The DAC outputs were checked for noise free drive output using an oscilloscope and generating sinusoidal functions. The ADC's were checked for their calibration using $4\frac{1}{2}$ digit digital voltmeter and speed of repsonse using an oscilloscope.

The tunnel control software is written in BASIC and compiled using a BASIC compiler. The object code was then linked to the machine to derive an executable code. The software was mounted on the system with dummy signal inputs of correct range, and the tunnel control software was executed using the execution module after compilation and checked for faults for nearly 5000 hours of operation without stop.

The time of execution for one computational cycle is very important, since the dynamic refreshing of the tunnel control commands must be related to the bandwidth of the tunnel control loop and must satisfy Nyquist sampling criterion. The sampling time aimed at is 100 ms for all the control loops. The IBM PC/AT takes about 102 ms to execute one full cycle of automatic control of all the tunnel control loops, and is near the goal. This speed could be realised only on a system with 12 MHz clock. Initial trials on a 8 MHz clock system gave higher cycle time of nearly 150 milliseconds. The cycle time mildly varies with the modes chosen. On manual mode for the temperature, pressure and Mach number loop the time taken for execution is less than 95 milliseconds. In Auto loop it takes about 102 milliseconds. This variation arises because of the number of statements executed in each cycle varies in each path. The number of paths in the software are many. Operation of the keyboard commands also slows down the execution to a small extent. The following breakup provides typical time for each software function execution, based on a 12 MHz clock.

ADC of seven channels	5 ms
DAC of seven channels	7 ms
Computation of the control laws on AUTO	40 ms
Display writing, executed once in 3 cycles	42 ms
Keyboard mode of inputs	1 ms
Variability by different paths	12 ms
Emergency displays	5 ms

The timing involved in executing the various functions is determined by executing the software 1000 cycles using a counter and measuring the time taken by use of the beep command embedded in the software. This measured average cycle time of about 100 ms has been chosen for DEL to be used in the program so that integral or derivative control laws are in real time.

The tunnel control software modules are in a free running serial mode and no internal clock has been used, since synchronization is not an issue. Variability of a few milliseconds with software taking different paths does not affect the slow dynamics of the tunnel states.

TUNNEL CONTROLLER COMMISSIONING AND TUNNEL PERFORMANCE

The microcomputer based controller has been commissioned and its performance was evaluated by a series of planned tests made during aerodynamic drag polar tests on 2-D supercritical airfoils. The procedure used for initial commissioning and the performance test results are presented below.

The Motorola 6800 microprocessor based pressure-temperature controller and the Intel SBC 80/20 microprocessor based Mach number controller were replaced by the new integrated microcomputer system. Sensor signals from the various signal conditioners connected to the Motorola 6800 system and Intel SBC 80/20 based controllers were connected to the IBM PC/AT controller in parallel. The display of all the tunnel variables on the IBM PC/AT monitor were checked during tunnel operation with old controllers. The LN_2 pump pressure control system was commissioned first. The LN_2 injection valve drive coils were transferred from the Motorola 6800 controller to the new controller and the temperature loop was commissioned next. The pressure control valve drive coils were then transferred over to the new controller, to realize tunnel total pressure control. Finally the rheostat drive signals were transferred from the Intel system to the new controller, thereby transferring total integrated control of the 0.3-m TCT to the new microcomputer based controller. The old systems were disconnected. The new controller was fine tuned to obtain stable and fast control with minimal cross coupling interactions.

Instumentation scheme for tunnel controller performance evaluation:

The closed loop control performance of the 0.3-m TCT was evaluated by studying the tunnel total temperature, total pressure, static pressure and fan speed as functions of time for set point command changes and disturbances. The ability of the controller to hold the conditions under extraneous disturbances or to follow the commands of the controller for various set point changes is evaluated

from these time trajectories. A separate set of tunnel sensors with slower response and higher accuracy are used for aerodynamic data acquisition and for the tunnel controller performance evaluation. They consist of a platinum resistance thermometer located in the settling chamber to measure the tunnel gas temperature, and a pair of capacitance type Barocells for the tunnel test section total and static pressures. The fan speed and the LN_2 pressure sensors are the same as the ones used for tunnel control. The signals are carried to the data acquisition MODCOMP computer through autoranging NEFF amplifiers. MODCOMP software uses the calibration data and generates the output in proper engineering units. The results presented are from this chain of data gathering system of the 0.3-m TCT.

The MODCOMP based data acquisition software package uses time base from drag rake traverse position drive system. The sampling is triggered by the rake position and is not very uniform in time, since the read pulse is derived from the rake drive mechanism which waits for the rake to settle. However, even if the sampling is not uniform in time, as long as the correct time and tunnel variables at the time of sampling are available, the trajectories provide faithful representation of the tunnel state dynamics. All the tunnel time trajectories have been generated using this time base mechanism.

Closed loop regulation of the tunnel states during 2-D model aerodynamic tests:

In all the tests described in the following section, the tunnel controller is in an automatic control mode with loop closures on temperature, pressure, and Mach number. In some cases, the Reynolds number mode has also been invoked. The tunnel controller is globally stable, it can accept large set point commands and hence the tunnel is always on closed loop control.

6.5 Inch Chord HSNLF Model Tests M= 0.200:

First set of results of tunnel automatic control are presented for tests on a 6.5 inch chord airfoil which was tested for Reynolds numbers ranging from 1 to 20 million/chord at various Mach numbers ranging from 0.200 to 0.750. To cover this range, tunnel temperature had to be varied between 100 to 300 K with pressure ranging from 18 to 75 psia.

Figure 25 shows the tunnel condition regulation under closed loop control during a rake traverse. The trajectories are for Mach number, pressure, temperature, fan speed and flow Reynolds number as functions of time or rake position, at M=0.2, P=18 psia, T=102 K and Re=3.95 million/chord. Clearly, the tunnel pressure and temperature are held very tightly, with stability of 0.1 K in temperature and 0.07 psi in pressure during the 100 s of data acquisition. The Mach number time trajectory shows a

peak error ±0.003 and a mean error of about ±0.001. At a flow Mach number of 0.200 the difference between total pressure and static pressure is about 0.48 psia. Even a small error of 0.01 psia in any one of these pressures dynamically, results in a 0.002 Mach number error. Considering this, the Mach number regulation is good.

A statistical analysis of the Mach number plot was made to evaluate the mean and the variance. The mean is precisely on 0.200 and the variance is less than 0.001. The fan speed also shows a variation of about 20 rpm about mean. The Reynolds number plot shows that it has been regulated well. The tunnel has operated at a very low speed of 990 rpm and at this extreme case of low pressure, and low Mach number the controller performance is reasonably good.

Figure 26 shows a control trajectory similar to figure 25 at M=0.200, P=18 psia, and T=125 K at a lower Reynolds number of 3 million/chord. The Mach number time plot shows a peak to peak variation of about ±0.004 maximum. Even here the Mach number regulation in a statistical sense is about ±0.002. The tunnel pressure and temperature are held constant to within 0.2 K and 0.07 psia.

Figure 27 shows same model run at tunnel conditions of M=0.200, P=71 psia, T=199 K and Re=6.00 million/chord. The pressure and temperature have been regulated very well to tight tolerances where as the Mach number shows an oscillation of about 0.004 peak to peak around the mean value of 0.200. This instability could not always be repeated but generally arose at high tunnel pressures and low Mach numbers.

Figure 28 shows same tests made at a very low Reynolds number of 2 million/chord at M=0.200, P=18 psia and T=164 K. The control of all the tunnel states is excellent with Mach stability better than ±0.001, temperature stability is ±0.15 K and pressure to within 0.07 of tunnel set points.

6.5 inch chord HSNLF model tests at M=0.300-0.360 and 0.730:

Figure 29 shows the tunnel condition regulation and the control trajectories of 0.3-m TCT for M=0.302, P=48 psia, T=199 K and Re= 6.00 million/chord. The tunnel condition regulation is acceptable for all the variables. The stability is ±0.1 K in temperature, ±0.05 psia in pressure, ±0.002 in Mach number and Reynolds number is held tightly to within 0.05 million/chord. Mild limit cycle type oscillations can be noted in the Mach number response. The Mach number is well within the accuracy band sought.

Figure 30 shows the control trajectory for the case of M=0.350, P=68 psia,T=229 K and Re=8.00

million/chord. The tunnel regulation of all the states is very good throughout. Regulation accuracy is to 0.1 K in temperature, 0.07 psia in pressure and 0.001 in Mach number of the set point. The control is on Reynolds number mode.

Figure 31 shows the tunnel condition regulation during rake traverse for case at M=0.730, P=17 psia, T=210 K and Re=4 million/chord. The pressure and temperature regulation are to within 0.07 psia and 0.2 K of set value. The Mach number shows a mild scatter of about ± 0.002. At this transonic Mach number of 0.730, the growth of wake is to be expected and is evident in the form of variation in fan speed as the rake approaches the model wake. In this run, the tunnel control is on Reynolds number mode and hence the Reynolds number is very steady.

9 inch chord Canadian CAST 10 model tests:

Three transonic test condition tunnel control trajectories are presented for the 9 inch chord CAST 10 supercritical airfoil. This is huge model relative to the test section of 13 inch^2, since the model also fully spans the test section. In each case the rake traverse in the wake causes considerable disturbance on the tunnel Mach number loop.

Figure 32 shows the tunnel condition regulation during a rake traverse at M=0.762, P=68 psia, T=231 K with Reynolds number at Re=20.00 million/chord. The tunnel regulation is excellent with temperature held to within 0.1 K, pressure to 0.07 psia and Mach number to 0.001 of the set values. The test conditions included nicely streamlined walls at α=1.2°. As the rake moves in the wake of the model, it changes the flow blockage. The Mach number disturbances caused by the rake movement is nicely corrected by the fan speed variation. The fan speed shows a dip very similar to the pressure profile in the wake of the model. This signature of the fan speed is a demonstration of the abilty of the Mach loop to accommodate blockage changes.

Figure 33 shows a similar tunnel condition time plot during a rake traverse at M=0.762, P=68 psia, T=231 K with Reynolds number at 20 million/chord. The angle of attack is α=2 °. The tunnel regulation is good, with temperature held to 0.1 K, Pressure to 0.07 psia and Mach number to 0.002 of the set values. The rake traverse does create a dip in fan speed and show some blockage change, but not of the same magnitude as in figure 32. This is due to fact that the walls have not been streamlined.

Figure 34 shows tunnel conditions during a rake traverse at M=0.780, P=64 psia, T=231 K with Reynolds number at 20 million/chord, α=1.3° and the walls streamlined. The tunnel temperature is

held to within 0.2 K and pressure to 0.1 psia of the set values. The Mach number regulation is very good till the rake starts moving out of the wake. It seems to initiate a major blockage change which transiently upsets the Mach number by about ± 0.003 which quickly settles out. Because of higher inlet Mach number, the magnitude of blockage induced Mach distrubance is higher. The fan speed shows the characteristic wake signature, superimposed by oscillatory corrections for the sharp Mach disturbance.

Tests with French CAST 10 model of 0.18 m chord:

Tests were made with a supercritical airfoil of 0.18 m chord at transonic Mach numbers and the tunnel test section flow parameters were monitored for evaluating the quality of tunnel controller performance. Fan speed was not recorded. In all the cases the walls have been streamlined prior to rake traverse.

Figure 35 shows the tunnel control regulation during a rake traverse at M=0.765, P=51 psia, T=150 K and Reynolds number hold mode set to Re=21.36 million/chord and α=0°. The tunnel condition is stable to 0.1 K, 0.1 psia and 0.002 Mach number around the set point. The rake induced blockage change is countered reasonably well.

Figure 36 shows tunnel control trajectories during rake traverse for same tunnel conditions as in figure 35 except that α=0.25° and walls are streamlined for this angle. The tunnel conditions are regulated to 0.2 K, 0.07 psia and 0.001 Mach number around the set point. Again, the effect of rake traverse on Mach number is corrected for by the controller.

Figure 37 shows tunnel states during a rake traverse for the same conditions as figures 35 and 36, except that α=2°.

Figure 38 is a similar plot of tunnel states during a rake traverse as figure 37. The Reynolds number is reduced to 20 million/chord. In both figures 37 and 38 the regulation is very good.

Figure 39 shows the Mach number has been increased to a higher value of 0.780. During the rake traverse, the rake moves from top of test section to the bottom. As the rake leaves the area behind the normal shock and the wake, it creates a blockage change which mildly upsets the Mach number. It is corrected for by fan speed changes. The regulation of Mach number in this case is only about ± 0.003.

In summary, the plots of the tunnel temperature, pressure and test section Mach number under closed loop control conditions indicate that the new microcomputer based controller is capable of maintaining the conditions accurately to about 0.1 K in temperature, 0.07 psia in pressure and on the average about 0.002 in Mach number around the set values, during aerodynamic data acquisition. The tests have covered a temperature range of 100-300 K, pressure range of 18-80 psia and Mach numbers from 0.200 to 0.800. One important feature to note is that at high entry Mach numbers the rake induced disturbances (as the rake moves down from behind the airfoil upper surface flow field down to airfoil lower surface field) are much larger. It may be necessary to stop the rake movement and wait for the Mach number to settle down before taking data in such cases, if the Mach number control performance is considered unacceptable.

Dynamic performance tests on the 0.3-m TCT microcomputer controller:

The 0.3-m TCT controller is able to regulate the tunnel conditions at desired set point values, as demonstrated in the previous section. To evaluate its dynamic behavior for various set point command changes and associated coupling disturbances it is likely to encounter, a series of tests were made and the results are presented in this section. Figure 40 shows the control scheme and the intrusive disturbances that are inherent during data acquisition. The disturbances to the control system while in stable equilibrium belong to the following category.

1. Single or multiple set point changes of small and large amplitudes.
2. Geometrical disturbances to the test section.
3. Mass enthalpy disturbances.

A set of tunnel runs have been made at a typical operating point of the tunnel, at a Mach number of 0.760, tunnel pressure of 68 psia and temperature of 231 K, with a CAST 10, 9 inch chord supercritical airfoil. Two adaptive wall shapes derived from optimised streamline conditions for α=0° (figure 41) and α=2° (figure 42) have been chosen for all the dynamic performance tests. The tests were made with all loops closed to show the control response including the coupling that exists amongst the three control loops.

Set point changes:

Figure 43 demonstrates the effect of a temperature set point unsymmetic pulse on the tunnel states. The temperature set point is taken from 231 to 227 K and after a time delay of 80 s, back to 233 K. The gas temperature settles to final value in about 15 s to within 0.3 K for steps in both directions.

The change in temperature has no effect on the pressure loop at all, and the pressure is held to within 0.07 psia throughout. The Mach number is well regulated to better than 0.001 of the set value except when the temperature jumps from 227 to 233 K. Even here, the Mach number uncertainty is within 0.002. In the figure 43, a simultaneous rake traverse exists. Despite this geometrical disturbance, the tunnel conditions are held tightly. The cross coupling between loops is insignificant. The fan speed accommodation to hold the Mach number arises from the gas temperature changes. The wake shadow effect occurs exactly when the temperature step occurs. The temperature loop is basically slow and takes 10-15 s for settling. Cooling response is not symmetrical with warmup response indicating the non-linear nature of the control system. The tunnel temperature response is very stable.

Figure 44 demonstrates the effect of pressure set point changes on the tunnel states, during a rake traverse. The pressure set point is stepped from 68 to 64 psia and after a delay of 40 s, it is stepped back to 68 psia. The tunnel pressure response for downward pressure is very quick and is completed in about 2 seconds. No overshoot occurs. The pressure rise from 64 to 68 psia takes about 6 s and is a function of the incoming mass flow. The system behavior is non-linear. Pressure set point change shows a strong coupling on test section Mach number. The Mach number settles down to the set point within 8 seconds. The tunnel temperature is also affected by pressure because of coupling, showing nearly 1 K transient change during pressure change. A mass discharge results in temperature drop. However, it is quickly corrected. This is to be expected because of major enthalpy loss due to discharge of GN_2. This also presents evidence to the effect that the mass enthalpy coupling is an isothermal phenomena. The tunnel temperature settles down to set point within about 8 seconds. The fan speed curve shows the effect of rake movement superimposed by fan speed corrections needed to correct the Mach number fluctuations. Rake blockage effect is visible as a trough in the fan speed plot.

Mach number set point for the tunnel is changed in two steps from 0.700 to 0.730 and 0.730 to 0.760, with a delay of 60 seconds. The response of the tunnel states to this set point disturbance is shown in figure 45. The Mach number faithfully follows the command and settles to the final value within about 6 seconds. The total pressure is unaffected by the Mach steps despite increases in fan speed. The tunnel temperature sees the fan speed increase and the extra energy. The temperature is disturbed by coupling from the Mach number loop. It takes about 6 s to settle after the first step in Mach number. After the second step, it takes a longer period to settle. Temperature error grows to about 0.4 K initially, and converges to zero in time. The fan speed varies automatically to obtain the required Mach number by about 200 rpm for each step. The effect of rake traverse is evident and visible in the fan speed response.

A second Mach number pulse response of the tunnel involving set point change from 0.762 to 0.777 and 0.777 to 0.762 with a time delay of about 70 s between the two is shown in figure 46. The Mach number faithfully follows the Mach step command and settles to the final value in less than 10 seconds. The ability of the controller to command and maintain such small Mach number differences of the order of 0.015 is nicely demonstrated in the figure 46. The Mach number stability is about 0.001 after the transient has died down. The pressure loop maintains the steady pressure without any visible coupling due to change of Mach number. The tunnel temperature loop maintains the temperature well with a small transient of about 0.4 K which dies down well before the Mach number stabilises. The fan speed plot shows variation required to hold the Mach number steady. Superimposed on the fan speed is the signature of rake movement through the wake in the form of a trough, which occurs after the Mach number pulse.

The tunnel controller, while on Reynolds number control mode, automatically changes the pressure set point when Mach number changes. Figure 47 shows the response of the tunnel to a Mach number set point change from 0.760 to 0.730 and from 0.730 to 0.760 with a time dwell of 80 seconds. The tunnel Mach number nicely follows the incremental Mach number change of 0.030 and settles in about 15 seconds. The change of Mach number induces a pressure set point change automatically, and the pressure changes from about 68 to 70 psia. The Reynolds number demand of 20 million/chord is regulated to within 0.03 of the set value. The tunnel temperature is also regulated stably except when Mach number is changing. But the regulation in temperature is within 0.2 K after the transient.

The set of figures 43 to 47 demonstrate the ability of the controller to accept single or multiple set point changes of small magnitude simultaneously. The stability of the all the loops is very good. There are no or minimal overshoots in response of any loop. Coupling does exist between the various loops but, as has been demonstrated, the coupling effects are corrected quickly and have no stability problem inherent in them.

Large amplitude set point changes:

Typically, at the start of 0.3-m TCT operation, the tunnel structure is cooled down from ambient to cryogenic operating temperature under closed loop control conditions. Before the new microcomputer based controller was put into operation, this cooldown was always perfromed manually to keep the structural cooldown rate to less than 10 K/min and the gas-metal temperature difference to less than 50 K. With the new controller, the cooldown functions are entirely under automatic control. The tunnel cooldown or warmup can be looked upon as a large set point control problem. Performance of the 0.3-m TCT and controller for large set point changes during three tunnel tests are now discussed.

Figure 48 illustates the time trajectories of the tunnel conditions during a typical cooldown, aerodynamic data acquistion and the tunnel warmup covering a period of about 2 hours and 15 minutes. At time zero, the tunnel is on closed loop control with pressure set point at 30 psia, Mach number set point at 0.440 and temperature set point to match the ambient value of 300 K. At time 50 s, a temperature set point of 100 K has been commanded. Initially the metal and gas are at same temperature, and hence the tunnel gas starts cooling at a rate of 20 K/min. Since the tunnel structure does not respond at such a high rate, the metal to gas temperature difference grows to about 45 K at a time of 150 seconds. The controller now has slowed down the rate of gas cooling automatically to match the structural cooling rate of about 3.6 K/min. The tunnel gas temperature cools down to 100 K in about 3000 s, and throughout these 50 min the tunnel pressure is kept constant at 30 psia and the Mach number at 0.440 by the controller. The metal temperature slowly follows the gas temperature with a lag. The fan speed has been continually varied by the controller to maintain the Mach number. A single command for temperature set point of 100 K at 50 s has been faithfully executed by the controller and safely cooled the tunnel gas as well as the metal structure to desired temperature. After the temperature has stabilized, a number of large Mach number set point changes, 0.440 to 0.800 at 3700 s, 0.800 to 0.250 at 4100 s, 0.250 to 0.800 at 4300 s, 0.800 to 0.500 at 4500 s, and 0.500 to 0.800 at 5050 s, have been executed by the controller in the tunnel. During periods of Mach number change, the tunnel pressure and temperature have remained constant at their set values. A set of large pressure changes have also been imposed through the controller, with a 30 to 50 psia step at 3900 s, 50 to 75 psia at 4600 s and 75 to 40 psia at 4900 seconds. The rapid drop of pressure at 4900 s has coupled into Mach loop, but is quickly compensated. A temperature step from 100 to 125 K is evident at 5300 seconds. The tunnel metal wall does not reach the gas temperature. This is because the sensor is at the external wall which reaches a final steady state temperature which is higher than the internal gas temperature. A tunnel warmup command is executed at 5400 s while keeping a constant Mach number of 0.600 and 0.700. The tunnel pressure has gradually leaked off. Since no LN_2 injection exists, the pressure loop cannot build the pressure. However, the mass control law can build the pressure by injection of LN_2 by the time the tunnel reaches the final temperature.

Figure 49 illustrates another cooldown of the 0.3-m TCT intended for CAST 10 airfoil data acquisition. This time, the cooldown is under conditions of constant fan speed and has been commanded as a temperature set point change at 50 seconds. The cooldown characteristics are very similar to cooldown at constant Mach number shown in figure 48. During the cooldown the Mach number gradually increases with decreasing gas temperature. Because of the improved heat transfer, the cooldown from 275 to 150 K has been completed in a relatively shorter time of 1200 seconds. The controller is able to maintain the pressure constant at 30 psia, and keep the metal-gas temperature difference to 45 K.

Structural cooldown rate is at an average rate of about 6 K/min. After the final temperature set point has been reached, a Mach number step to 0.765 has been commanded and airfoil tests have been performed. At a time of about 2850 s, the Mach number shows a drop to 0.580 for some checks on the tunnel. The Mach number has been brought up to 0.765 and the tests continued. The tests consist of flexible wall contouring, rake movement and other data acquisition oriented disturbances to the tunnel geometry. The fan speed fluctuations seen in figure 49 are due to tunnel geometrical activity, which has been nicely compensated by the Mach loop which shows a much steadier response. The airfoil tests have been conducted with Reynolds numbers held constant at 20 million/chord at a Mach number of 0.765. At time of 5800 s, the tunnel has been shutdown without a warmup. The tunnel pressure has gradually leaked off in about 15 minutes.

Figure 50 illustrates the purging process and subsequent cooldown of the 0.3-m TCT to evaluate the boundary layer removal compressor system at a low temperature of 100 K. During the purge, the tunnel fan has been runup to 2400 rpm fan speed with the pressure gradually builtup to 30 psia at ambient temperature of 275 K. The pressure buildup has occured from 14.7 to 30 psia in about 50 seconds. At the end of pressure buildup, an equilibrium condition exists where LN_2 injection as well as steady discharge of warm gas occurs simultaneously. This process gradually removes moisture within the tunnel and the boundary layer system which is run at a low idling speed. At about 800 s, the tunnel resident gas is discharged by commanding 16 psia pressure. This process takes away most of the remaining moisture in the system. The figure 50 shows a number of activities from 850 to 2500 seconds involving routine checks on some instrumentation problems while the tunnel is idled at about 1000 rpm fan speed. Before idling pressure was builtup tp 50 psia and dropped twice.

At time of 2500 seconds, the tunnel has been cooled down to 100 K at constant fan speed with a large temperature set point command from 275 to 100 K. The tunnel pressure is kept constant at 30 psia during cooldown. The cooldown is complete by time of 4700 seconds. During boundary-layer system evaluation, the tunnel Mach number is varied from 0.800 down to 0.300 in steps of 0.100. In each dwell of Mach number, the boundary-layer compressor system has been run at varying compressor speeds to vary removed mass flow from 0.5 to 4% of test section flow. The tunnel controller is able to work against the mass disturbances as well as the compressor induced heat disturbances. The tunnel conditions are held steady while the boundary-layer mass flow removal is varied. The start of tunnel warmup is shown from time after 6800 seconds.

The 0.3-m TCT microcomputer based controller is able to accept very large set point commands and execute them safely on the tunnel. This feature has resulted in considerable reduction of the work load on the operator. The nonlinear control laws effectively address the limitations in structural cooling

rate, metal-gas temperature limitations and provide globally stable controls. The large set point changes do cross couple to other loops but are quickly corrected for by the respective loops. The Mach number loop is also very stable due to velocity limits imposed in the control laws. The pressure loop is also very stable globally for large set point commands.

Geometrical disturbances to the tunnel test section:

As indicated in figure 40, tunnel test section geometry is disturbed by flexible adaptive wall, angle of attack, and rake traverse systems. These changes of geometrical shape during tunnel operation constitute a necessary part of aerodynamic data acquisition. They modify the Mach control loop for static as well as dynamic response. In order to evaluate the effects of geometrical changes in the test section on the tunnel control, a set of runs were conducted with the disturbance occurring during data acqusition. The tunnel conditions for these tests were around M=0.765, P=68 psia, T=230.6 K (corresponding to 20 million/chord Reynolds number) with streamlined wall shapes and angles of attack setting.

Figure 51 provides the tunnel responses, while in closed loop control, to geometrical disturbances caused by rake traverse in the model wake. The figure nicely illustrates the fan speed accommodation needed to maintain the test section Mach number during rake traverse. The tunnel Mach number is regulated to better than 0.001 of the set point. The tunnel temperature and pressure are also held stable to within 0.1 K and 0.07 psia of the set values. The fan speed varies by about 20 rpm when the rake enters the wake shdow of the model demonstrating a nice signature of rake movement on speed plot. This signature repeats in all the records discussed in this document because the time ramp for all the plots has been obtained only by a rake traverse. This figure also demonstrates the sensitivity of the Mach control loop for rake induced blockage changes. The Mach number tracking is very good.

Figure 52 provides the tunnel response, while in closed loop control, to blockage changes caused by angle of attack geometrical disturbance. The angle of attack of the large 9 inch chord full span CAST 10 model is changed from α=2° to 0°. The tunnel Mach number is upset immediately during model motion, but it quickly returns to the set value in about 10 s to within 0.001 of the Mach number set point. The tunnel total pressure is not disturbed by the angle of attack change. The tunnel fan speed changes by nearly 160 rpm to accommodate the changed blockage. Because of this quick fan speed change, the tunnel temperature loop shows a coupling from angle of attack change of about 0.6 K which dies out within about 10 seconds. This coupling arises from the fact that temperature control loop is slower than the fan speed loop dynamics. The fan speed shows the signature of rake traverse in the form of a trough in the speed plot.

Figure 53 indicates the tunnel responses while in closed loop control, to disturbances caused by a pulse change in angle of attack, from 0° to 2° and after a wait of about 80 s from 2° to 0°. The tunnel Mach number set at 0.760 shows a change of 0.010 during the period angle of attack induced blockage is varying. Simultaneously, the Mach loop changes the fan speed to bring the Mach number back to set value. The Mach number correction occurs within about 8 seconds. Then the Mach number is stable to 0.001 of the set value. Angle of attack change from 2° to 0° causes a similar response from the tunnel. The tunnel pressure control is totally unaffected by the angle of attack change and stays within 0.07 psia of the set value. The tunnel temperature shows a mild coupling from fan speed which is quickly corrected within 8 seconds. The fan speed curve clearly demonstrates the Mach loop operation to correct the Mach number. Superimposed on the fan speed response is the rake induced signature appearing as a trough.

The next type of geometrical disturbance is the major shape change caused by flex wall adaptive control system. After sensing the wall pressure distribution, the 21 sets of actuators are moved to change the wall geometry to realize zero wall interference. (ref. 10) As indicated in figures 41 and 42, the magnitude of change can be of the order of an inch on each wall just to correct for an angle of attack change of 2°. This is a major geometrical change when compared to the test section size of 13 square inch. In the following tests, the wall shapes are changed between two standard shapes to evaluate their effect on the tunnel control system. Figure 41 refers to zero angle of attack wall adaptation contours at M=0.760, Reynolds number of 20 million/chord at 231 K. Figure 42 refers to wall shape streamlined under same conditions except that α=2°.

Figure 54 shows the tunnel responses, while in closed loop control, to disturbances caused by moving walls from shape 2 to shape 1, and by the rake traverse. The tunnel conditions are M=0.700, P=68 psia, T=231 K, and α=0°. The wall shapes 1 and 2 are from M=0.760 case and not for the present test Mach number of 0.700 and hence the wall shapes are arbitrary. The walls take nearly 120 s to move between the two positions. During this period the Mach number has been held steady to within 0.001 of the set value, despite considerable blockage reduction caused by wall shape change. The shape change can be considered to be equivalent to a ramp input disturbance, except that the static correction is nonlinear. The effect of blockage reduction on the Mach number has been compensated by the fan speed reduction of nearly 110 rpm. The tunnel total pressure has been held steady to within 0.07 psia and the temperature to within 0.2 K of the set values. The fan speed shows the rake signature on the speed. The tunnel controller is able to counter the geometrical changes caused by wall movement effectively.

Figure 55 shows the tunnel responses, while under full closed loop control by the microcomputer, to geometrical disturbances caused by moving walls from shape 1 to shape 2 and by rake traverse. In this case the tunnel conditions are same as the case presented in figure 54, except that α=2°. Again, the Mach number is held steady to within 0.001 of the set value over the period of 120 s during which time test section blockage increases. The increase in blockage results in fan speed increase of about 100 rpm. The rake signature on the fan speed is evident here also as the rake passes through the wake of the model. The tunnel pressure and temperature are held tightly during this wall shape change induced disturbance.

Figure 56 shows the tunnel responses, while in closed loop control, to geometrical disturbances caused by adaptive wall movement from shape 2 to shape 1. The wall shapes are optimised for the tunnel conditions of M=0.760, P=68 psia, T=231 K, and α=0°. The walls take about 120 s to move and represent a streamlining reduction of blockage. The Mach number is held steady to within 0.002 or better of the set value throughout the wall movement period. The fan speed decreases by nearly 200 rpm, to accommodate the decreasing blockage, to maintain the Mach number. This fan speed change is larger than the cases discussed in figures 54 and 55 because the wall shapes are fully optimised for least wall interference for the tunnel conditions. The rake signature is visible in the fan speed plot. The tunnel temperature and pressure are held well within the required 0.2 K and 0.1 psia of the set value.

Figure 57 provides the tunnel responses, while under closed loop control of the microcomputer, to geometrical disturbances caused by the wall shape being changed from shape 1 to shape 2 and by the rake traverse. Again the walls take nearly 120 s to move fully. The tunnel Mach number has been regulated at a steady value of 0.760 within $\pm$0.001, except for about 10 s when the excursion is about 0.003. In this case, the blockage is increasing due to the fact that α=0° the wall shapes are for α=2°. This increase in blockage demands an increase in fan speed to maintain the Mach number. Nearly 200 rpm increase is necessary to account for increased blockage. The fan speed plot shows the rake signature while it is passing in the wake of the CAST 10 model.

The effect of movement of the walls from shape 1 to 2 is not necessarily linear with time on the tunnel Mach number. This is evident from the fan speed-time plots in figures 51 to 54, all of which show non-linear behavior in speed as a function of time. This is possibly due to the complex manner in which stepper motor commanded wall movement translate to area and Mach number changes.

Disturbances caused by mass enthaply changes:

The 0.3-m TCT has an auxiliary system to treat the boundary layer by removing mass from the walls of the tunnel test section. The thermodynamic effects of this boundary layer treatment on the tunnel control system has been exhaustively discussed in reference 15. Presently, the 0.3-m TCT has two modes of boundary layer treatment possible. (ref. 7) They are,

1. Passive discharge of test section mass flow out of the tunnel up to nearly one percent of the test section mass flow at high tunnel pressure.
2. Removal, compression, cooling and reinjection of the test section mass flow up to nearly 8% of the test section mass flow.

In the first case, instead of removing mass out of the settling chamber for tunnel pressure control, it is removed from test section through the passive boundary layer treatment valves. This imposes no extra control problems as long as mass flow removed is less than the injected mass flow. In the second case, extra mass enthalpy are added to the tunnel in the form of compressor heat and LN_2 injection to cool this extra compressor induced heat. If the temperature control in this circuit is good there is no control burden at all on the tunnel control system. Imperfections in this control as well as surge conditions in the compressor recirculation mode can result in mass-enthalpy loads on the tunnel control. The new control laws can adequately accommodate these disturbances.

Preliminary commissioning tests on the boundary layer treatment system both active and passive shows that the new microcomputer controller is least affected by this system. In the passive mode the only limitation is that the test section mass flow magnitude removed cannot exceed the tunnel injected LN_2 mass flow. The effect of boundary layer control system on the tunnel control since the effects were insignificant and no dynamic problems were encountered as illustrated in figure 50.

Summary of tunnel control performance with the integrated microcomputer controller:

The closed loop control of the 0.3-m TCT using the microcomputer based integrated tunnel controller is globally stable and provides excellent control of all the tunnel variables. The performance for small perturbation disturbances can be summarised as follows. When large enthalpy and energy disturbances are involved, these numbers are not valid till system converges near final point to within about 3 K in temperature, 4 psia in pressure and 0.03 in Mach number.

Tunnel Mach number mode:

Stability in Mach number during rake traverse	±0.001 rms (variance)
	±0.002 peak to peak
Stability in Mach number during angle of attack and wall induced disturbances	±0.0015 rms (variance)
	±0.003 peak to peak
Response time of Mach number for small step inputs and disturbances	5 - 10 s
Mach number change during pressure step	±0.010 peak
Mach number change during small temperature set point changes	±0.003 rms

Tunnel temperature mode:

Temperature stability during steady state operation	±0.1 K
Temperature stability during sharp pressure step	±1.0 K
Temperature stability during fan speed/Mach number step	±0.3 K
Temperature stability due to wall changes	±0.2 K
Temperature stability due to angle of attack step	±0.3 K
Response time of temperature for small step	10-15 s

Tunnel Pressure mode:

Pressure stability during steady state	±0.07 psia
Pressure stability during wall movement	±0.07 psia
Pressure stability during angle of attack step	±0.07 psia
Pressure response time for step input	2 s down, 6 s up
Pressure stability during temperature step	±0.12 psia
Pressure stability during Mach number step	±0.10 psia

Tunnel Reynolds number mode:

Reynolds number stability with no disturbances	±0.03 million
Reynolds number during Mach number step change	±0.06 million

OPERATION OF THE MICROCOMPUTER BASED 0.3-m TCT CONTROLLER

The IBM PC/AT tunnel controller has a Phoenix BIOS and is setup so the DOS is resident in hard disk C. The AUTOEXEC.BAT file (an DOS file) starts the system on disk C. For tunnel control

operation in a dedicated mode, the BASIC compiler, Linker, the BASIC libraries are loaded in to hard disk C. The tunnel controller software is compiled and linked to obtain the executable element on disk C. The AUTOEXEC.BAT file is setup so that every time the system is powered up, the microcomputer starts up, transfers to C disk, loads and executes the tunnel control program automatically. The execution of the tunnel control program cannot be stopped by any commands from the keyboard. It can be terminated only by power stoppage. For tunnel control program modifications, the system has to be booted with DOS software diskette in disk A.

Once the microcomputer is powered, the tunnel control program starts executing and the monitor screen displays the tunnel status. Figure 58 shows a view of the monitor display format. Forty four display blocks are identified on the screen which provide tunnel information to the operator. These are detailed in Appendix C. Figure 59 shows a typical tunnel operational display.

The 0.3-m TCT requires a number of auxiliary systems to be working before the tunnel can operate. These include air supply for the pneumatic control vlaves, lubrication system for the fan bearing, LN_2 supply pump motor, hydraulic supply for gas discharge valves, cooling water system for oil systems, and the variable frequency generator auxiliary systems. The microcomputer based system does not control these auxiliary systems directly but can function logically for all states of the auxiliry systems. Interlockes to protect these systems exist outside of the tunnel microcomputer.

If the microcomputer controller is powered up without the auxiliary systems being on, the controller sees an emergency situation. It commands closure of LN_2 injection vlave, opening of discharge valve and zero set point to fan speed. These are executed only when the relevent auxiliary systems are on. The tunnel control can start only after the auxilairy systems are functioning normally and all the sensors are in normal range.

Normal tunnel startup proceeds with the LN_2 pump system operation takes the LN_2 pressure to 160 psia with the bypass on (shown in figure 21). The tunnel LN_2 pressure controller sees a high pressure, and since the set point is 11 psia (for fan off conditions), the back pressure valve is commanded full open to relieve the pressure. No control occurs because of the bypass.

The tunnel controller is next taken to Auto loop on temperature with a set point corresponding to ambient. The temperature loop does not function until the fan speed is brought up to a minimum of 600 rpm, as commanded by the software. The pressure set point is set to about 30 psia. At the start, the tunnel pressure is atmospheric, and hence the gas discharge valves close fully as commanded by control law. The tunnel fan system is started with a manual set point of 2400 rpm for the motor.

After the variable frequency generator drives the fan motor to its low end of about 600 rpm the tunnel controller takes over. When the fan speed of 600 rpm is reached, the LN_2 pump pressure set point shifts to 132 psia and closed loop control begins. The fan speed also enables the temperature loop and tunnel cooling starts with LN_2 injection cancelling the fan heat. Temperature is maintained at ambient by the controller, once the fan speed stabilises. The tunnel pressure slowly builds to about 30 psia by evaporation of injected LN_2. Once the tunnel pressure is built up to the set point, gas discharge starts and the pressure is regulated at the set value. A steady LN_2 input and gas discharge output from the 0.3-m TCT slowly dilutes and removes the moisture in the tunnel over a period of about 5 minutes.

After this purging process is complete, desired set points for the final tunnel test conditions are keyed in through the keyboard. All commands are safe and the system reaches the final desired point using the simple trajectory control law in the software in due course of time.

0.3-m TCT simulator:

To familiarise the tunnel operators with the microcomputer based tunnel controller, a simulator has been built around the IBM PC/AT. This simulator has the exact same tunnel display and keyboard controls as the tunnel controller. The dynamics of the tunnel has been mathematically represented as a module of software. This software takes about 15 ms to execute and it has been added to the main tunnel control software with minor modifications in respect of analog/digital and digital/analog conversion. Appendix D details the precise model used with its discrete version for numerical simulation. The realism of simulation is good from the point of operator control commands. It is reasonable in terms of the tunnel static and dynamical behavior. To cooldown the metal shell this simulator takes about 25 min which is comparable with the actual tunnel cooldown rate.

CONCLUSIONS

This paper gives details of the successful development and operation of a microcomputer based controller for the 0.3-m TCT. The controller is capable of integrated closed loop control of all the tunnel flow variables or flow parameters.

New nonlinear global tunnel control laws for pressure, temperature, Mach number and Reynolds number have been generated using some previous results, long operating experience and new analysis. The new laws overcome safety concerns in respect of metal thermal management. They automatically generate tunnel trajectories in P-T plane for fast set point changes. They provide much tighter tunnel

control thereby improving the quality of data and increasing the efficiency of operation.

Feasibility of using commercial standard microcomputer systems for control has been demonstrated by choice of a reliable and flexible microcomputer system capable of real time communication to and from analog systems, with its own flexible operating system. Emphasis has been on exclusion of custom built electronic hardware. This is a highly versatile and reliable low cost solution to the problem.

Software has been generated to realise the control laws in real time. These laws are in the well understood BASIC language and hence is very transparent for modifications. Despite the use of this language, the speed of control computation for all the control laws burden, multicolored complex display and the operator interface is accommodated in 100 ms. The operator interface with tunnel operation is at a supervisory level and is through a simple and functional display on the monitor. The keyboard commands are safe and reject inadvertent and wrong commands. The software performs in an endless loop for all conceivable data inputs and keyboard commands.

The tunnel microcomputer based controller has been successfully commissioned and operated in an aerodynamic data generation mode for more than 150 hours on three 2-D airfoils at Mach numbers ranging from 0.2 to 0.780 and Reynolds numbers from 1 to 20 million/chord. The tunnel controller performance yields stability in temperature to 0.2 K, pressure to 0.07 psia and Mach number to 0.002 around the set point. These conditions are held for normal operating disturbances. Even in the case of intrusive data acquisition from geometrical distrubances, like rake traverse, angle of attack change, and flexible wall contour change the tunnel regulation is very good. The tunnel settles to a final Mach number and pressure set points within 20 to 30 s for most cases. Temperature takes a longer time depending upon the amplitude of command.

Though the tunnel process dynamics is multivariable and strongly coupled, for small perturbation around an equilibrium point, the closed loop responses show very little interaction between the variables. The dynamic response under closed loop control shows no inherent instabilities. The microcomputer based controller integrates all the tunnel control functions and safely controls all the tunnel states automatically. The number of operators for 0.3-m TCT control operation has come down from the previous two intensely active operators to one supervisor.

In summary a low cost, high performance, commercial microcomputer is able to control a nonlinear multivariable process in the 0.3-m TCT operation efficiently. This system has been demonstrated to save operating time and improve the efficiency of operation. The aerodynamic data quality and reliability have been improved considerably by tight control of tunnel conditions.

APPENDIX A

DYNAMICS OF LN_2 INJECTION VALVE

Introduction:

The 0.3-m TCT requires a maximum LN_2 inflow of about 8 kg/s at an operating pressure of 6 atm, temperature of 105 K and Mach number 0.900 based on 2000 KW fan heat dissipation. The minimum flow of less than 0.04 kg/s required is at a low Mach number of 0.3, a tunnel pressure of 1.2 atm and a temperature of 300 K or above. The automatic temperature control laws for the tunnel demand fine control of LN_2 flow in to the tunnel at various operating conditions. The choice of a mass flow control valve for the 0.3-m TCT was initially a digital control valve. The digital valve had 10 elements providing a rangeability of 1 in 1024. The digital valve provided excellent calibration of the LN_2 mass flow into the tunnel under static usage. A set of valves were procured in 1976 and the tunnel ran in manual control with excellent results.

After the tunnel went on microprocessor based closed loop control in 1979, the controller commanded the digital valves at a rate of 10 Hz. This high speed switching was necessary in closed loop operation because of stability and accuracy requirements. In about 30 hours of operation, the valve small elements were exposed to millions of cycles resulting in damage to various gasket elements. This deteriorated the valves considerably resulting in poor control. Studies were made to find a sturdy LN_2 injection valve with good response, repeatability, rangeability and ruggedness in operation. Diaphragm operated pneumatic control valve driven by an electropneumatic controller is considered to be an ideal choice for LN_2 injection. In the following section, the performance tests on an electropneumatically signalled LN_2 injection valve is detailed.

Valve performance tests:

A standard 300 psia air to open diaphragm operated globe valve has been converted to electro-pneumatic operation. The pneumatic diaphragm actuator is driven by a Moore electropneumatic flapper nozzle type transducer. The flapper nozzle is moved by an electrical signal to provide 3-15 psig proportional signal corresponding to 4-20 mA electrical input. The 3-15 psig pneumatic signal is power amplified through a pneumatic booster to actuate the diaphragm chamber. The purpose of the test is to evaluate the performance of electrical signal to valve position transfer function for static and dynamic commands.

A schematic diagram for performance tests on the LN_2 valve is shown in figure 60. The Moore amplifier/electropneumatic transducer is excited by a signal generator capable of DC to 10 Hz excitation current of 4-20 mA on the coil. The valve position is sensed by an infinite resolution potentiometer excited from a DC source and the wiper provides the accurate position of the valve. The position pot and valve position alignment/calibration were conducted first. The Moore electropneumatic transducer is supplied from a 100 psig air pressure source through a pressure reducer set to 30 psig. The 100 psig source also feeds the booster driving the diaphragm under control of electropneumatic transducer.

Frequency reponse tests were conducted first. The electropneumatic coil was excited at frequencies varying from 0.1 Hz to 8 Hz in about 12 steps. The amplitudes of excitation were varied from 6%, 14%, 16%, 25%, 34% and 90%. Mean position of 50% datum was held all through the tests. The input output wave forms were recorded on the galvonometric recorder. In order to establish transport delay characteristics step response tests were also conducted. The amplitude responses were normalized to 0.1 Hz response to serve as the base. The phase shifts were determined by normalising the wave peak to peak as 360° and evaluating the phase lag by the shift in the response on the galvonometric records. The galvonometers had very high frequency response of the order of 400 Hz. The recorded data was analysed to obtain the Bode plots. The transport delay was estimated by using the paper speed as a reference and determining the delay in the response of the stem pot during step input.

Classical Bode plots for the various input/output frequencies are shown in figure 8 in respsect of responses for amplitudes upto 25% peak to peak. Higher input amplitude modeling was not made because the math model sought was intended for small perturbation response only. Figure 8 shows the system response is amplitude dependent and hence nonlinear. There is also evidence of transport delay of the order of 0.1 s or higher. The Bode plot data was fitted for a transport lag τ and a first order time lag t_1. Also the frequency response data was fitted for a second order dynamics with damping and natural frequency adjustments for best fit. The fitting was based on postulating the model and comparing the errors in the fit to both the amplitude and phase. The single best fit for a linear description of all the responses upto 25% peak to peak turns out to be the transport lag and a first order time lag

$$\frac{\text{valve position}}{\text{position command}} = \frac{e^{-\tau S}}{1 + t_1 S} = \frac{e^{-0.115\,S}}{1 + 0.201\,S}$$

This corresponds to a first order time lag of 0.201 s and a transport lag of 0.115 s. The transport lag predictions from frequency response tests were confirmed by the step response study. A typical step reponse for full command is shown in figure 9. The step response indicates a transport delay of 0.100 s.

The model description varies as a function of the input amplitude and some typical fits are as follows. For peak to peak amplitude 6% command, the model is

$$\frac{\text{valve position}}{\text{position command}} = \frac{e^{-0.106\ S}}{1 + 0.36\ S}$$

Tests were also performed for larger inputs of 90% peak to peak and a model was fitted. This is not a representative case for small perturbation modeling required for stability analysis. For peak to peak amplitude of 90%, the model is

$$\frac{\text{valve position}}{\text{position command}} = \frac{e^{-0.124\ S}}{1 + 0.206\ S}$$

Results of static position response tests are shown in figure 10. For input current signals varying from 4-20 mA the stem steady state response position are recorded and shown as input/output response plots. The plot indicates a mildly non-linear response with about 5 to 10% nonlinearity as well as hysteresis of about 1 to 2%. Hysteresis tests were conducted by recoding response for ascending and descending commands. The repeatability was found to be less than 1%.

Summary:

Electropneumatically actuated globe valve have a good response and repeatability for use as a LN_2 injection valve in cryogenic tunnels. The response has a time constant of about 0.200 s and a transport lag of 0.115 s for small perturbation commands. This performance is adequate for use in the 0.3-m TCT as a primary actuator.

APPENDIX B

FLOWCHART FOR 0.3-m TCT CONTROL

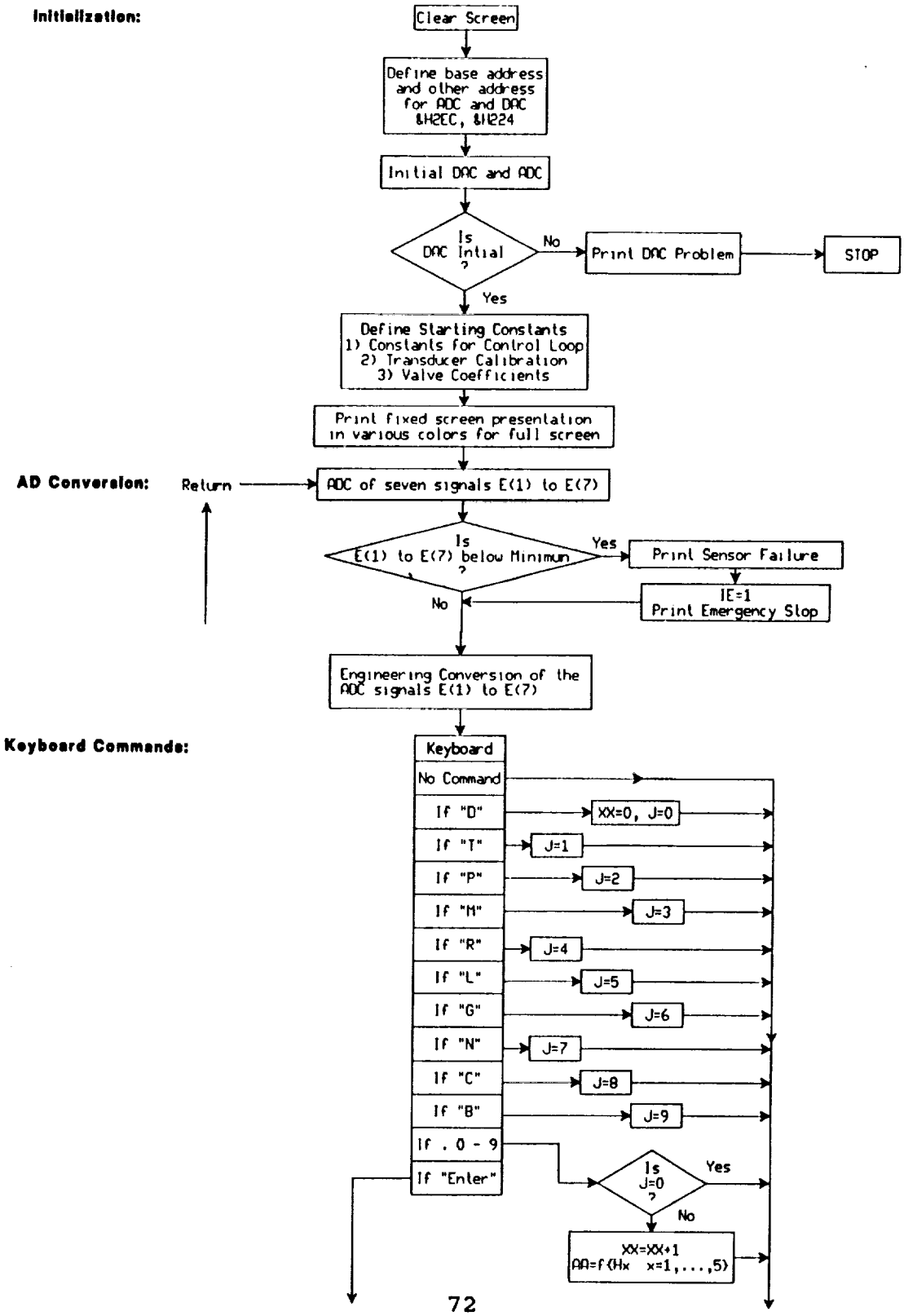

ORIGINAL PAGE IS
OF POOR QUALITY

Parameter Estimation and Set Point Supervision:

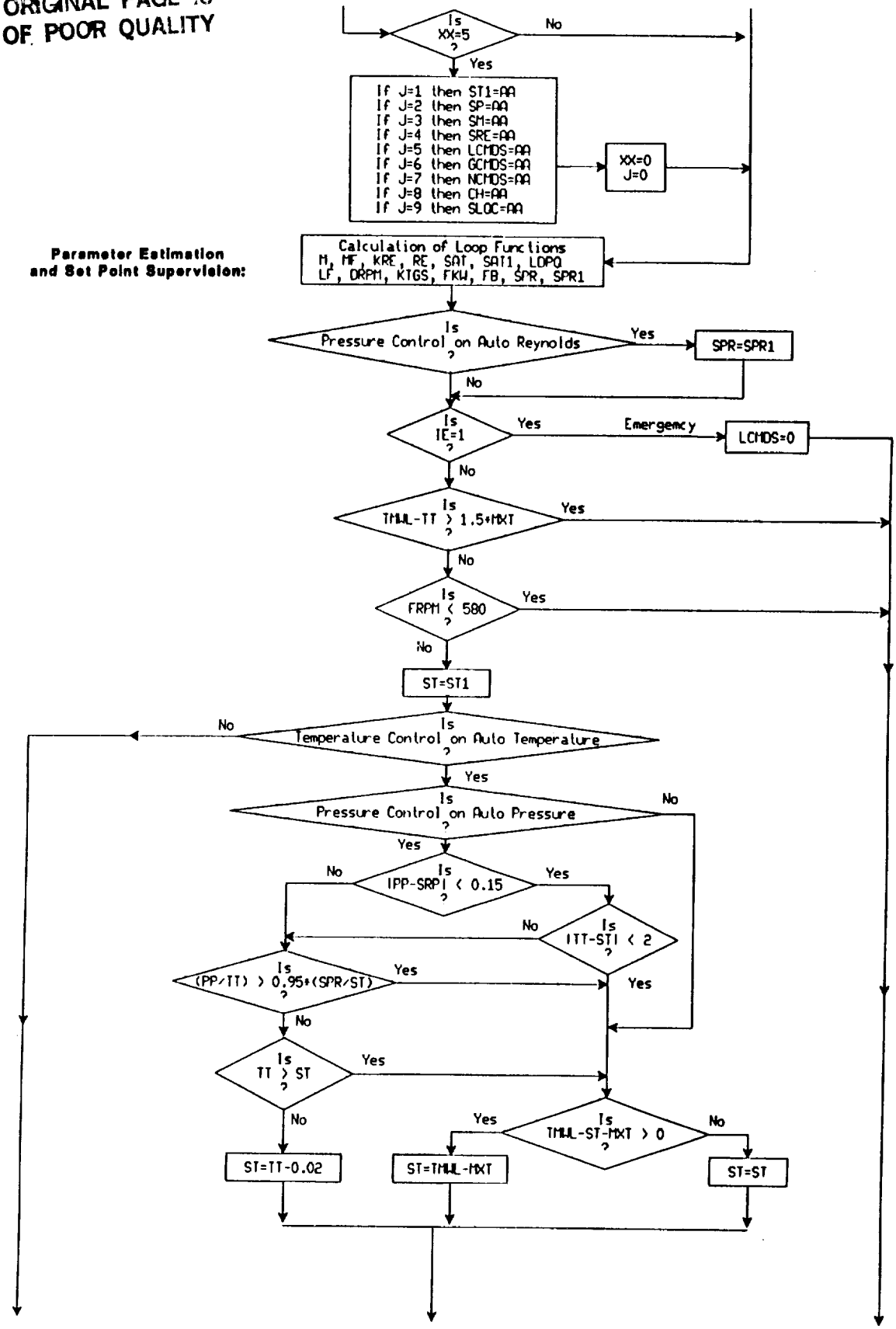

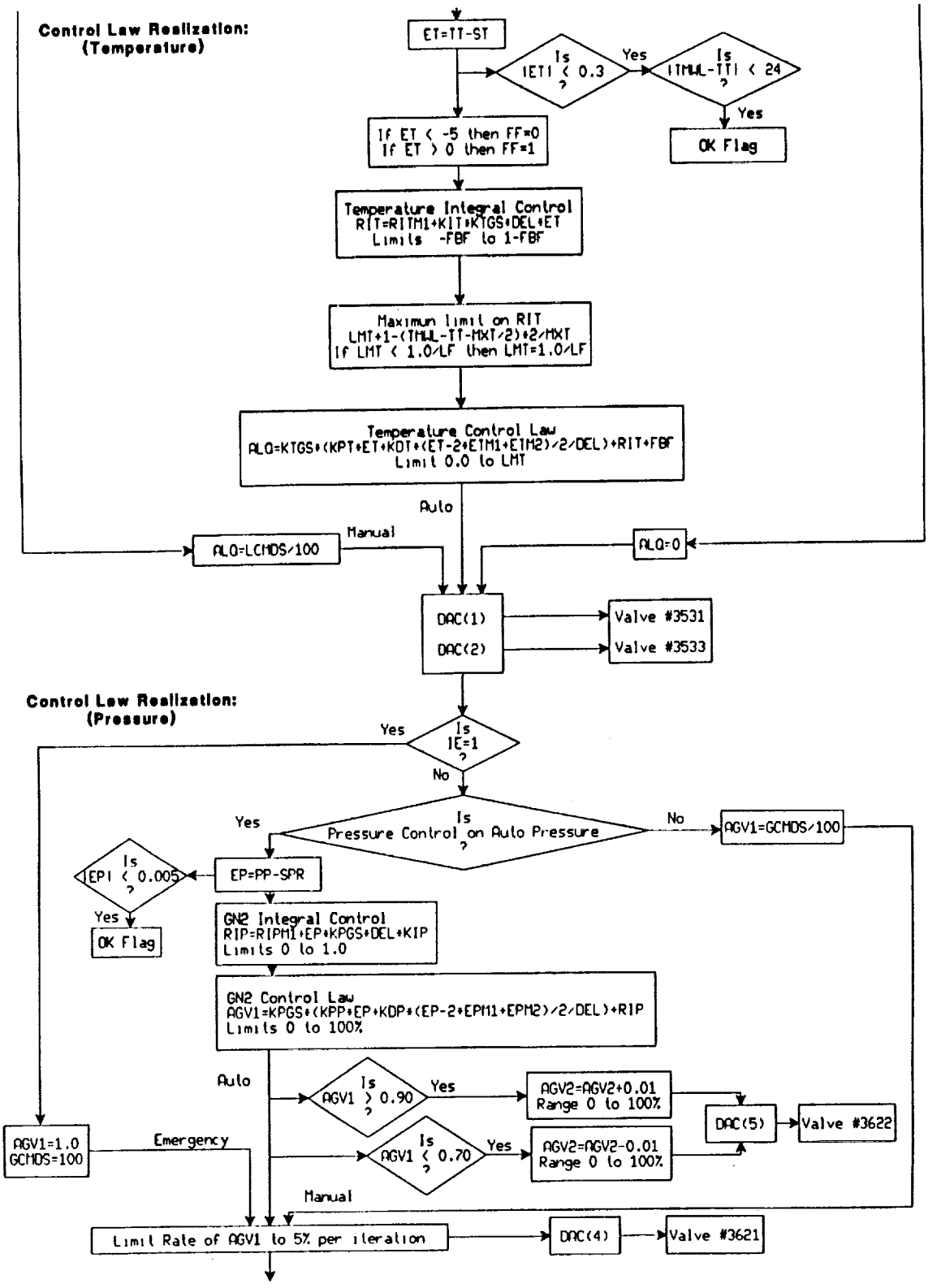
Control Law Realization:
(Temperature)
ET=TT-ST
Is |ET| < 0.3 ?
Yes
Is |TMWL-TT| < 24 ?
Yes
OK Flag
If ET < -5 then FF=0
If ET > 0 then FF=1
Temperature Integral Control
RIT=RITM1+KIT*KTGS*DEL*ET
Limits -FBF to 1-FBF
Maximun limit on RIT
LMT=1-(TMWL-TT-MXT/2)*2/MXT
If LMT < 1.0/LF then LMT=1.0/LF
Temperature Control Law
ALQ=KTGS*(KPT*ET+KDT*(ET-2*ETM1+ETM2)/2/DEL)+RIT+FBF
Limit 0.0 to LMT
Auto
Manual
ALQ=LCMDS/100
ALQ=0
DAC(1)
DAC(2)
Valve #3531
Valve #3533
Control Law Realization:
(Pressure)
Yes
Is IE=1 ?
No
Yes
Is Pressure Control on Auto Pressure ?
No
AGV1=GCMDS/100
Is |EP| < 0.005 ?
EP=PP-SPR
Yes
OK Flag
GN2 Integral Control
RIP=RIPM1+EP*KPGS*DEL*KIP
Limits 0 to 1.0
GN2 Control Law
AGV1=KPGS*(KPP*EP+KDP*(EP-2*EPM1+EPM2)/2/DEL)+RIP
Limits 0 to 100%
Auto
Is AGV1 > 0.90 ?
Yes
AGV2=AGV2+0.01
Range 0 to 100%
DAC(5)
Valve #3622
AGV1=1.0
GCMDS=100
Emergency
Is AGV1 < 0.70 ?
Yes
AGV2=AGV2-0.01
Range 0 to 100%
Manual
Limit Rate of AGV1 to 5% per iteration
DAC(4)
Valve #3621

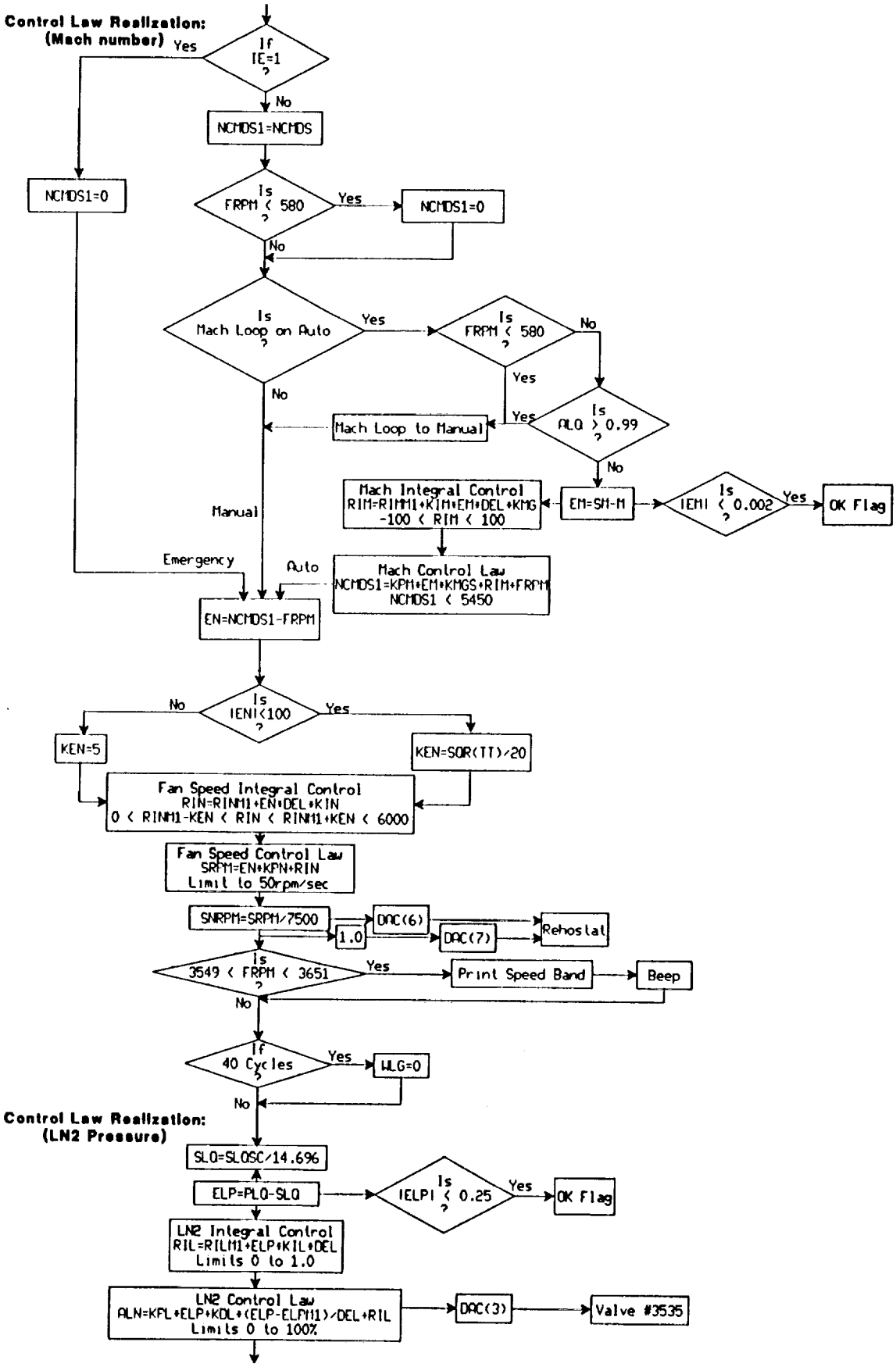
Control Law Realization:
(Mach number)
Yes
If IE=1 ?
No
NCMDS1=NCMDS
NCMDS1=0
Is FRPM < 580 ?
Yes
NCMDS1=0
No
Is Mach Loop on Auto ?
Yes
Is FRPM < 580 ?
No
Yes
No
Yes
Is ALQ > 0.99 ?
Mach Loop to Manual
No
Mach Integral Control
RIM=RIMM1+KIM+EM+DEL+KMG
-100 < RIM < 100
EM=SM-M
Is IEMI < 0.002 ?
Yes
OK Flag
Manual
Emergency
Auto
Mach Control Law
NCMDS1=KPM+EM+KMGS+RIM+FRPM
NCMDS1 < 5450
EN=NCMDS1-FRPM
No
Is IENI<100 ?
Yes
KEN=5
KEN=SQR(TT)/20
Fan Speed Integral Control
RIN=RINM1+EN+DEL+KIN
0 < RINM1-KEN < RIN < RINM1+KEN < 6000
Fan Speed Control Law
SRPM=EN+KPN+RIN
Limit to 50rpm/sec
SNRPM=SRPM/7500
1.0
DAC(6)
DAC(7)
Rehostat
Is 3549 < FRPM < 3651 ?
Yes
Print Speed Band
Beep
No
If 40 Cycles ?
Yes
WLG=0
No
Control Law Realization:
(LN2 Pressure)
SLQ=SLQSC/14.6%
ELP=PLQ-SLQ
Is IELPI < 0.25 ?
Yes
OK Flag
LN2 Integral Control
RIL=RILM1+ELP+KIL+DEL
Limits 0 to 1.0
LN2 Control Law
ALN=KPL+ELP+KDL+(ELP-ELPM1)/DEL+RIL
Limits 0 to 100%
DAC(3)
Valve #3535

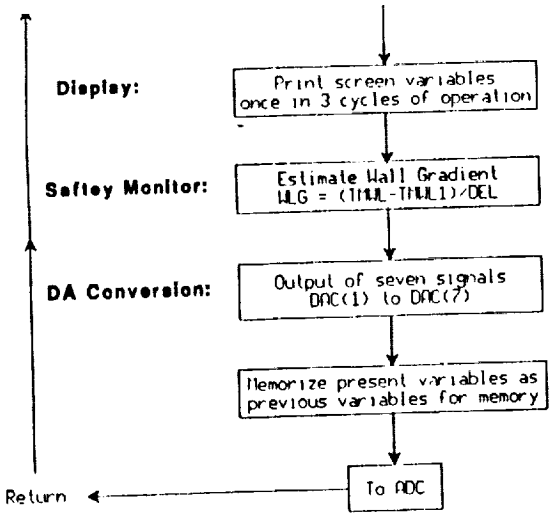

APPENDIX C

DETAILS OF THE MONITOR DISPLAY FOR TUNNEL CONTROL (Figure 58)

W1 Displays the status of LN_2 control as "AUTO". It cannot be changed. The LN_2 control is always on automatic mode.

W2 Displays the status of temperature control loop. Three modes are possible.
"AUTO" in yellow for temperature control operation using temperature set point.
"MANUAL" in yellow for LN_2 injection valve area control.
"MANUAL" in red for emergency command.

W3 Displays status of pressure control loop. Four modes are possible.
"AUTOP" in yellow for pressure control operation using pressure set point.
"AUTORE" in yellow for pressure control with Reynolds number generated pressure set point.
"MANUAL" in yellow for GN_2 discharge valve area control.
"MANUAL" in red for emergency command of 100% for GN_2 discharge valve position.

W4 Displays status of fan speed control. Three modes are possible.
"AUTO" in yellow for fan speed control operation using Mach number set point.
"MANUAL" in yellow for fan speed control using fan speed set point.
"MANUAL" in red for emergency command of zero fan speed.

W5 Displays the LN_2 pressure control set point. Set to 11 psia for fan speed below 580 rpm.
Switches to 132 psia for fan speed $\geq$ 580 rpm.
Is loaded from the keyboard by letter command "B". Updated only on a new set point command.

W6 Displays the tunnel temperature control set point.
Is loaded from the keyboard by letter command "T". Updated only on a new command.

W7 Displays the tunnel temperature set point actually used as estimated by control law based on gas-metal temperature difference, set point magnitude and direction, tunnel trajectory direction (like in zone 4). Updated every 0.3seconds.

W8 Display of the tunnel pressure set point as desired by operator in "AUTOP" mode.
Is loaded from the keyboard by letter command "P". Updated on a new set point command.

Also displays pressure set point as estimated by Reynolds number when in "AUTORE" mode. Updated every 0.3 seconds.

W9 Displays Reynolds number set point desired by operator.
Is loaded from the keyboard by letter command "R". Updated on a new set point command.

W10 Displays Mach number set point as desired by operator.
Is loaded from the keyboard by letter command "M". Updated on a new set point command.

W11 Displays fan speed set point as desired by operator.
Is loaded from the keyboard by letter command "N". Updated on a new set point command.

W12 Displays the true LN_2 supply pressure measured by the transducer. Updated every 0.3 seconds.

W13 Displays the true gas temperature in the tunnel settling chamber. Updated every 0.3 seconds.

W14 Displays the true metal temperature on the tunnel aluminum shell at the third corner.
Updated every 0.3 seconds.

W15 Displays the tunnel total pressure measured in the tunnel settling chamber.
Updated every 0.3 seconds.

W16 Displays the tunnel flow Reynolds number based on the chord.
If chord data is not given Reynolds number is based on default value of a chord of 0.1800 m.
Updated every 0.3 seconds.

W17 Displays the true flow Mach number in the test section using the difference between measured total and static pressures. For no flow conditions, the estimate is clipped to be > 0.001 to avoid arithmetic problems in program. Updated every 0.3 seconds.

W18 Displays the true measured fan speed in rpm from the sensor. Updated every 0.3 seconds.

W19 Displays the command to LN_2 back pressure valve generated by the LN_2 pressure control law.
Display is in percent for 4-20 mA current drive. Updated every 0.3 seconds.

W20 Displays the command to the LN_2 injection valves in percent. This correponds to 4-20 mA signal

going to the coils. In "AUTO" mode the command is from the temperature control law. In "MANUAL" the command is from position command, limited by metal-gas temperature difference.

W21 Displays the command to gas discharge electrohydraulic valve 1.
In "AUTO" mode the drive is derived from the pressure control law.
In "MANUAL" mode the driver is derived from the area control command.
Display of 0-100% corresponds to 1-5 VDC set point commands to electrohydraulic valve 1.

W22 Display corresponds to gas discharge electrohydraulic valve 2 in "AUTO" mode.
Display of 0-100% corresponds to 1-5 VDC set point command to electrohydraulic valve 2.

W23 Displays the fan speed rheostat position command in percent.
This is the set point to the position servo driving the field coil of the variable frequency generator.
0-100% corresponds to 0-5 VDC to position servo set point.

W24 Display area normally blank. When the fan speed is in the range of 3550-3650 rpm, the display shows "SPEED BAND" to alert the operator about the singularity of the speed control system.

W25 Letter "B" enables this display with flashing ",psia". Numeric inputs from the operator in the format ###.#, forms the LN_2 pressure set point and is displayed as loaded. Return command transfers the set point to the LN_2 control loop and clears the display.
"D" command clears the display without transferring it to control.

W26 Letter "T" enables this display with flashing ",K". Numeric inputs from operator in the format ###.#, forms the temperature set point and is displayed as loaded. Return command transfers the set point to temperature control loop, transfers the control to AUTO and clears the display.
"D" command clears the display without transferring it to control.

W27 Letter "L" enables this display with flashing ",% opn". Numeric inputs from the operator in the format ##.##, forms the LN_2 valve area set point and is displayed as loaded. Return command transfers the set point to the controller, transfers the control to MANUAL and clears the display.
"D" command clears the display without transferring it to control.

W28 Letter "P" enables this display with flashing ",psia". Numeric inputss from the operator in the format ##.##, forms the tunnel pressure set point and is displayed as loaded. Return command

transfers the tunnel pressure set point to the controller, transfers the control to AUTOP and clears the display. "D" command clears the display without transferring it to control.

W29 Letter "R" enables this display with flashing ",miln/chrd". Numeric inputs from the operator in the format ##.##, forms the Reynolds number set point and is displayed as loaded. Return command transfers the Reynolds number set point to the controller, takes the control to "AUTORE" and clears the display. "D" command clears the display without transferring it to control.

W30 Letter "G" enables this display with a flashing "% opn". Numeric inputs from the operator in the format ##.##, forms the discharge valve 1 position set point and is displayed as loaded. Return command transfers theset point to the controller, transfers control to "MANUAL" and clears the display. "D" command clears the display without transferring it to control.

W31Letter "C" enables this display with a flashing ",m". Numeric inputss from the operator in the format .####, forms the model aerodynamic chord for Reynolds number estimation, and is displayed as loaded. Return transfers this chord to Reynolds number estimation and clears the display. "D" command clears the display without transferring it to control.

W32 Letter "M" enables this display with a flashing ",Mach". Numeric commands from the operator in the format #.###, forms the Mach number set point and is displayed as loaded. Return command transfers the Mach number set point to the controller, transfers control to "AUTO" and clears the display. "D" command clears the display without transferring it to control.

W33 Letter "N" enables this display with a flashing ",rpm". Numeric inputs from the operator in the format ####., forms the fan speed set point and is displayed as loaded. Return command transfers the fan speed set point to the controller, transfers control to "MANUAL" and clears the display. "D" command clears the display without transferring it to control.

W34 Metal temperature time gradient as a cooling or a warm up rate in K/min is diplayed in this block. This display is updated every 4 seconds since this time is required to average the gradient.

W35 This displays the saturation temperature of tunnel test section gas, based on the tunnel static pressure. Updated every 0.3 seconds.

W36 This displays the mean aerodynamic chord used for Reynolds number estimation. The chord of the model can be loaded though "C" command. Default chord is displayed in white whereas the chosen chord length is shown in yellow. Updated on a new command.

W37 This displays measured tunnel test section static pressure. Updated every 0.3 seconds.

W38 The measured pressure drop across the screen in the settling chamber is shown in this display area. The actual pressure drop is compared with an ideal pressure drop. If the actual pressure indicates on set of icing, this display starts flashing.

W39 This display is normally blank. When the sensors go out of meaningful signal range, this display shows "SENSOR FAILURE" in red. This clears by itself once the signals are normal.

W40 This display is normally blank. When the tunnel is on an emergency shutdown, this displays "EMERGENCY SHUTDOWN". This can be cleared by "D" command or new set point commands, when the emergency condition no longer exists.

Flag1 On when the absolute value of LN_2 pressure loop error is less than 0.25 atm. Updated every 0.3 seconds.

Flag 2 On when the absolute value of the tunnel temperature loop error is less than 0.2 K. Updated every 0.3 seconds.

Flag 3 On when the absolute value of the pressure loop error is less than 0.006 atm. Updated every 0.3 seconds.

Flag 4 On when the absolute value of Mach number loop error is less than 0.002. Updated every 0.3 seconds.

APPENDIX D

REAL TIME SIMULATION OF 0.3-m TCT

Introduction:

The 0.3-m TCT is a high Reynolds number wind tunnel facility which is run at different Reynolds numbers, Mach numbers and dynamic pressures. The tunnel is a closed circuit fan driven tunnel capable of 6 atm of tunnel shell pressure, 78 to 340 K temperature and flow up to Mach 1. The control of these flow parameters Reynolds number, dynamic pressure and Mach number is realised by closed loop control of tunnel total pressure, tunnel temperature and fan speed. Though closed loop operation allows hands off operation, it is necessary for the tunnel operators to be familiar with the tunnel flow-variable dynamics for various actuator inputs. The tunnel gas temperature is usually controlled by fan speed induced heating or LN_2 mass flow induced cooling. The tunnel pressure is controlled by mass increase due to evaporated LN_2 mass flow and tunnel mass depletion caused by GN_2 discharge from the tunnel. The tunnel test section Mach number is controlled by the fan speed variation and incidental pressure ratio change.

The tunnel control laws are realised on a PC/AT computer and the software is able to update the tunnel control commands ten times a second for all the control loops. A need has been felt to mount a simple tunnel simulation package on the PC controller so that new tunnel operators can be trained to understand the basic dynamics of the tunnel. This presentation is concerned with development of a very simple tunnel dynamics simulator, which takes less than about 5-10 ms on a PC/AT computer.

Tunnel dynamical equations:

Consider a closed circuit cryogenic tunnel wherein the tunnel gas is derived from LN_2 evaporated in the tunnel, and whose temperature and pressure are controlled by injection of controlled LN_2 stream in to the tunnel and by dischargeing excessive gaseous nitrogen out of the tunnel. In such a tunnel the heat sources are the work done by the fan to circulate the tunnel mass flow at various Mach numbers and the metal wall heat release. The following equations provide the basic equations which detail the dynamics of the tunnel variables.

$$\frac{dT}{dt} = \frac{1}{W_G C_v}\left\{\dot{m}_L(h_L - C_vT)\, e^{-\tau_L S} - \dot{m}_G(C_p - C_v)\, e^{-\tau_G S}T + \dot{Q}_F\, e^{-\tau_F S} - \int \dot{Q}_m\right\}$$

$\tau_L = 0.8t_c \qquad \tau_G = 0.2t_c \qquad \tau_F = 0.8t_c$

t_c = circuit time and S = Laplace operator

$$\int_{\text{surface}} \dot{Q}_m = \frac{W_t C_m T\, S}{1 + t_m S} = (T - T_m)\, y$$

y= heat transfer coefficient

$$T_m = \frac{T}{1 + t_m S}$$

$$\frac{dP}{dt} = \frac{P}{T}\frac{dT}{dt} + \frac{P}{W_G}(\dot{m}_L - \dot{m}_G)$$

$$M\sqrt{T} = \frac{N\, e^{-\tau_G S}}{K_m(1 + t_p S)}$$

$$\frac{N}{N_{set}} = \frac{1}{1 + 0.56S + 0.2S^2}$$

$$\dot{m}_L = 0.8676 C_{Lqv}\sqrt{(P_{Lq} - P)}\; A_L$$

A_L = normalized valve area, full open=1.0

C_{Lqv} is the valve coefficient for LN_2 valve

$$\dot{m}_G = 2.725 C_{gv}\frac{P}{\sqrt{T}}\, A_{Gv1}$$

A_{Gv} = normalized valve area, full open=1.0

C_{gv} = valve coefficient for gas discharge valve

$W_G = 4375\,\frac{P}{T}$ (for 14.1 m^3 volume of the tunnel)

$W_t = 3200$ (mass of Al-6061 exposed to tunnel flow)

$C_m = 5.5\ T - 0.008\ T^2$ (specific heat of Al-6061)

Real gas properties of GN_2:

$C_p = 1.04$

$C_v = 0.751$

Heat transfer integrated over 60 m^2 internal surface area in the tunnel

$$t_m = \frac{948}{T^{0.12}\ (P\ M)^{0.8}}$$ (metal time constant of heat release)

Fan characteristics

$k_m = 521$

$$t_c = 6.08\ \frac{(1+0.2M^2)^3}{M\sqrt{T}}$$ (circuit time around the tunnel)

$h_L = -121.0$

$$\dot{Q}_F = \frac{K_f\ P\ M^3\sqrt{T}}{(1 + 0.2\ M^2)^3}$$

Real time simulation:

Using these basic equations for the dynamics of the tunnel a simple simulation version has been made. The simulation really consists of solving the above differential equations in real time for the various inputs, namely the LN_2 flow control valve area, the LN_2 pressure, the gaseous discharge valve area, and the fan rpm. For real time continuous inputs, the aim is to determine the tunnel states namely the tunnel total pressure, the tunnel total temperature, and the test section Mach number. The various equations are integrated to arrive at the tunnel dynamics. However, in view of the very tight time requirements, the approach of transforming the continuous system in to a discrete system in the form of difference equations has been used. Amongst many transformations available, Tustin transformation has been used to convert the differential equations in to difference equations involving use of previous few cycles of memory. Following equations provide the transformed versions. The Tustin

transformation provides Lapalce operator S to be replaced by a difference Z term as follows

$$S = \frac{2}{\Delta T}\,\frac{Z - 1}{Z + 1}$$

or

$$Z^{-1} = \frac{1 - \frac{S\tau}{2}}{1 + \frac{S\tau}{2}}$$

The differential equations can be transformed into their Laplace equivalents and the resultant continuous versions can be transformed in to difference equations with sampling interval Δ. In the following number 'n' coming after the variables correspond to data value $n\Delta$ seconds prior to current value. Subscript 'new' refers to the estimated new value of the tunnel state concerned after Δ seconds. It is also assumed that Δ, the sampling rate is much smaller than the highest modality of the tunnel dynamics.

$$\dot{Q}_m = [T - T_m]\,\frac{W_t C_m}{t_m}$$

$$\dot{Q} = \dot{Q}_m + \dot{Q}_F + \dot{m}_L(h_L - C_v T) - \dot{m}_G(C_p - C_v)T$$

$$T_{m\ new} = \frac{\Delta}{2t_m + \Delta}(T + T1) + \frac{2t_m - \Delta}{2t_m + \Delta}\,T_m$$

$$N_{new} = \frac{1}{\Delta^2 + 1.12\Delta + 0.8}[\Delta^2\{N_S + 2N_S1 + N_S2\} - N\{2\Delta^2 - 1.6\} - N1\{\Delta^2 - 1.12\,\Delta + 0.8\}]$$

$$\delta P = \frac{P}{T}\,\frac{\dot{Q}}{W_G C_v}\,\Delta + \frac{P}{W_G}(\dot{m}_L - \dot{m}_G)\Delta$$

$$P_{new} = P + \delta P$$

$$\delta T = \frac{\dot{Q}}{W_G C_v}\,\Delta$$

$$T_{new} = T + \delta T$$

These equations have been mechanised into the IBM PC/AT controller version to provide real time simulation of the tunnel with the new controller configuration.

APPENDIX E

LIST OF SENSORS, RANGES AND THEIR NAMES

Sensors

Variable	Channel	Units	Sensitivity	Transducer
PP	E(1)	0-88 psia	0-5 VDC	Barocell
PS	E(2)	0-88 psia	0-5 VDC	Barocell
TT	E(3)	78-342 K	0-5 VDC	Thermocouple
TMWL	E(4)	78-342 K	0-5 VDC	Thermocouple
FRPM	E(5)	0-6400 rpm	0-5 VDC	Tacho
PLQ	E(6)	0-200 psia	0-5 VDC	Transducer
DLP	E(7)	0-5 psid	0-5 VDC	Barocell

Electrical outputs from the controller:

Channel	Variable	Output	Type	Actuator
DAC(1)	ALQ	4-20 mA	position drive	valve #3531
DAC(2)	ALQ	4-20 mA	position drive	valve #3533
DAC(3)	ALN	4-20 mA	position drive	valve #3535
DAC(4)	AGV1	1-5 VDC	position drive	valve #3621
DAC(5)	AGV2	1-5 VDC	position drive	valve #3622
DAC(6)	SNRPM	0-5 VDC	fan drive command	Rheost servo
DAC(7)	IQ	5 VDC	fan drive reference	Rheost Ref(100%)

APPENDIX F

INPUT KEYBOARD COMMANDS

B,b Input LN_2 back pressure set point. LN_2 back pressure set point format is ###.#, range is LN_2 pressure to 150 psia.

C,c Input mean aerodynamic chord. Chord format is .####, range is 0.01 to 0.4 m.

D,d Delete the previous input keys memorized on screen and not yet executed.

G,g Input GN_2 discharge valve area. Takes the pressure controller and Reynolds number controller to manual control mode. GN_2 valve area format is ##.##, range is 99.99%=full open to 0%=closed.

L,l Input LN_2 valve area. Takes the temperature controller to manual mode. LN_2 valve area format is ##.##, range is 99.99%=full open to 0%=closed.

M,m Input Mach number set point. Takes fan speed to automatic Mach number control mode. Mach number set point format is #.###, range is 0.150 to 0.995.

N,n Input fan speed set point. Takes the fan speed to manual Mach number control mode. Fan speed set point format is ####., range is 0 to 5600 rpm.

P,p Input pressure set point. Takes the controller to automatic pressure control mode and manual Reynolds number control mode. Pressure set point format is ##.##, range is 14.7 to 88 psia.

R,r Input Reynolds number set point. Takes the pressure control to automatic Reynolds number control mode by generating the required pressure set point. Reynolds number set point format is ##.##, range is 1 to 50 million/chord.

T,t Input temperature set point. Takes the controller to automatic temperature control mode. Temperature set point format is ###.#, range is saturation temperature to 340 K.

REFERENCES

1. Kilgore, R. A. : Design Features and Operational Charecteristics of the Langley 0.3-meter Transonic Cryogenic Tunnel. NASA TN D-8304, 1976.

2. Balakrishna, S.; and Thibodeaux, J. J. : Modeling and Control of a LN_2-GN_2 Operated Closed Circuit Cryogenic Wind Tunnel. Proceedings of the First International Symposium on Cryogenic Wind Tunnels. Paper #23. Southampton University, England, 3-5 April 1979.

3. Balakrishna, S. : Synthesis of a Control Model fo a Liquid Nitrogen Cooled, Closed Circuit, Cryogenic Nitrogen Wind Tunnel and its Validation. NASA CR-162508, Febuary 1980.

4. Balakrishna, S. : Automatic Control of a Liquid Nitrogen Cooled, Closed-Circuit, Cryogenic Pressure Tunnel, NASA CR-162636, March 1980.

5. Thibodeaux, J. J.; and Balakrishna, S. : Development and Validation of a Hybrid -Computer Simulator for a Transonic Cryogenic Wind Tunnel, NASA TP-1695, September 1980.

6. Ladson, Charles S.; and Ray, Edward J. : Evolution, Calibration and Operational Characteristics of the Two-Dimensional Test Section of the Langley 0.3-Meter Transonic Cryogenic Tunnel, NASA TP-2749, September 1987.

7. Johnson, Charles B.; Murthy, A. V.; and Ray, Edward. J. : A description of the Active and Passive Side-Wall-Boundary-Layer Removal Systems for the 0.3-Meter Transonic Cryogenic Tunnel, NASA TM-87764, November 1986.

8. Palancz, B. : Analysis of the Performance of a Liquid Nitrogen Cooled, Closed Circuit, Cryogenic Nitrogen Wind Tunnel and its application to the DFVLR's 3 M -Tunnel in Cologne - Part Two Dynamical performance. DFVLR Interner Bericht, WKT 9/80.

9. Steinhauser, R. : Design of a Control System for a Cryogenic Wind Tunnel Optimising a Vector Performance Index. DFVLR-FB-85-37, Febuary 1986.

10. Wolf, Stephen W. D. : The Design and Operational Development of Self-Streamlining Two-Dimensional Flexible Walled Test Sections, NASA CR-172328, March 1984.

11. Balakrishna, S : Modeling and Control of Transonic Cryogenic Wind Tunnels - A Summary Report, NASA CR-159376, October 1980.

12. Chapin, W. G. : Evaluation of a Quartz Bourdon Pressure Gage for Wind Tunnel Mach Number Control System Application, NASA TM-88991, July 1986.

13. Balakrishna, S. : Minimum Energy Test Direction Design in the Control of Cryogenic Wind Tunnels, NASA CR-163244, June 1980.

14. Jacobsen, Richard T. : The Thermodynamic Properties of Nitrogen from 65 K to 2000 K with Pressures to 10000 Atmospheres; Ph.D Thesis submitted to Washington State University, 1972.

15. Balakrishna, S. : Effects of Boundary Layer Treatment on Cryogenic Wind Tunnel Controls, NASA CR-159372, August 1980.

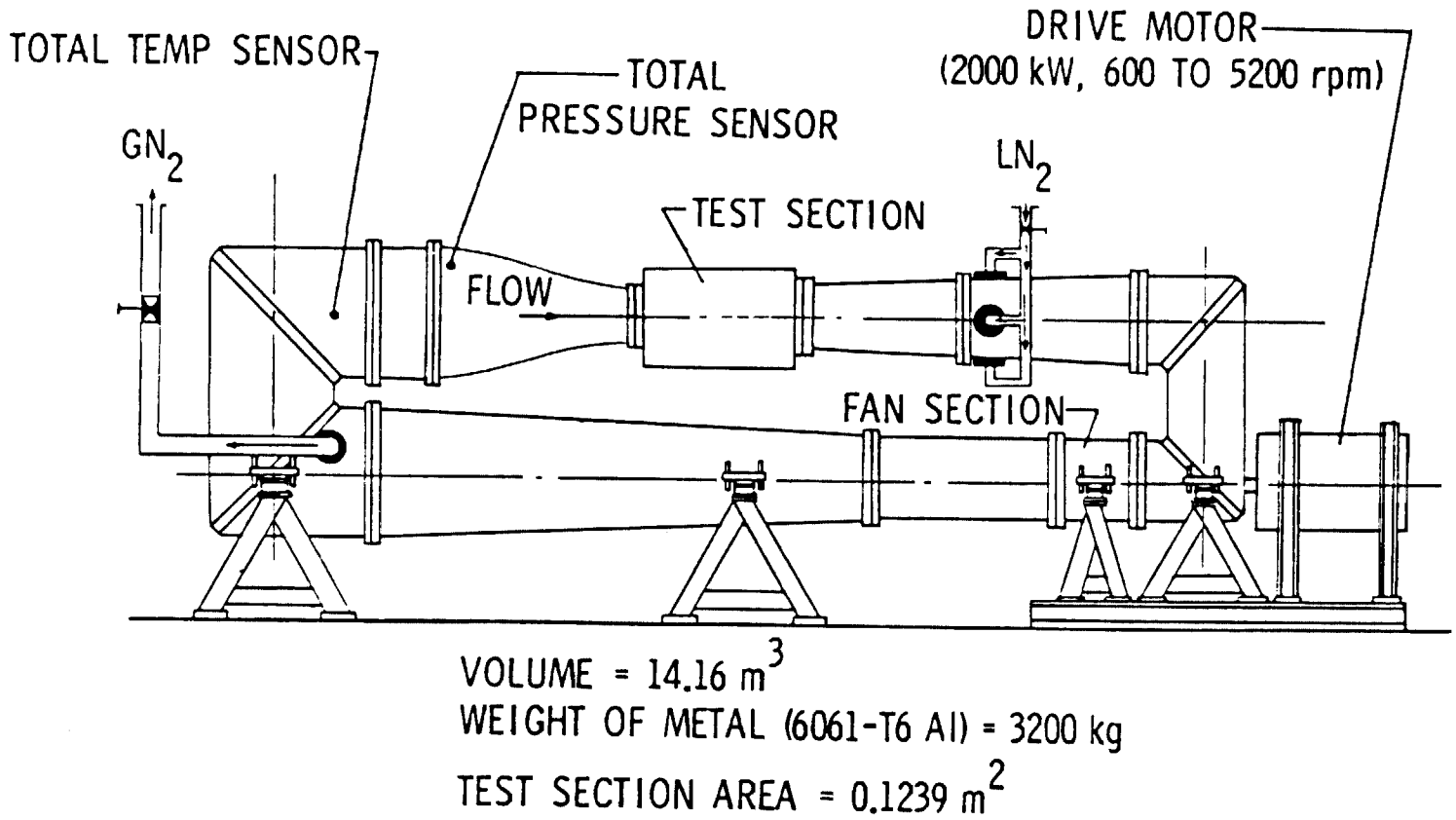

Figure 1 – Schematic of Langley 0.3-Meter Transonic Cryogenic Tunnel

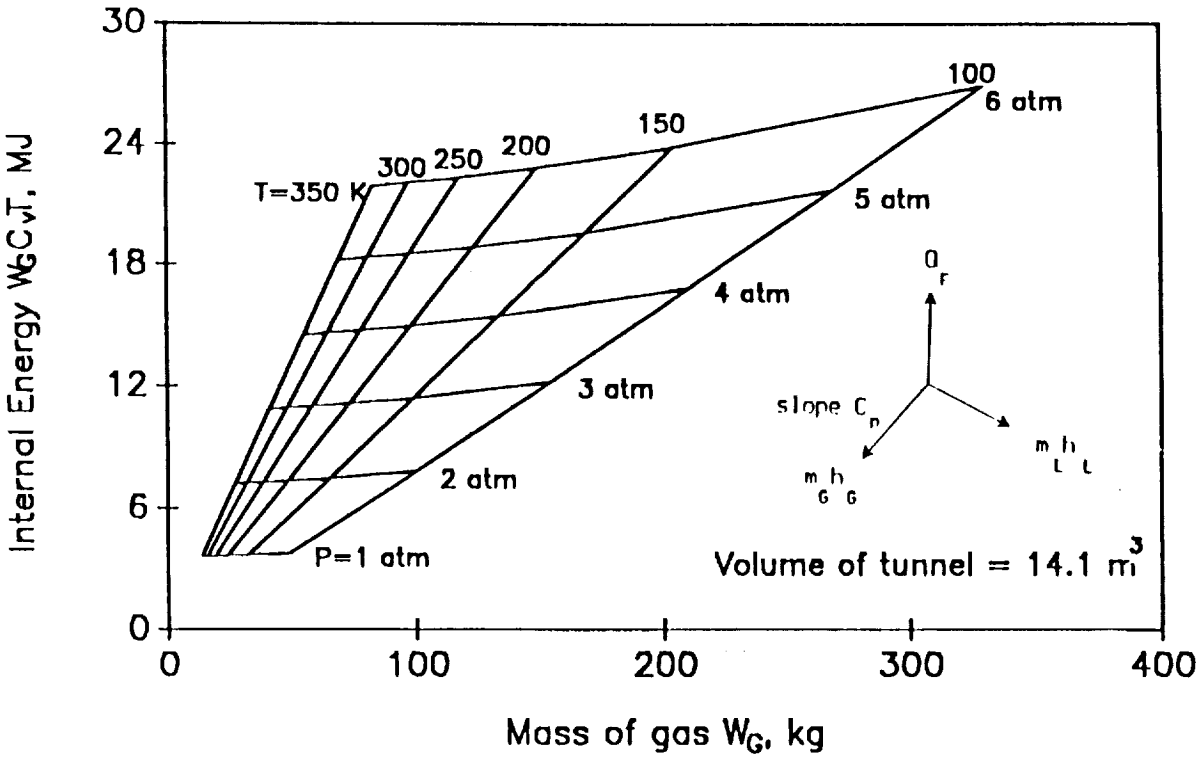

Figure 2.– 0.3–m TCT energy state diagram, ideal internal insulation.

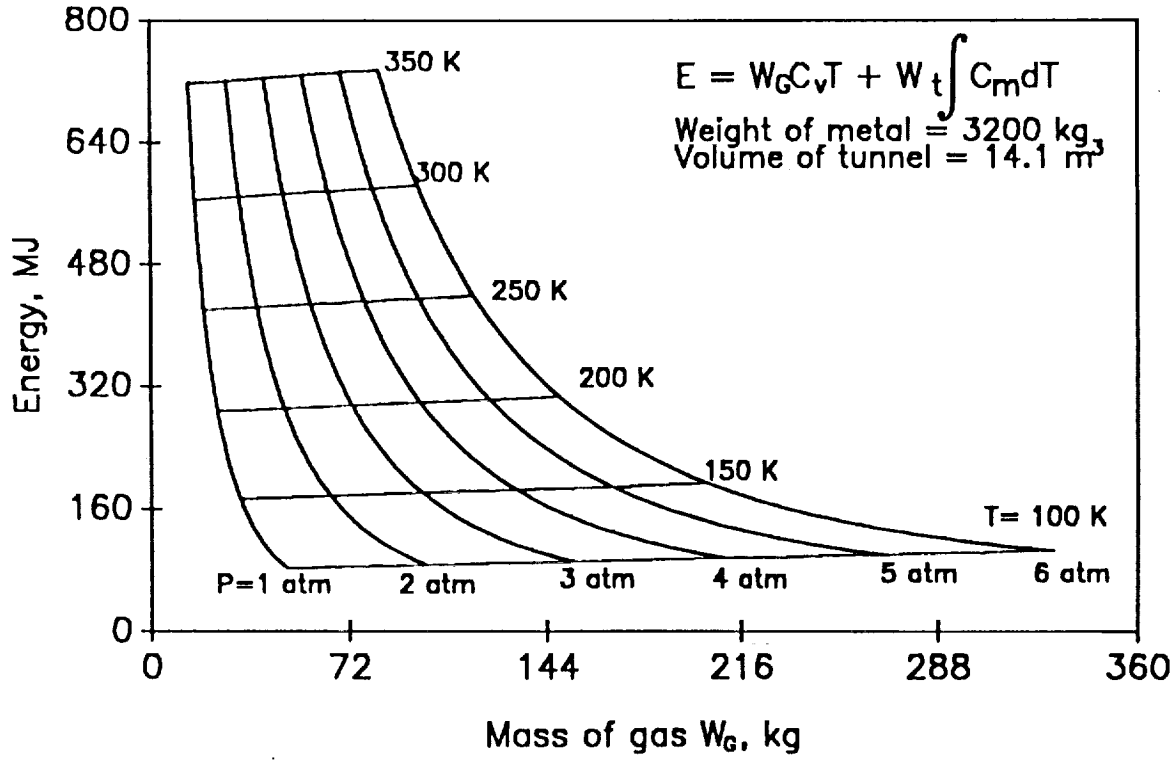

Figure 3.– 0.3–m TCT energy state diagram, ideal external insulation.

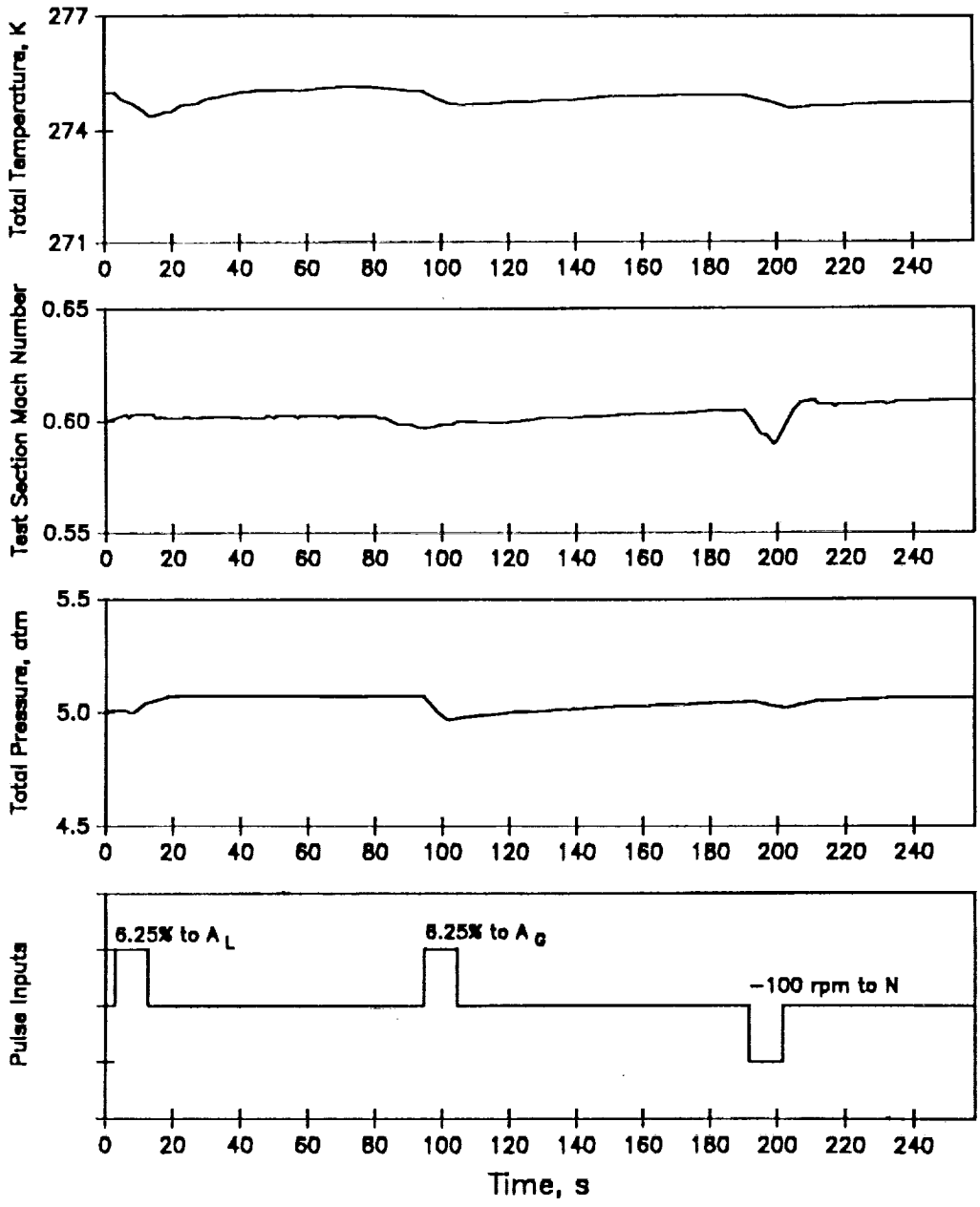

Figure 4.– 0.3–m TCT open loop response to pulsed inputs under equilibrium.

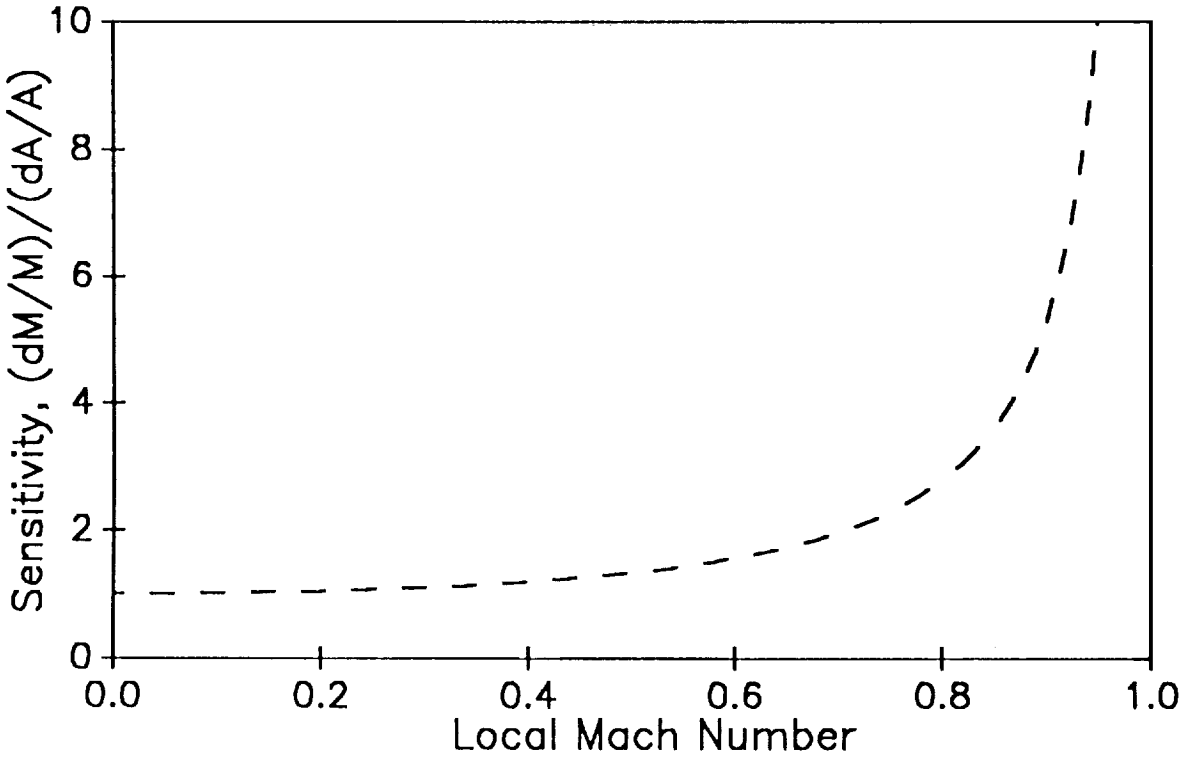

Figure 5.– Sensitivity of test section area change.
(one dimensional analysis)

A_t = Test section area
A = Local cross sectional area
M = Local one dimensional flow Mach number

$$\frac{dA}{A} = -\frac{dM}{M}(1 - M^2)$$

M_∞ = Entry Mach number

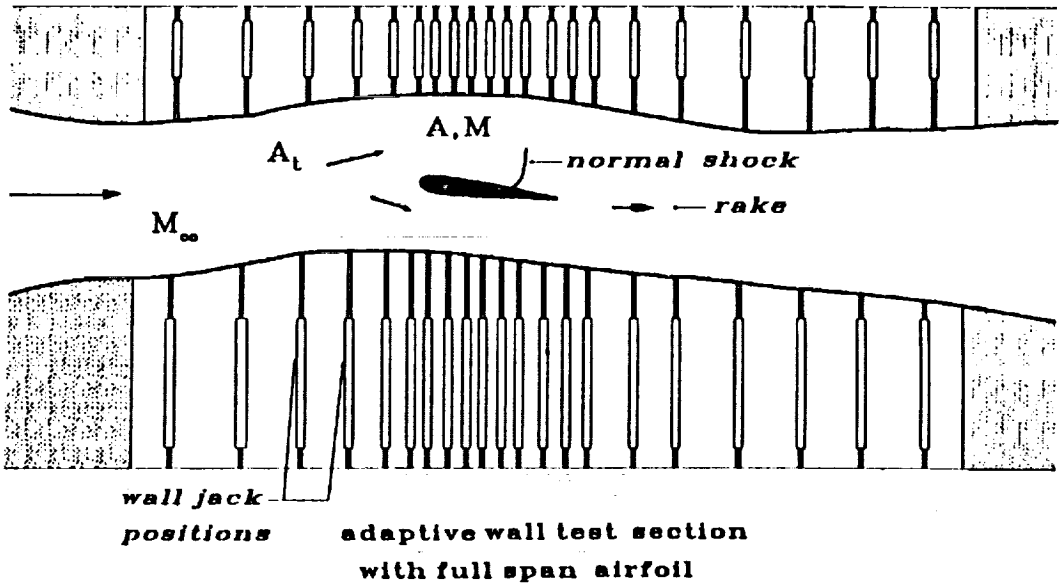

Figure 6.- Test section one dimensional flow approximation.

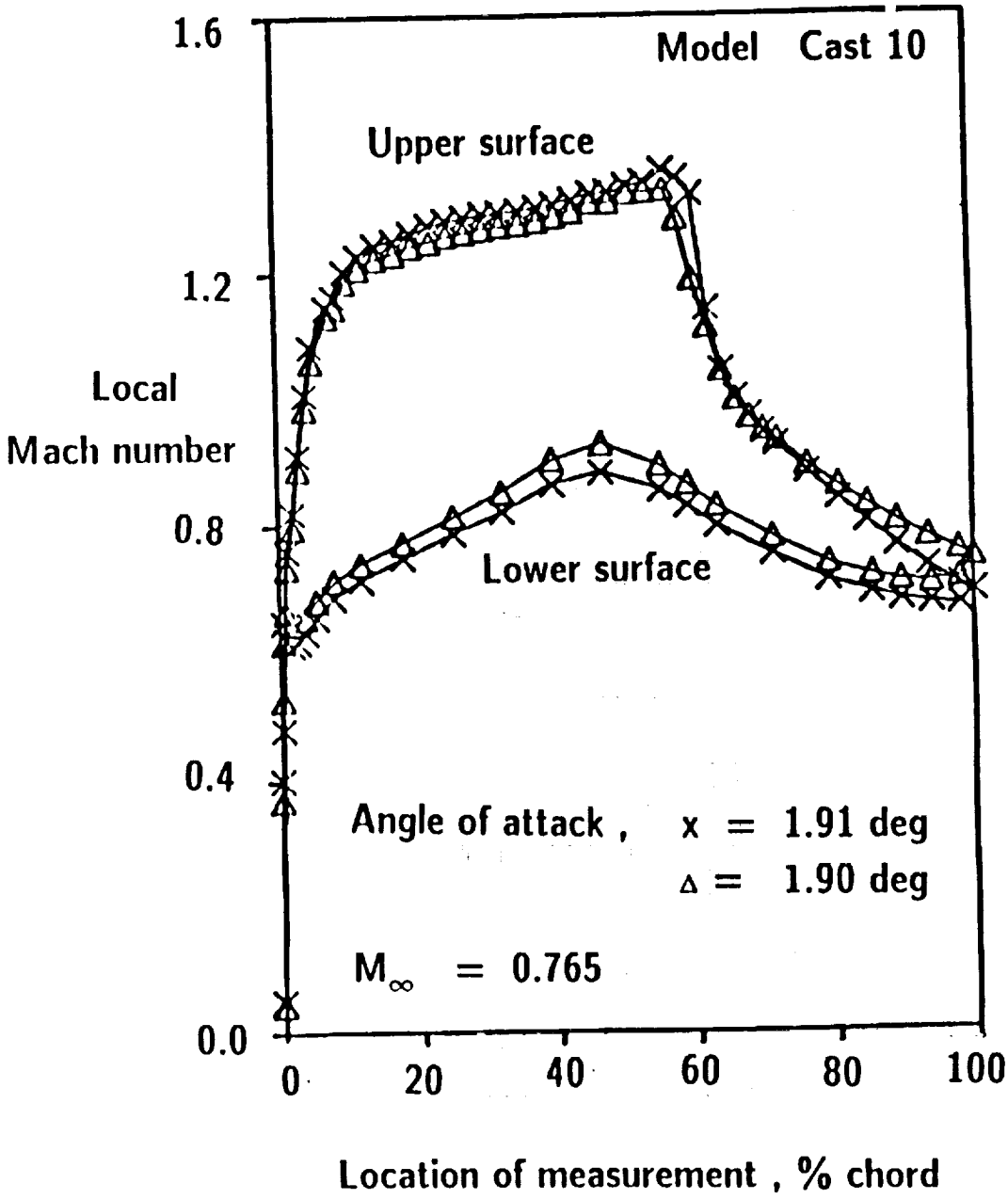

Figure 7 Local Mach number distribution over an airfoil.

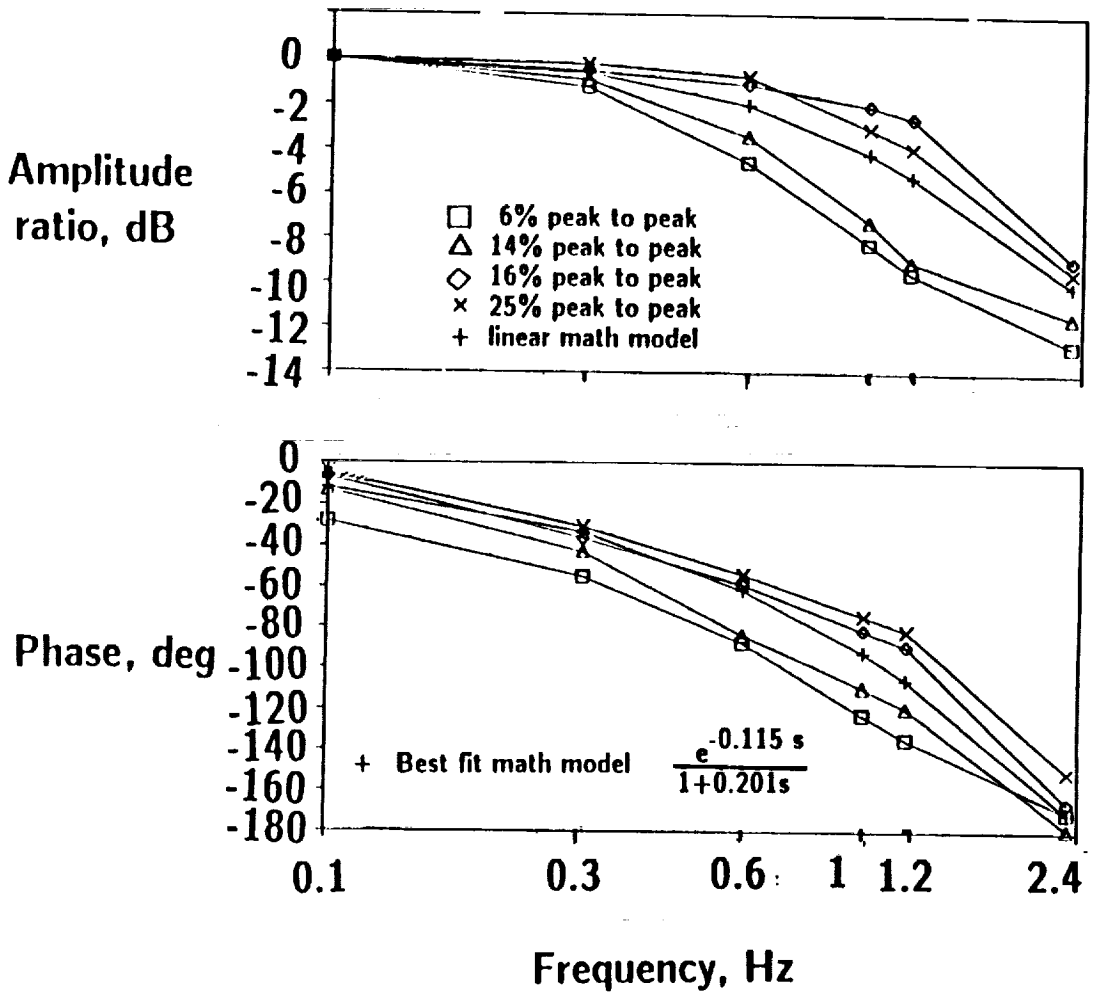

Figure 8.- Bode plots for the 0.3-m TCT LN2 injection valve frequency response.

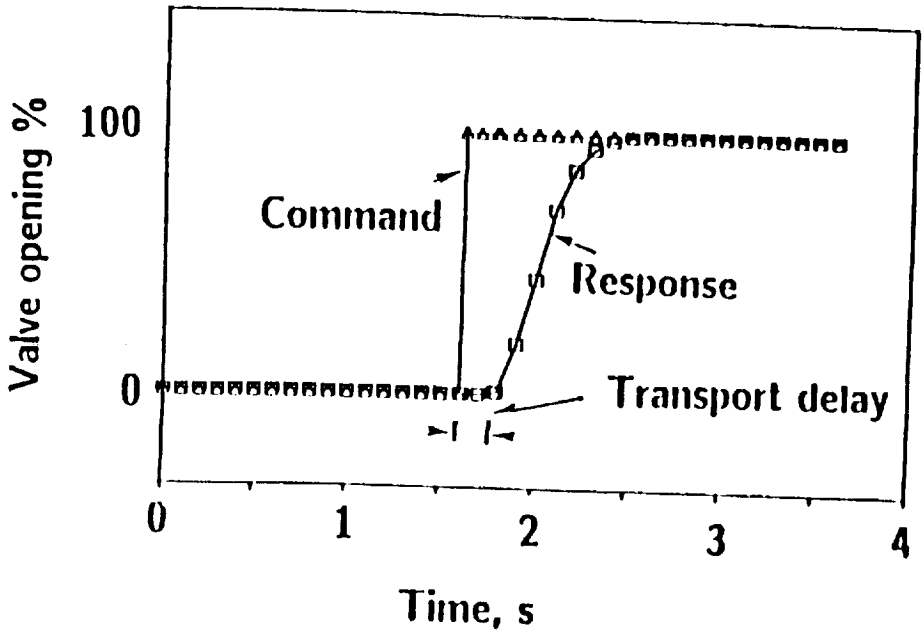

Figure 9.- Step response of the LN2 injection valve.

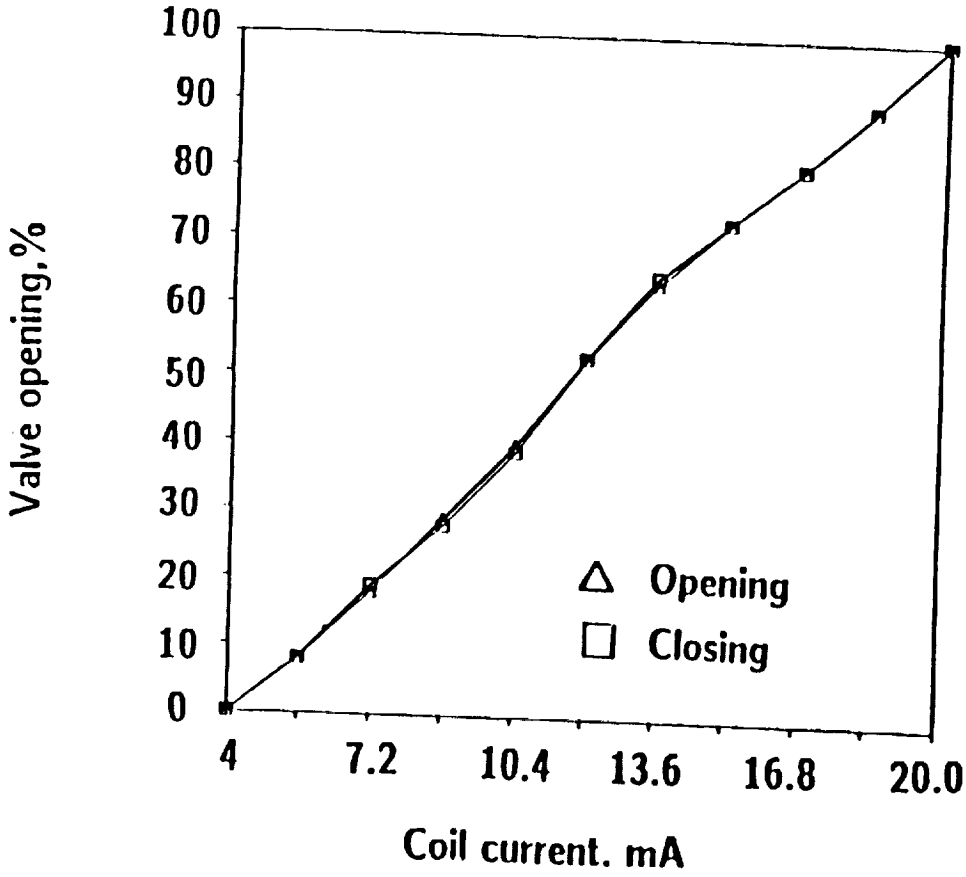

Figure 10.- Static calibration of LN2 injection valve.

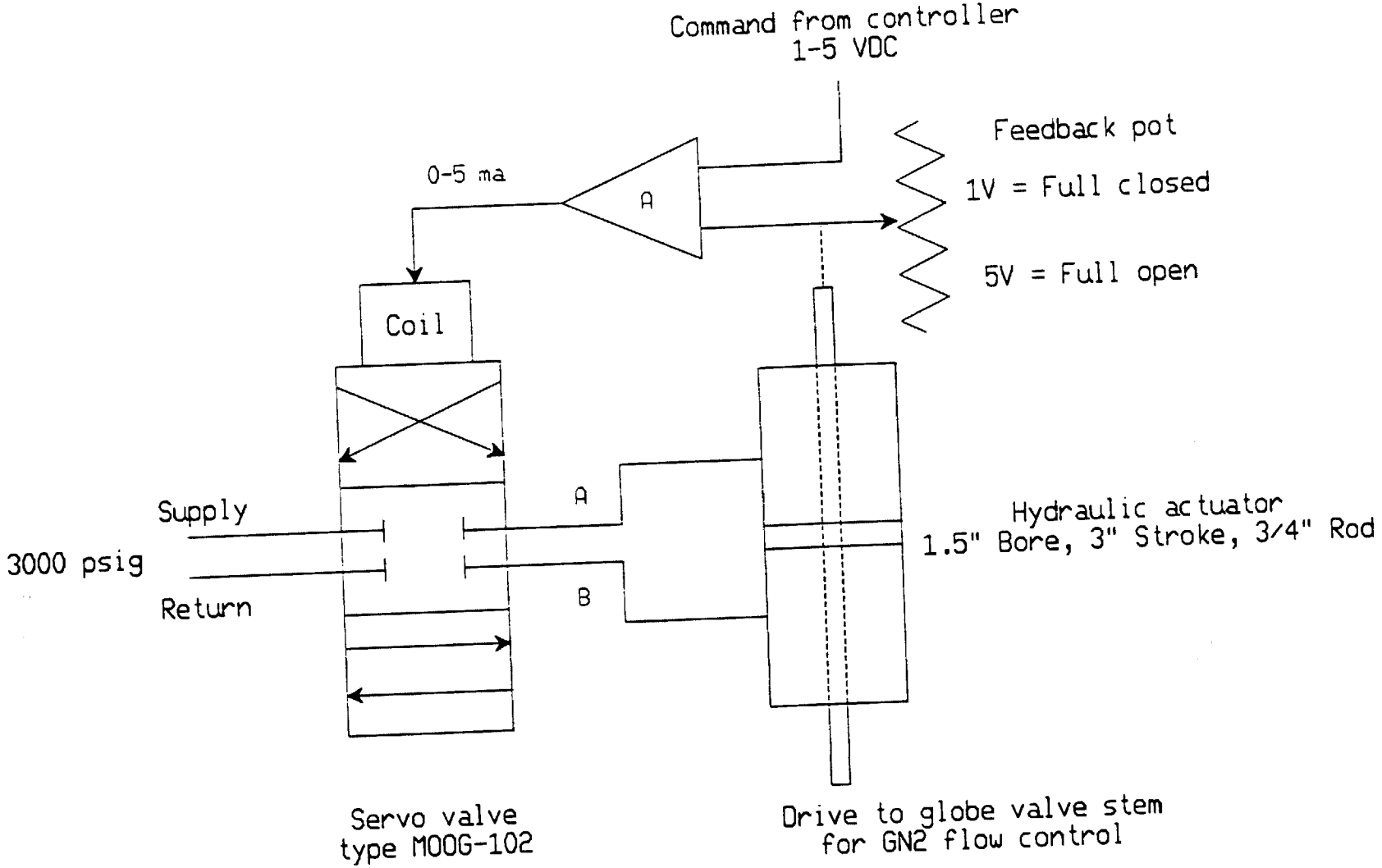

Figure 11.- Schematic of E-H valve for GN2 discharge control.

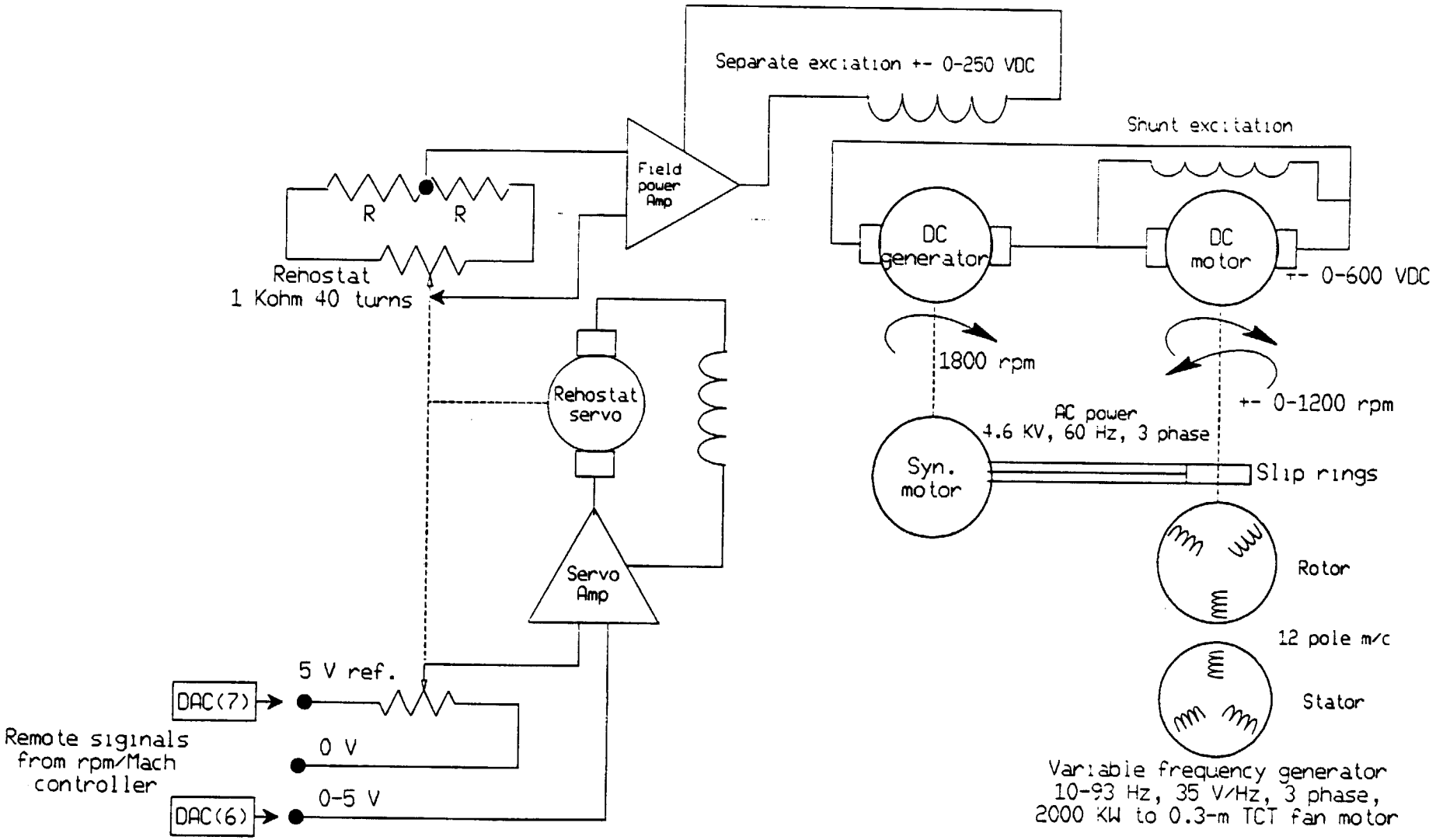

Figure 12.- Variable frequency generator control schematic.

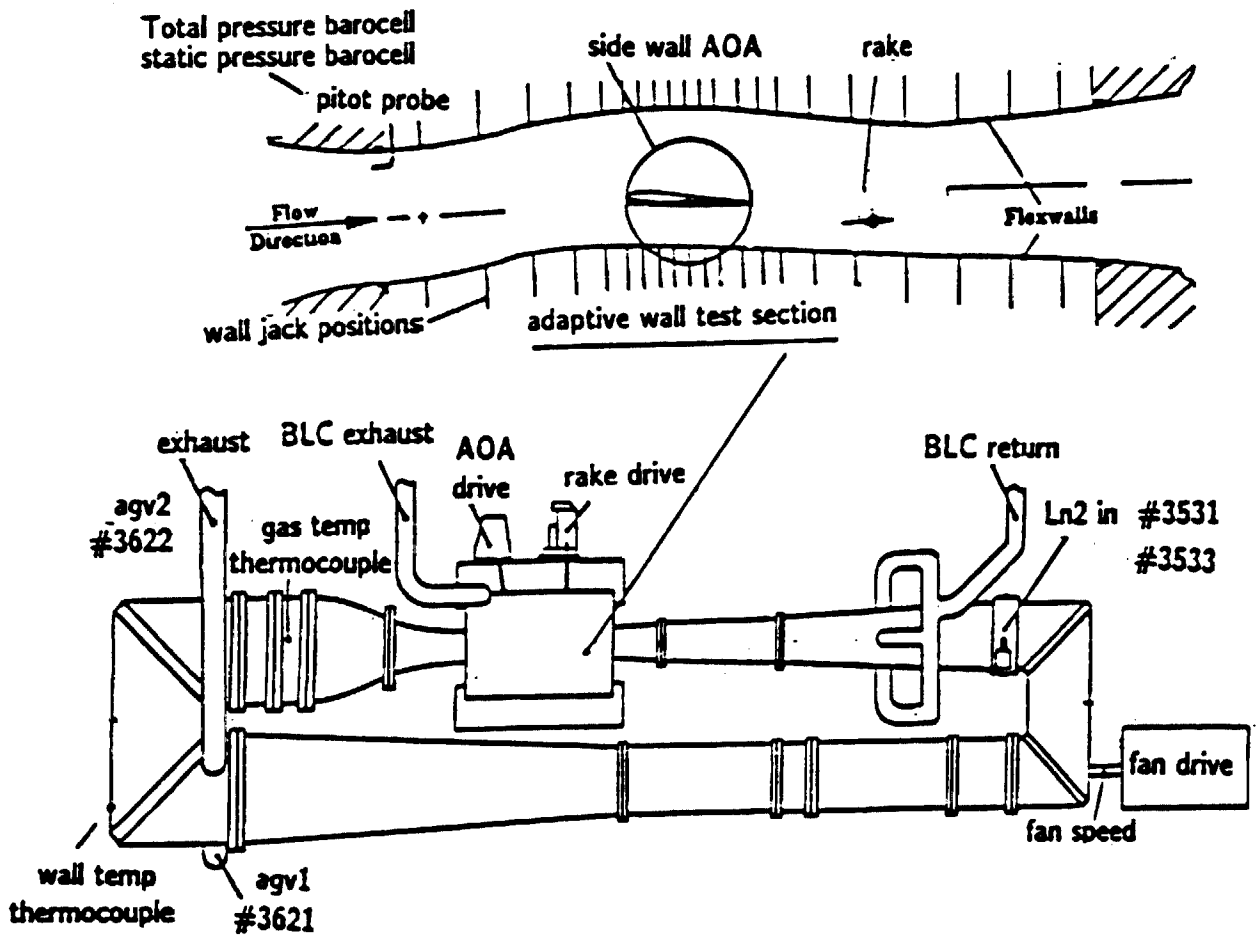

Figure 13.- 0.3-m TCT sensors and actuators for control.

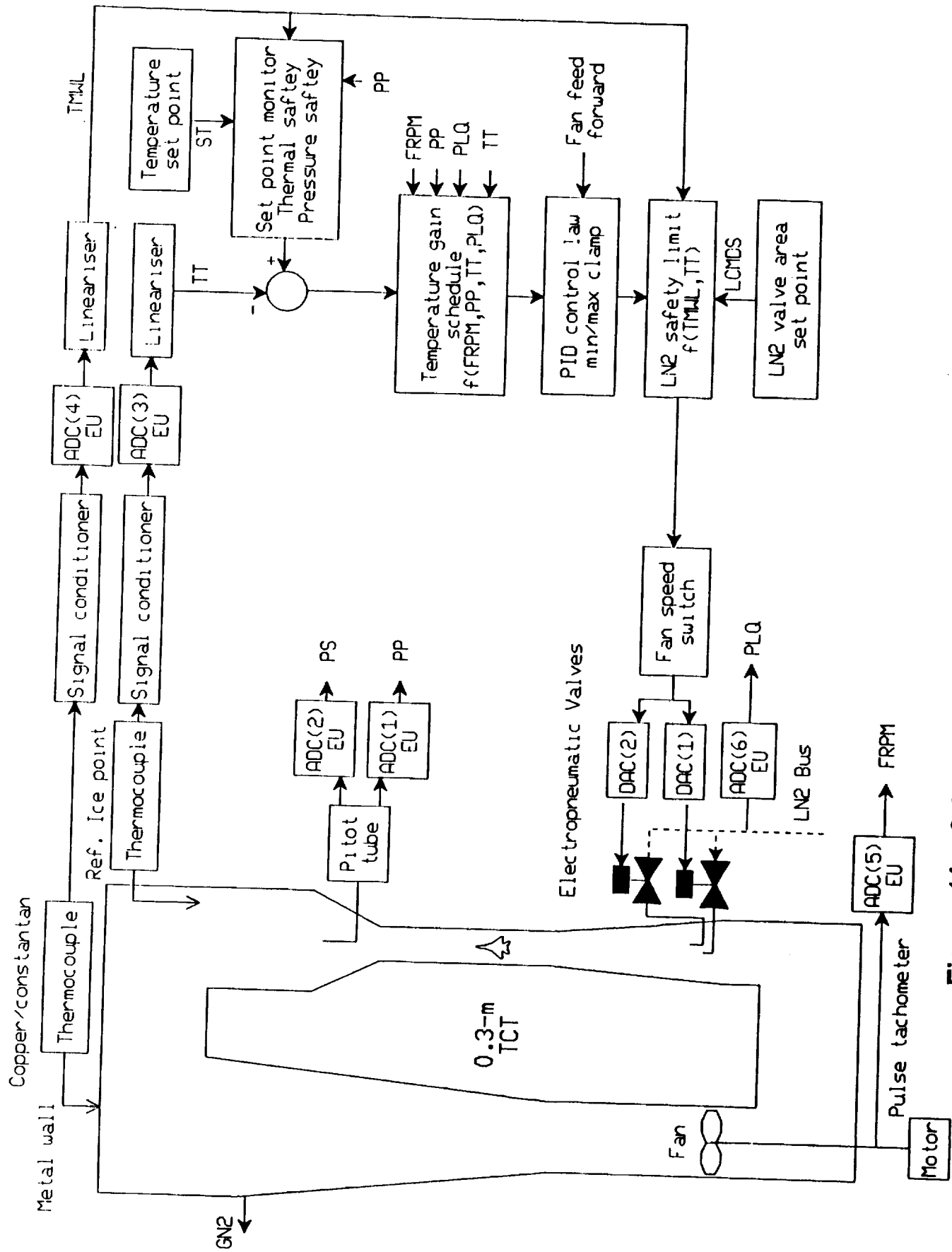

Figure 14.- 0.3-m TCT temperature control schematic.

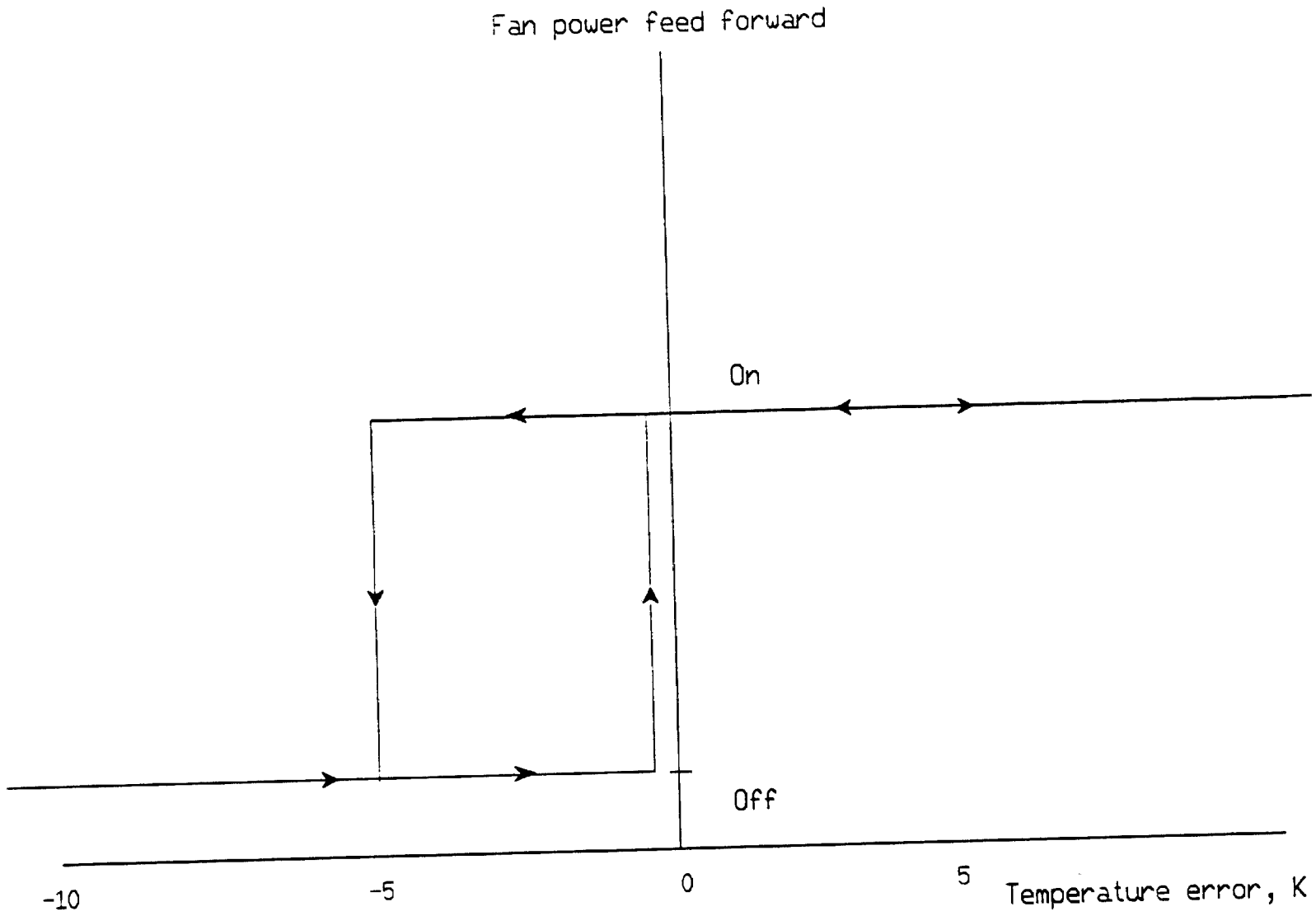

Figure 15.- 0.3-m TCT temperature loop feed foward logic.

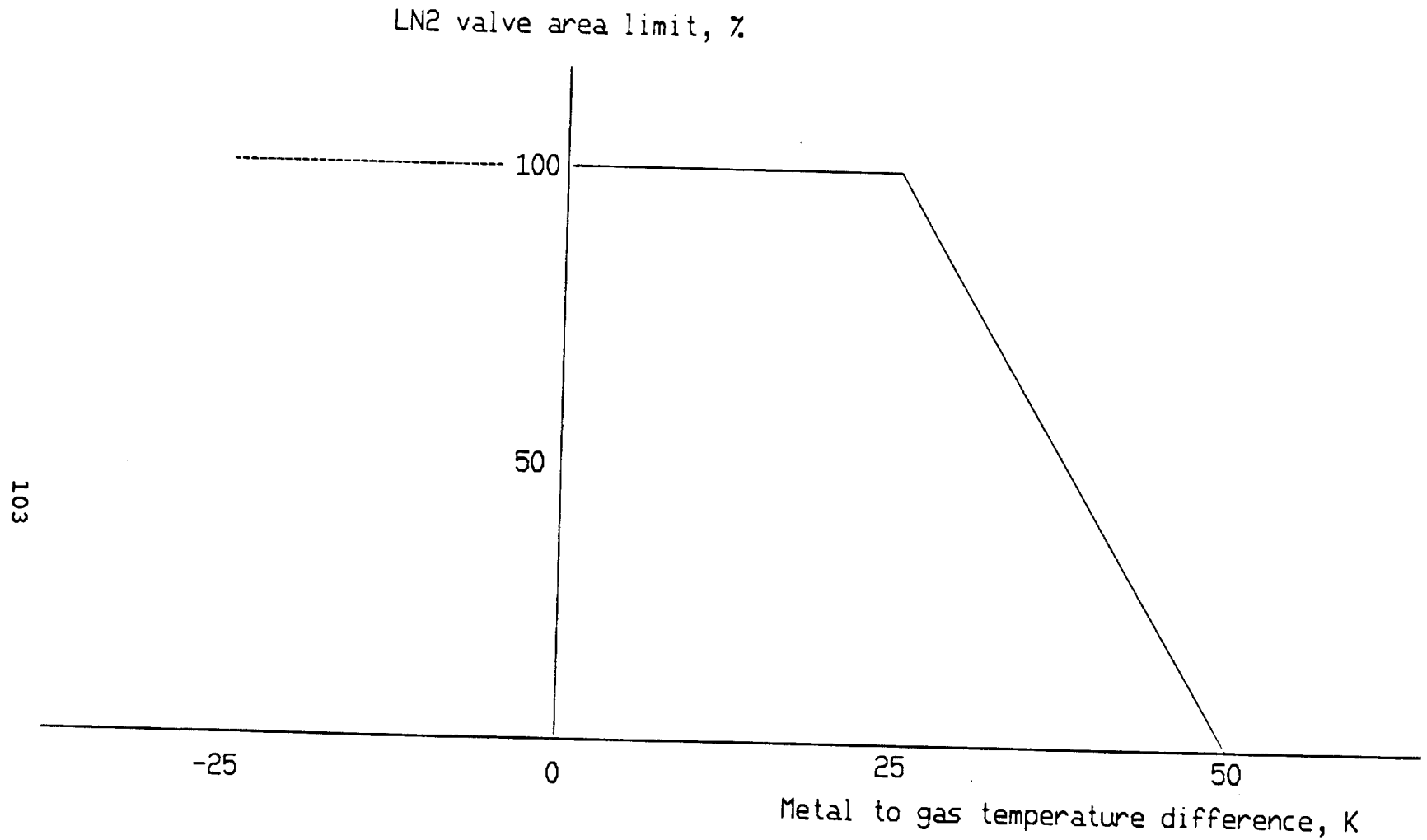

Figure 16.- Limit on LN2 valve area as a function of metal to gas temperature difference.

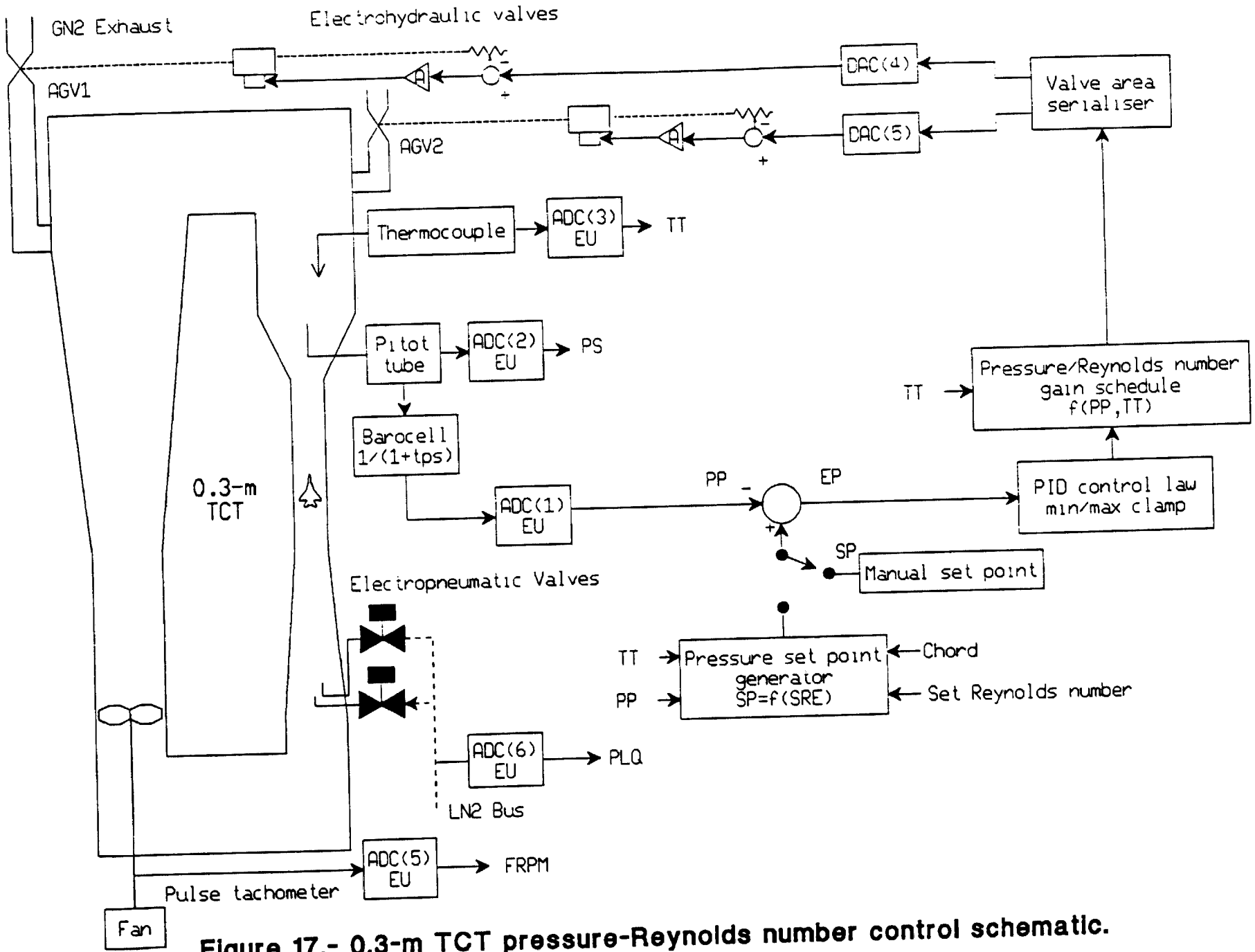

Figure 17.- 0.3-m TCT pressure-Reynolds number control schematic.

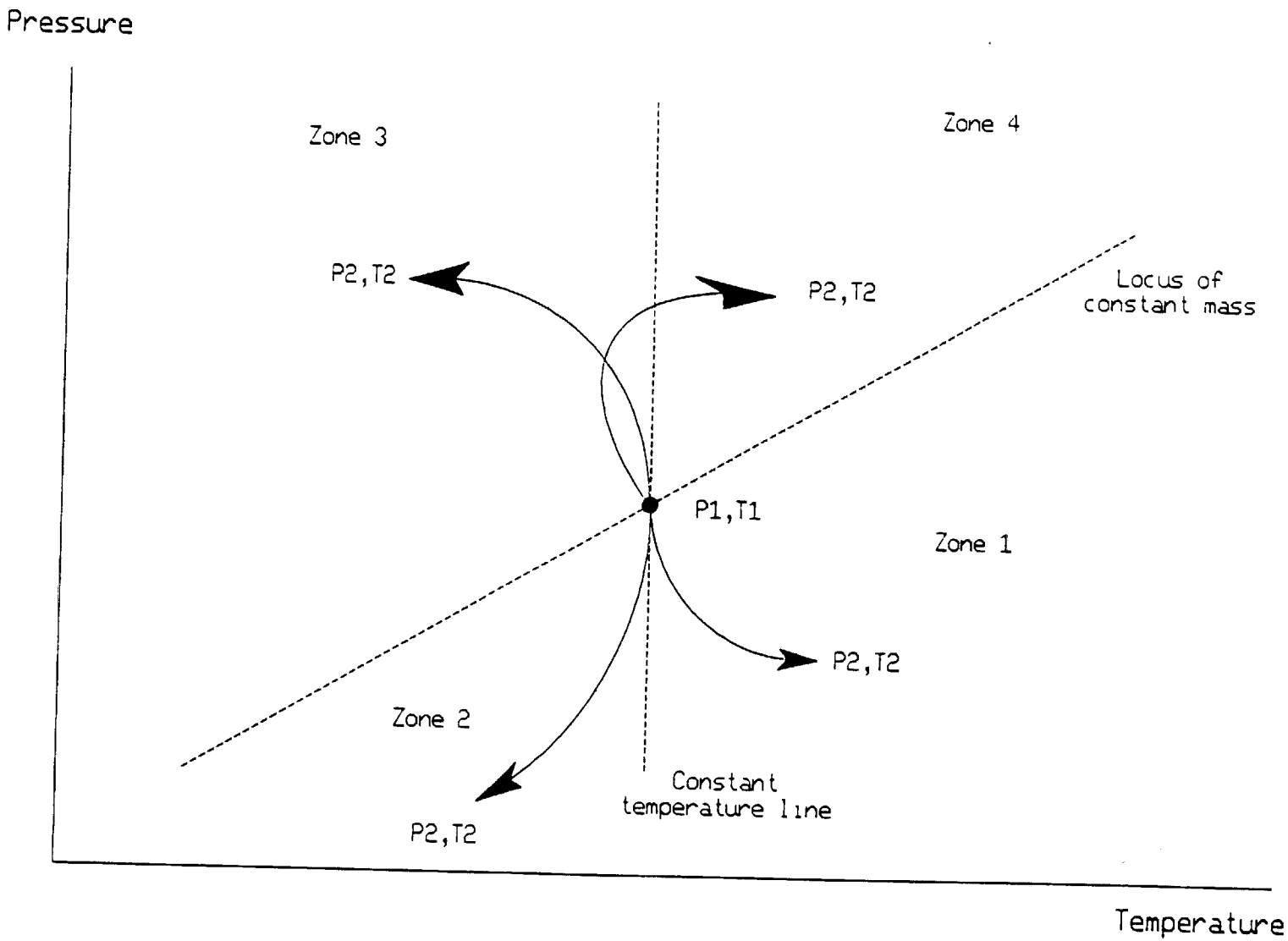

Figure 18.- Tunnel trajectory in pressure-temperature plane.

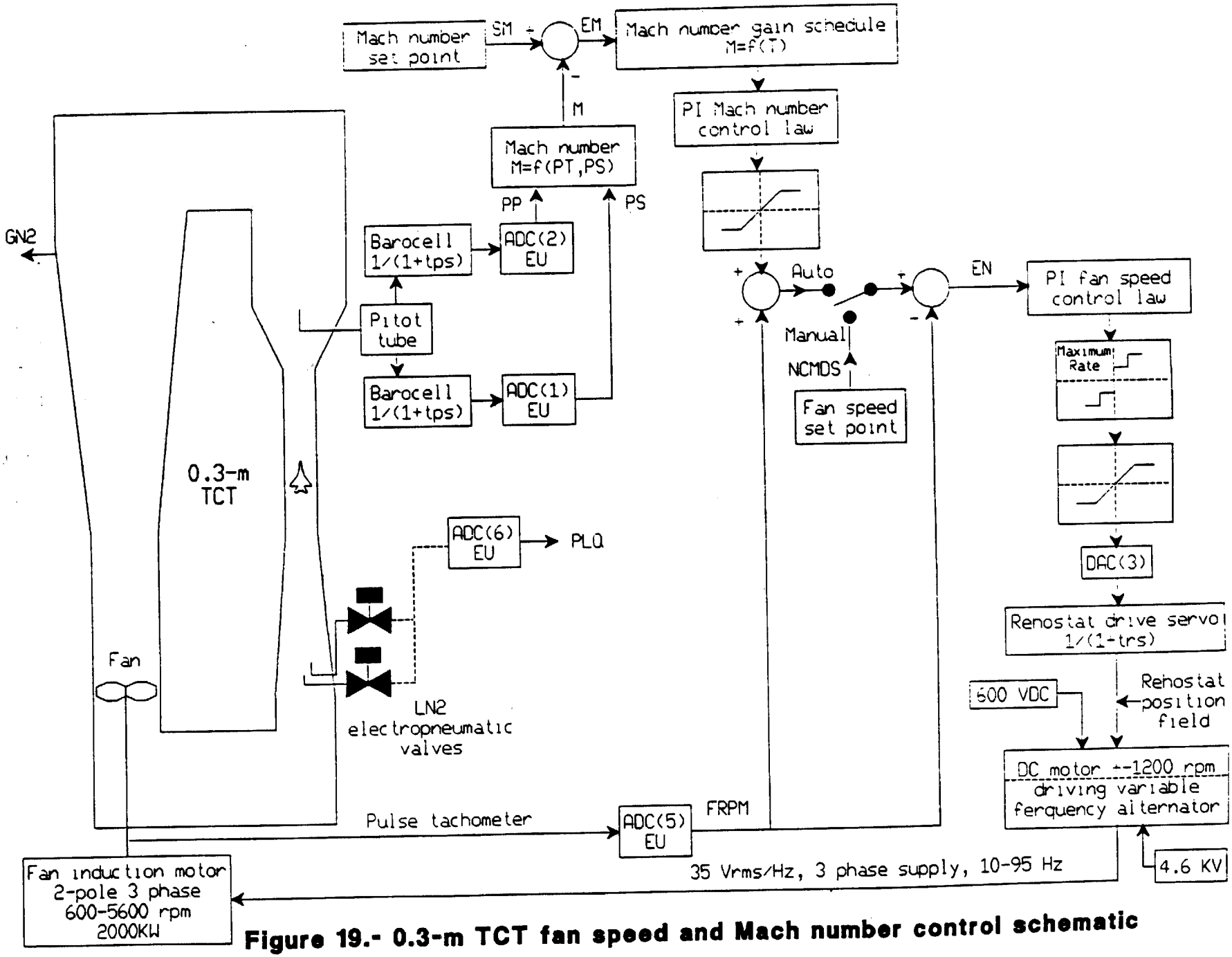

Figure 19.- 0.3-m TCT fan speed and Mach number control schematic

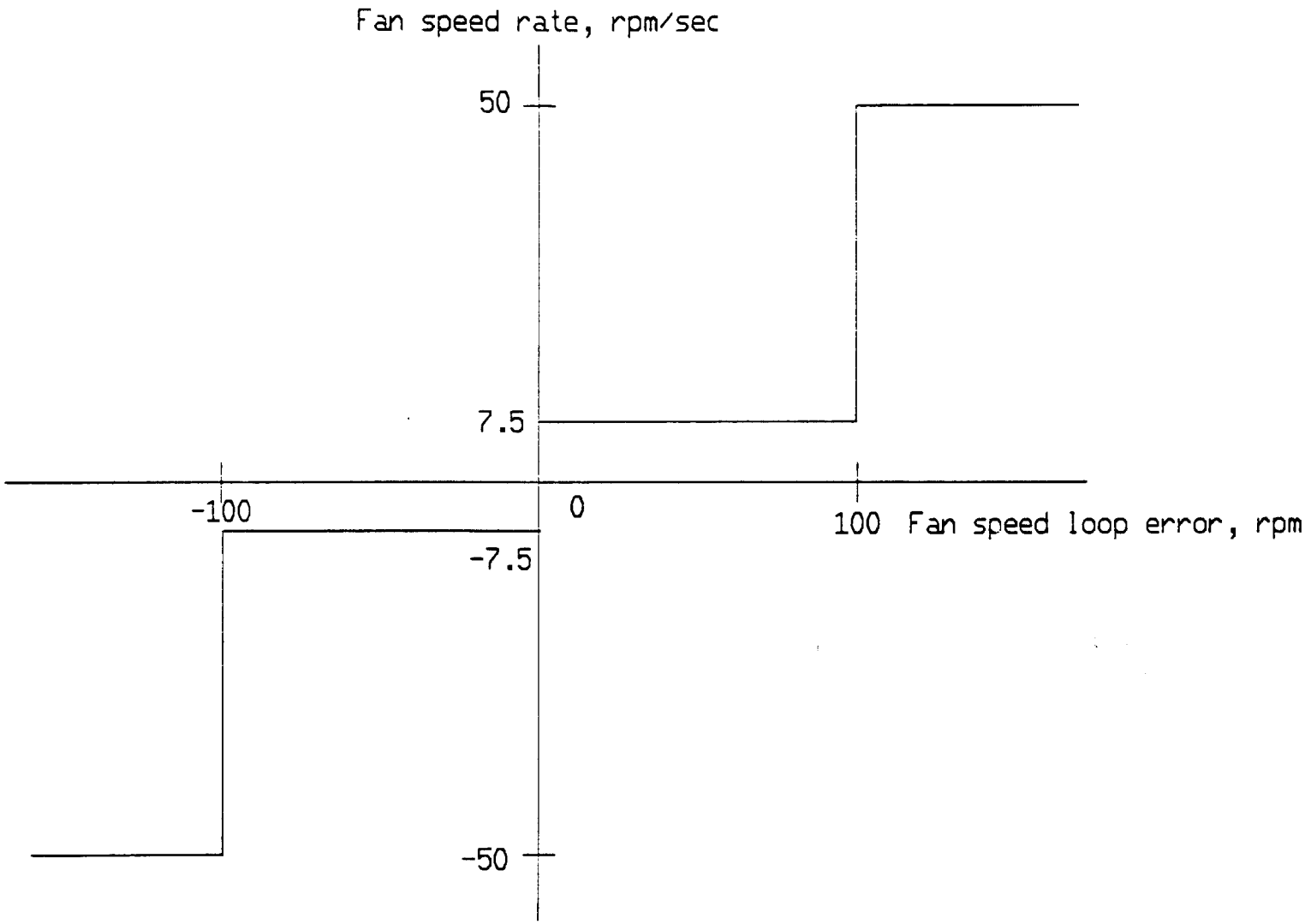

Figure 20.- Fan speed rate limit as a function of fan speed control loop error.

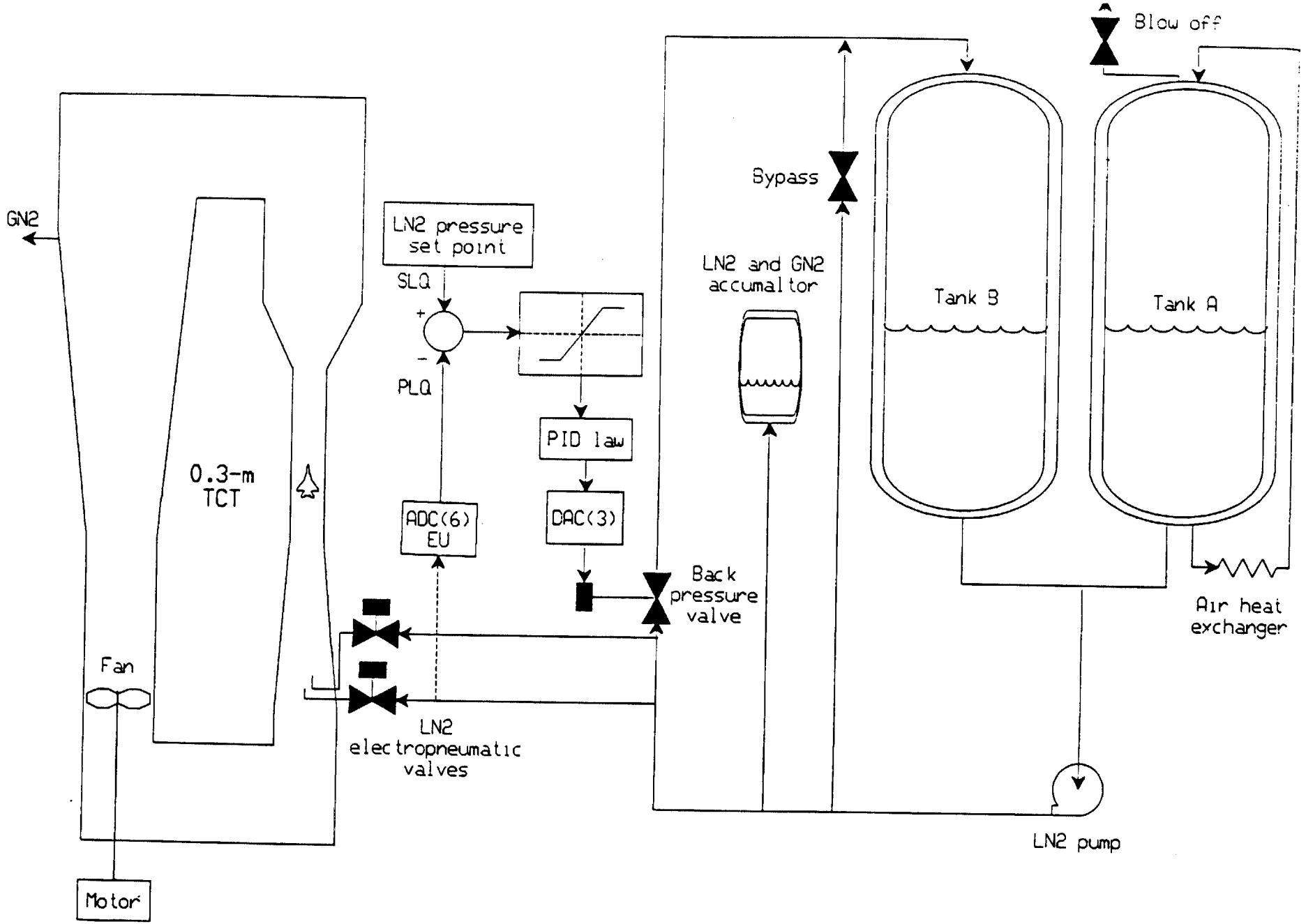

Figure 21.- LN2 storage and pressure control schematic.

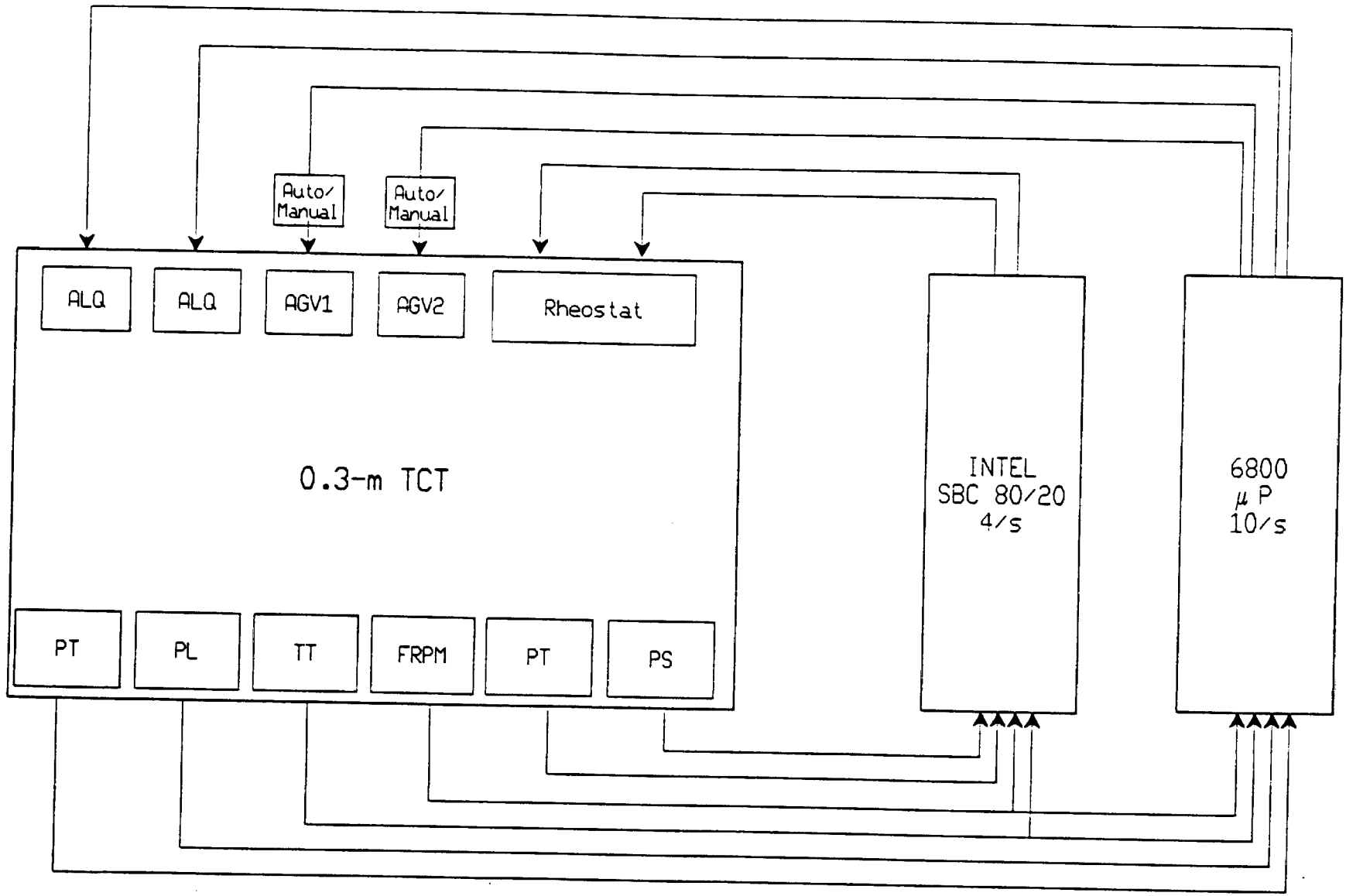

Figure 22.- Schematic for Motorola 6800 based P-T controller and SBC 80/20 based Mach number controller.

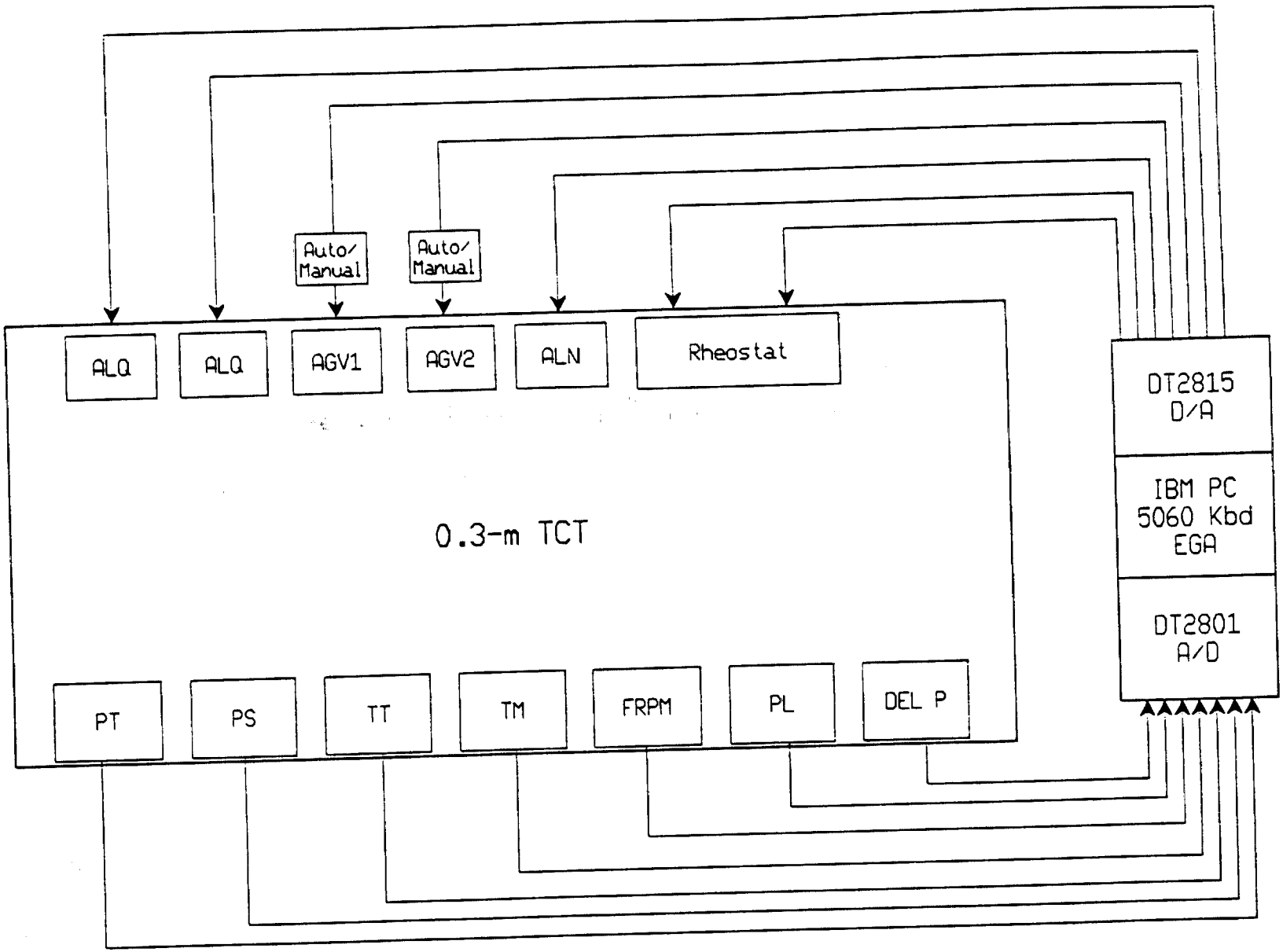

Figure 23.- Schematic for IBM PC-AT based temperature, pressure-Reynolds number and Mach number controller.

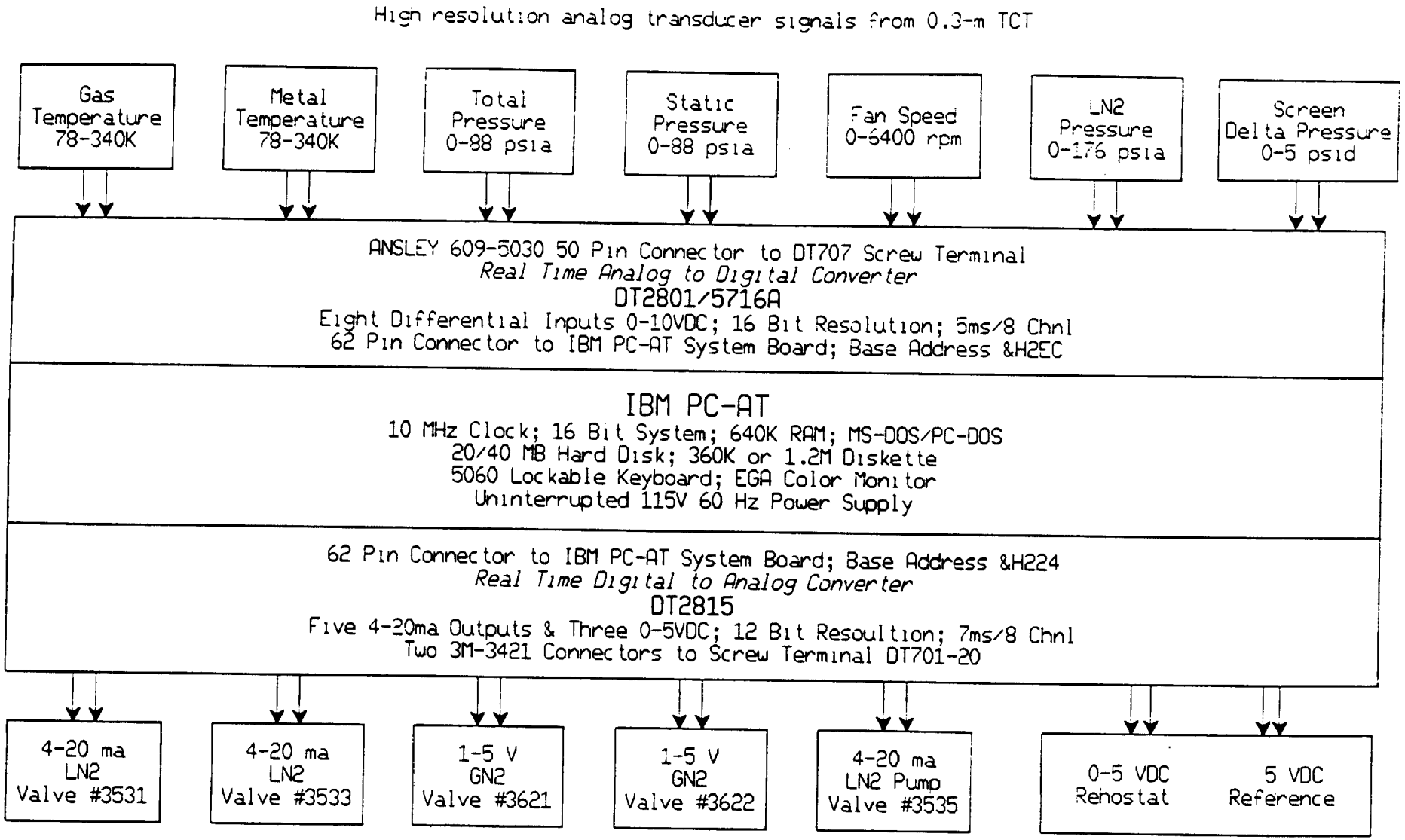

Figure 24.- IBM PC-AT based temperature, pressure-Reynolds number and Mach number controller.

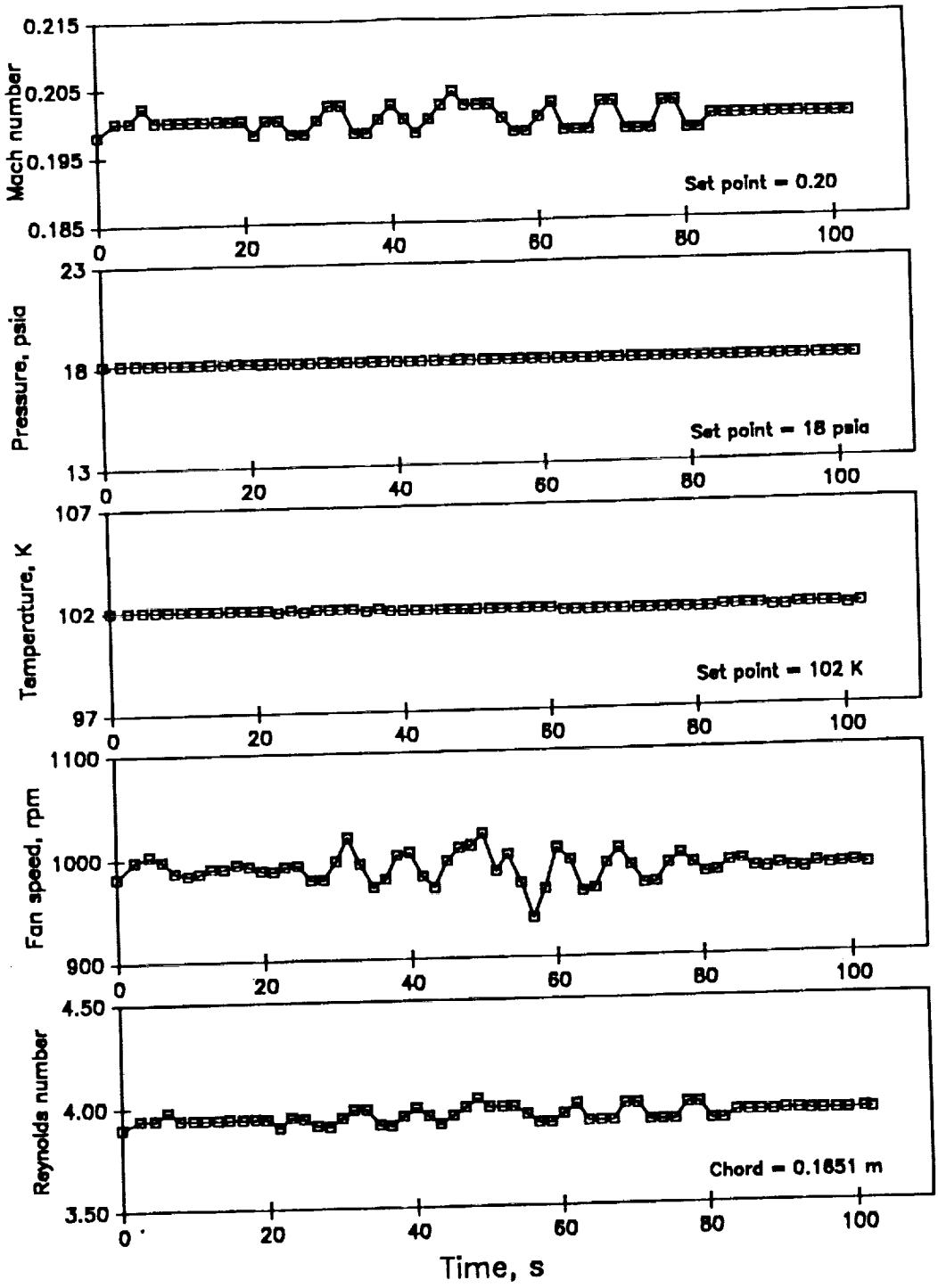

Figure 25.– Tunnel condition regulation under closed loop control. Drag rake traverse. (2 to 0 inches)

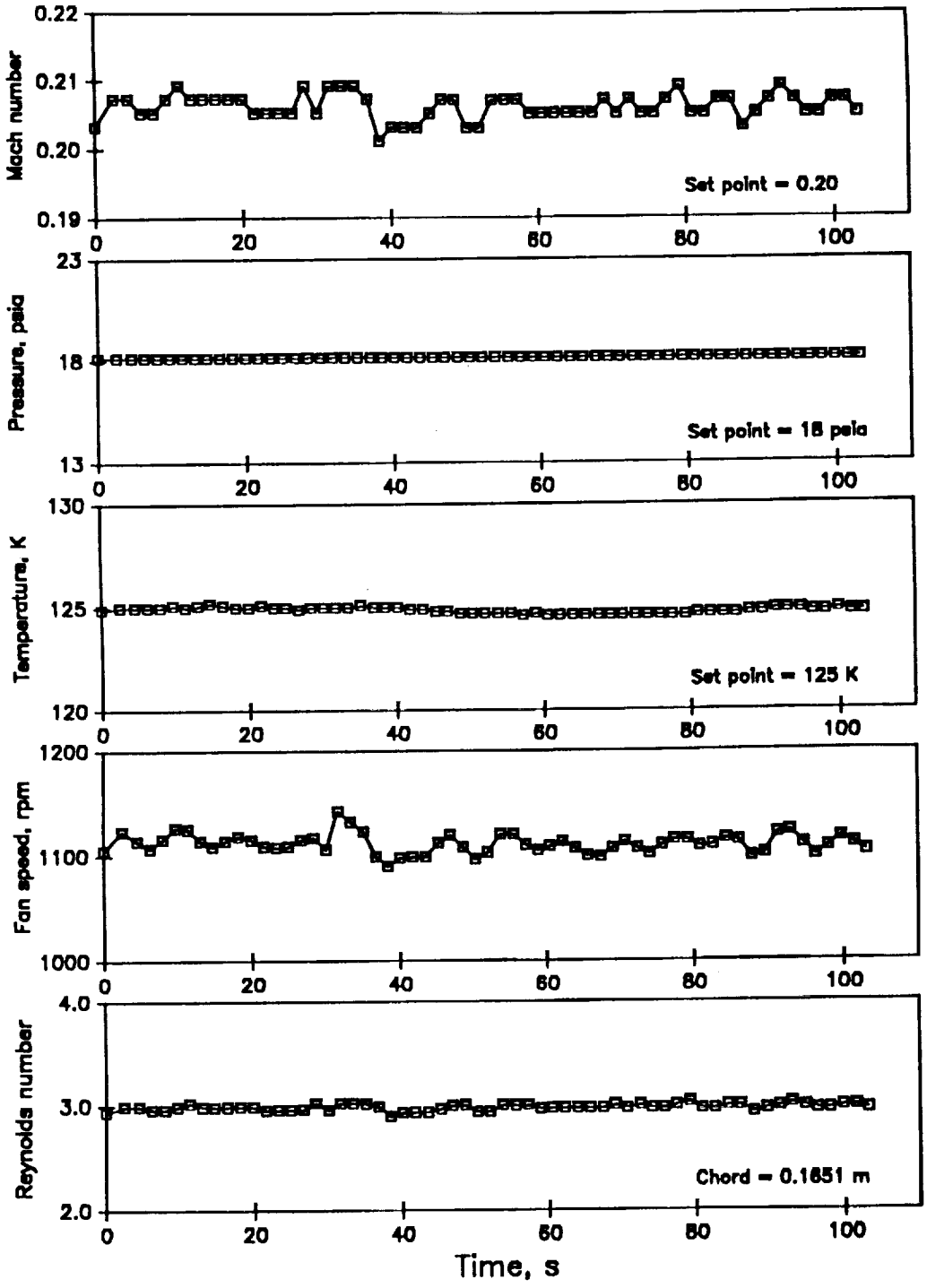

Figure 26.— Tunnel condition regulation under closed loop control. Drag rake traverse. (2 to 0 inches)

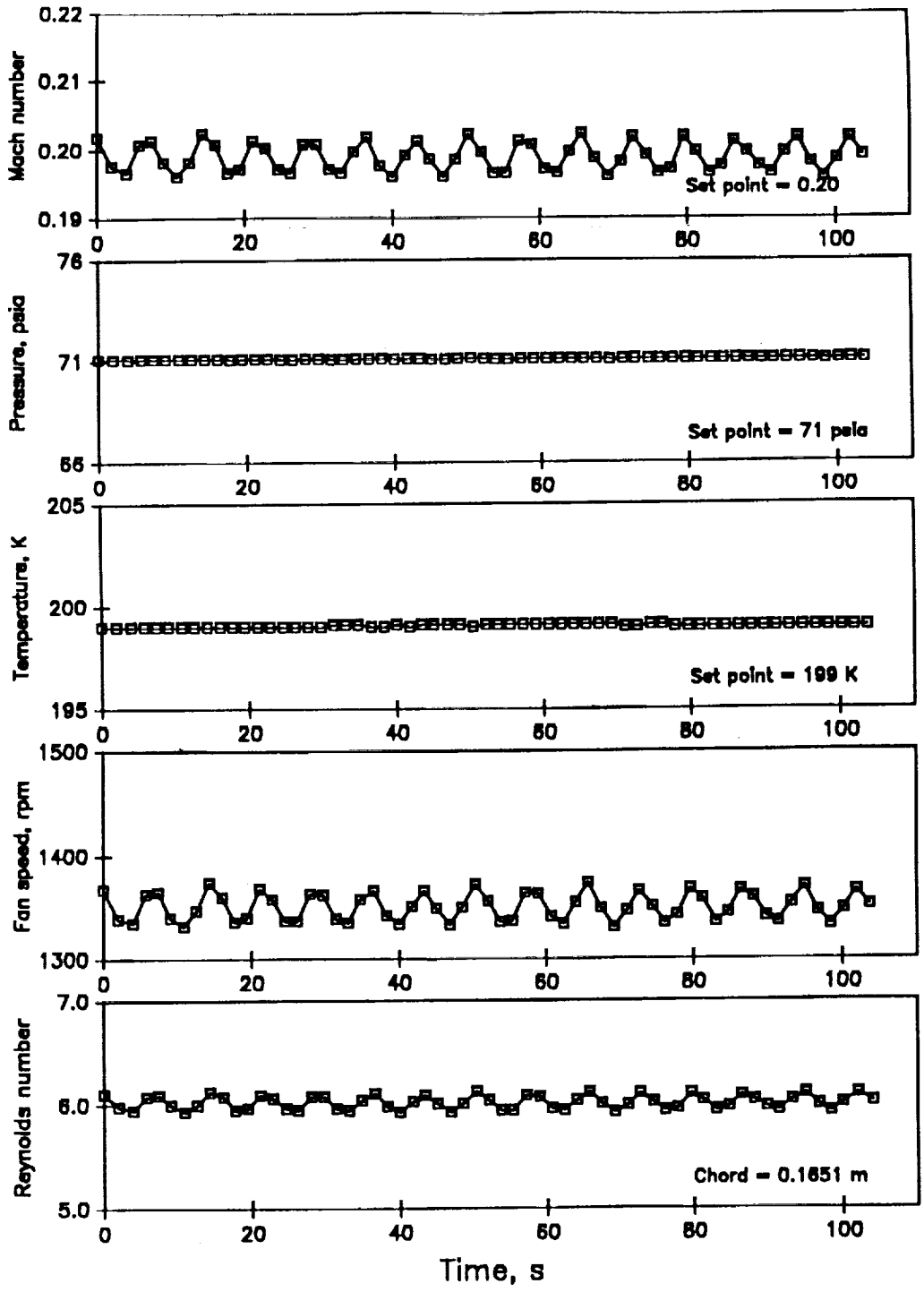

Figure 27.– Tunnel condition regulation under closed loop control. Drag rake traverse. (2 to 0 inches)

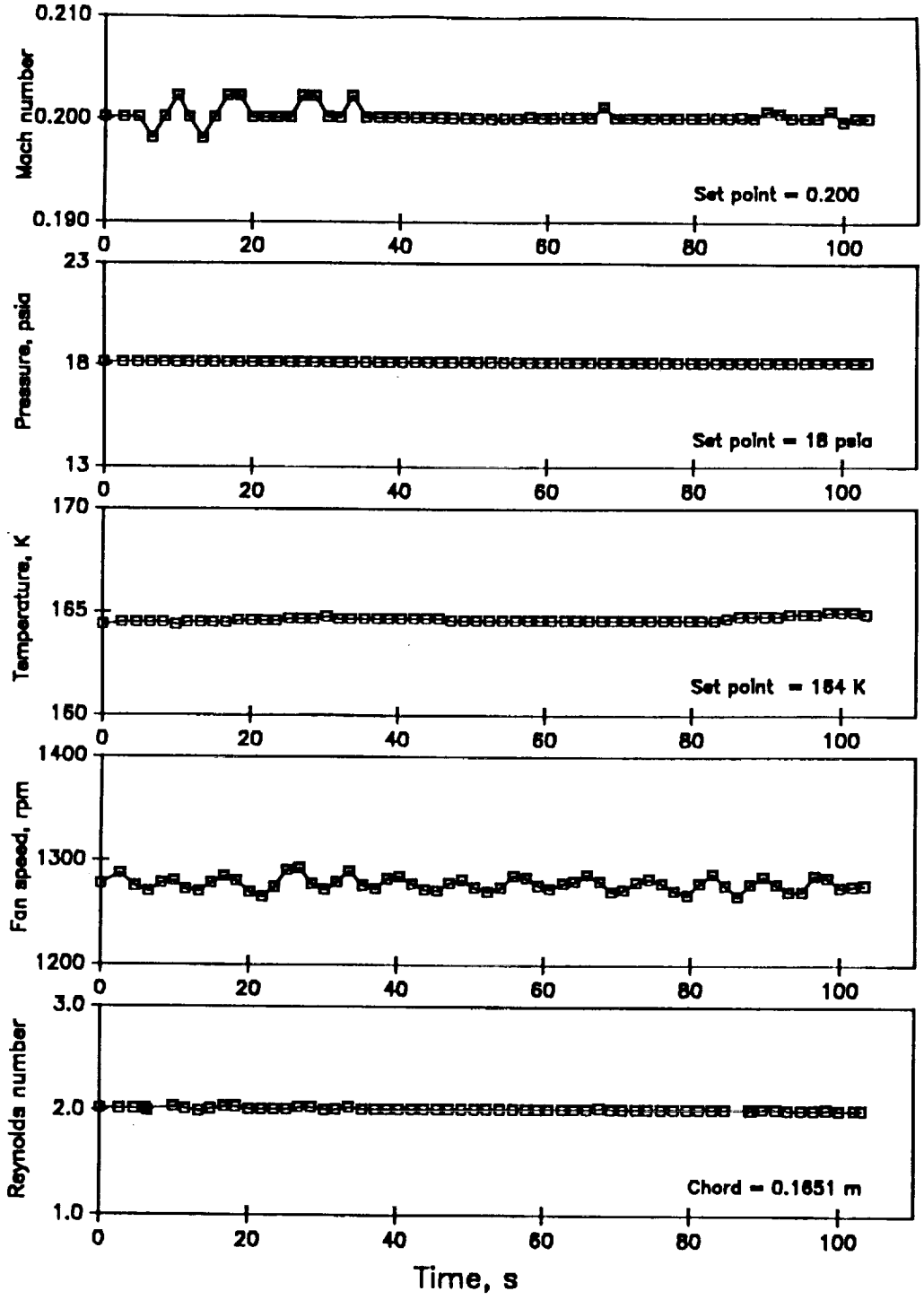

Figure 28.– Tunnel condition regulation under closed loop control. Drag rake traverse. (2 to 0 inches)

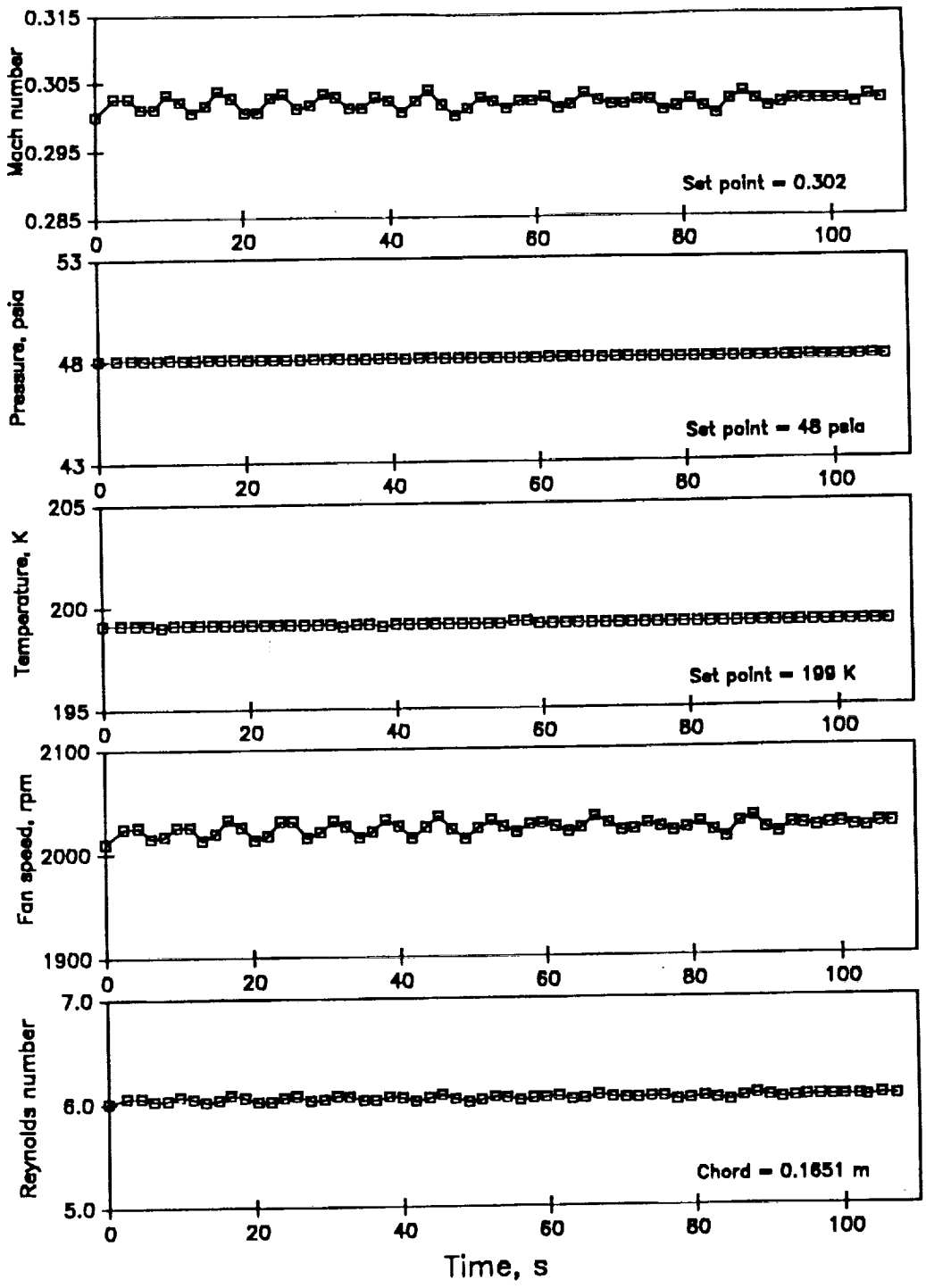

Figure 29.– Tunnel condition regulation under closed loop contol. Drag rake traverse. (2 to 0 inches)

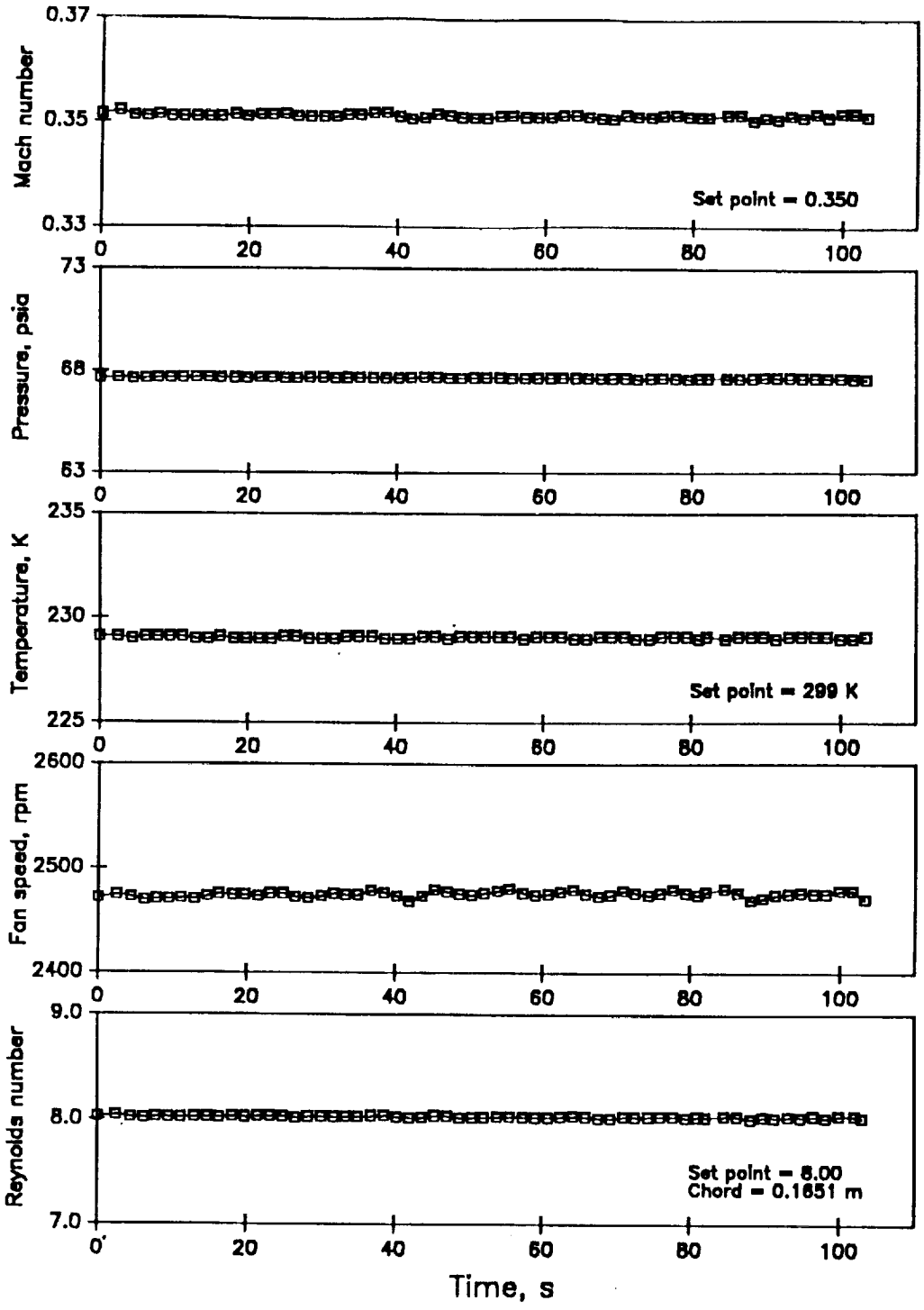

Figure 30.– Tunnel condition regulation under closed loop control. Drag rake traverse (2 to 0 inches)

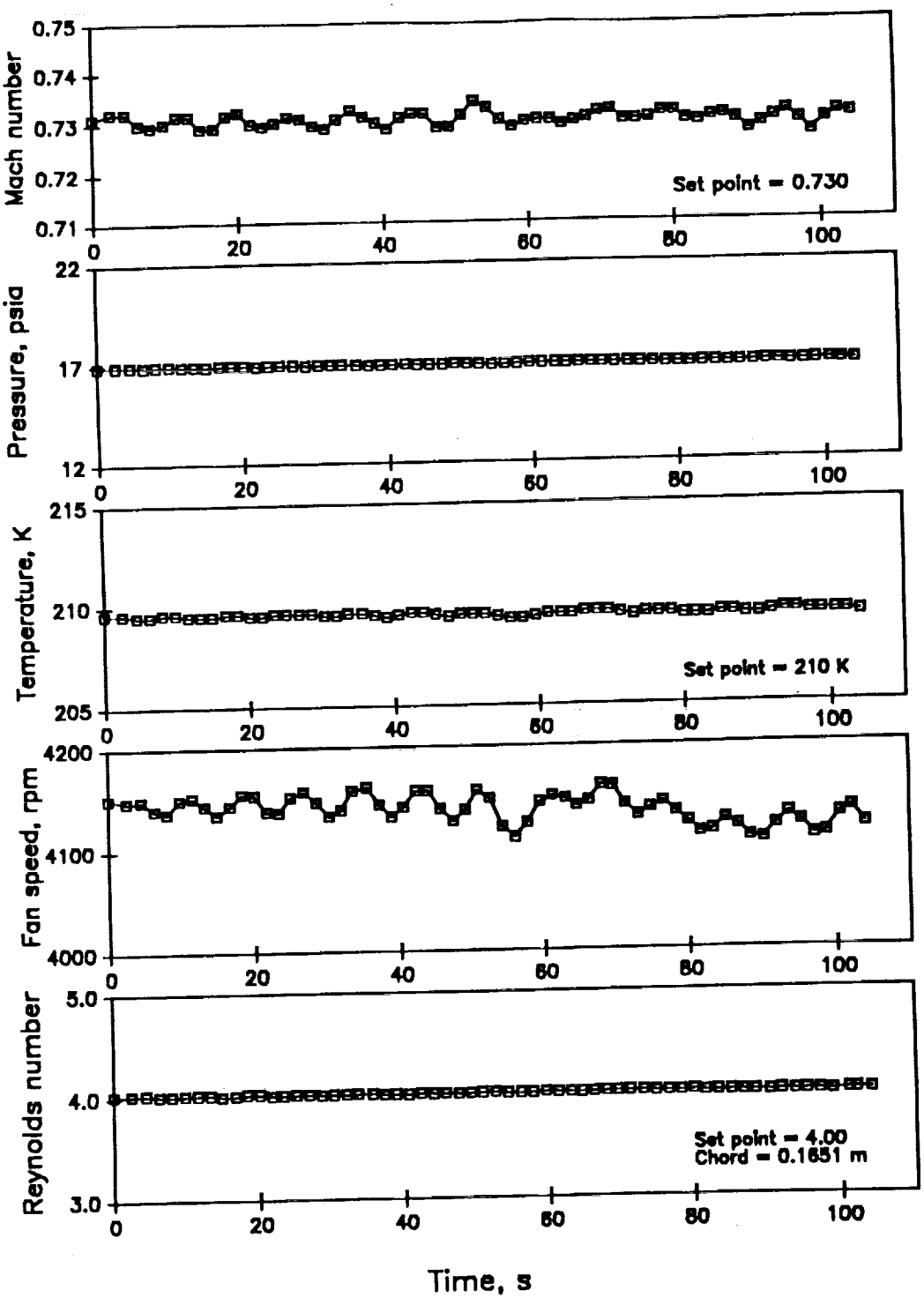

Figure 31.– Tunnel condition regulation under closed loop control. Drag rake traverse. (2 to 0 inches)

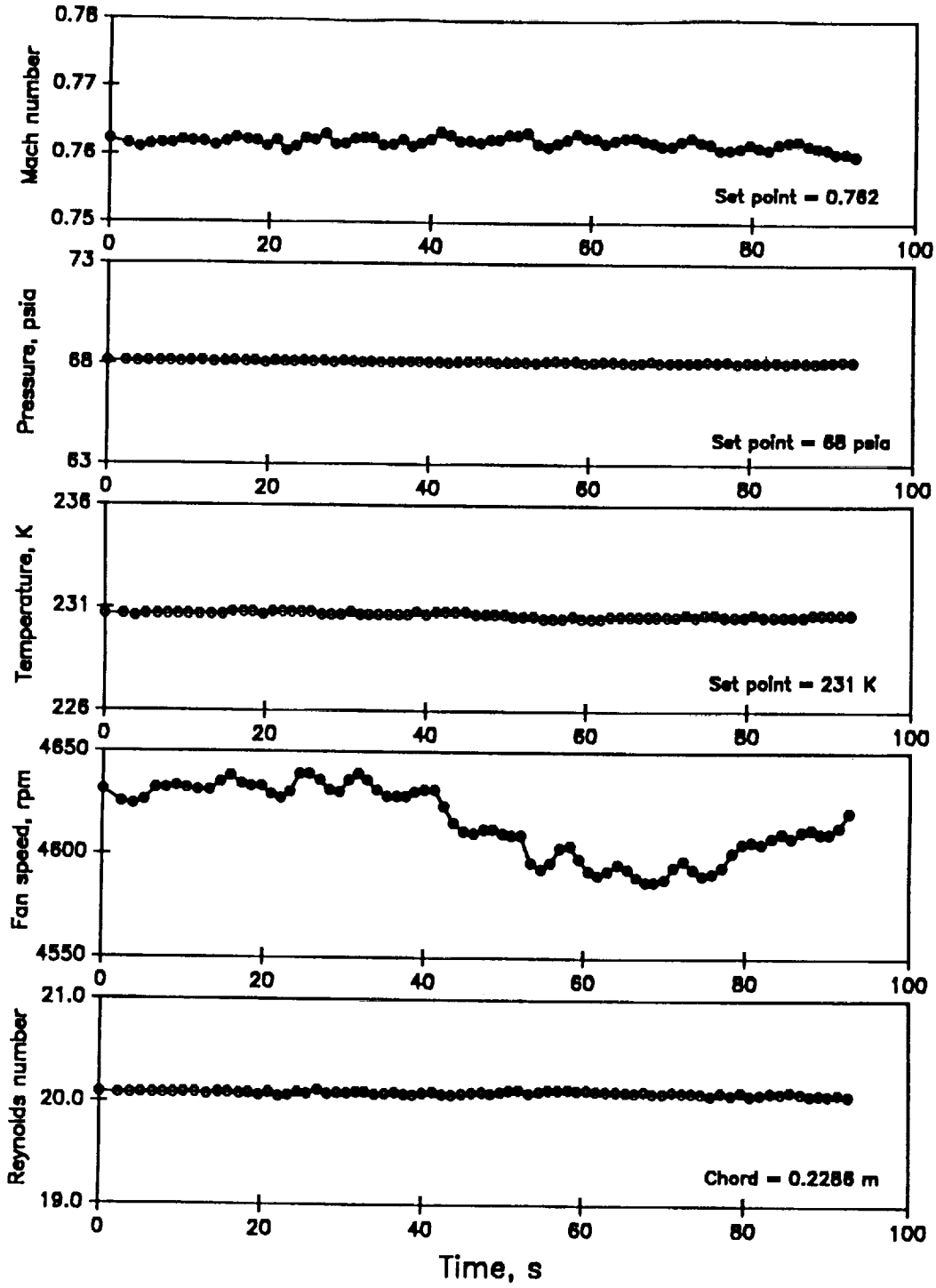

Figure 32.– Tunnel condition regulation under closed loop control.
Drag rake traverse. (1 to −1 inches)
CAST 10, α=0°, wall streamlined.

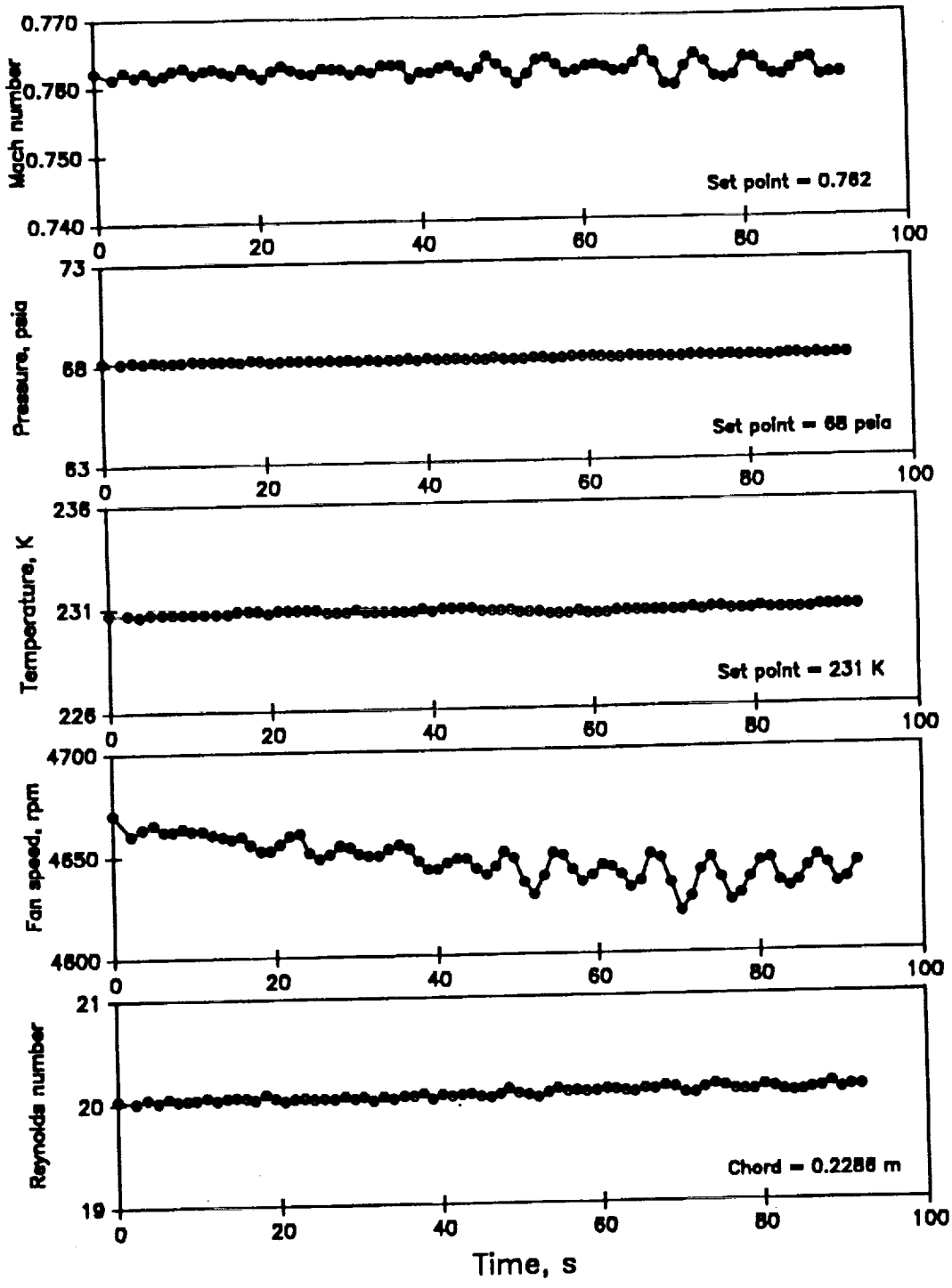

Figure 33.– Tunnel condition regulation under cloased loop control.
Drag rake traverse. (1 to −1 inches)
CAST 10, α=2°.

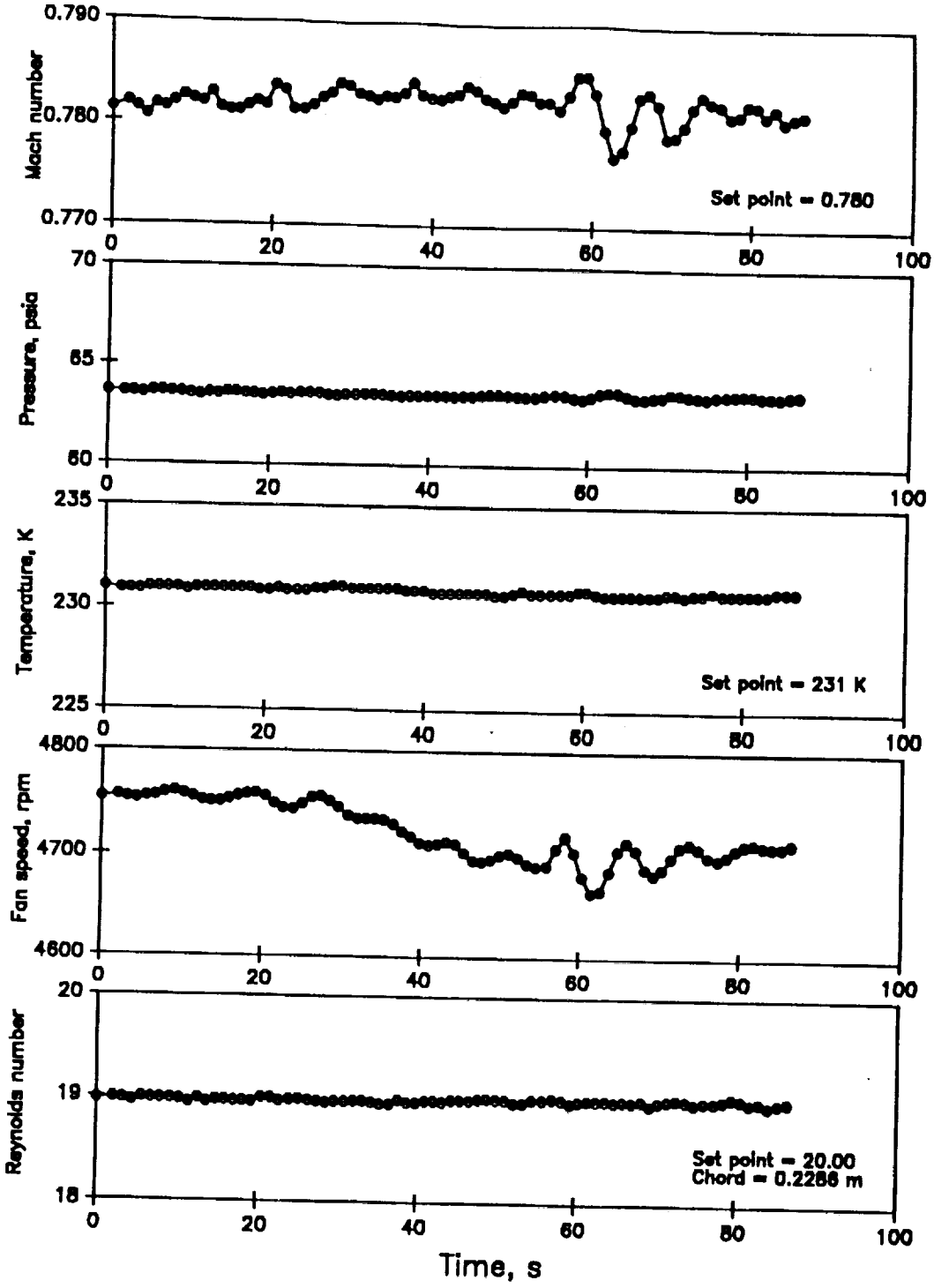

Figure 34.– Tunnel condition regulation under closed loop control.
Drag rake traverse. (1 to −1 inches)
CAST 10, α=0°, walls streamlined.

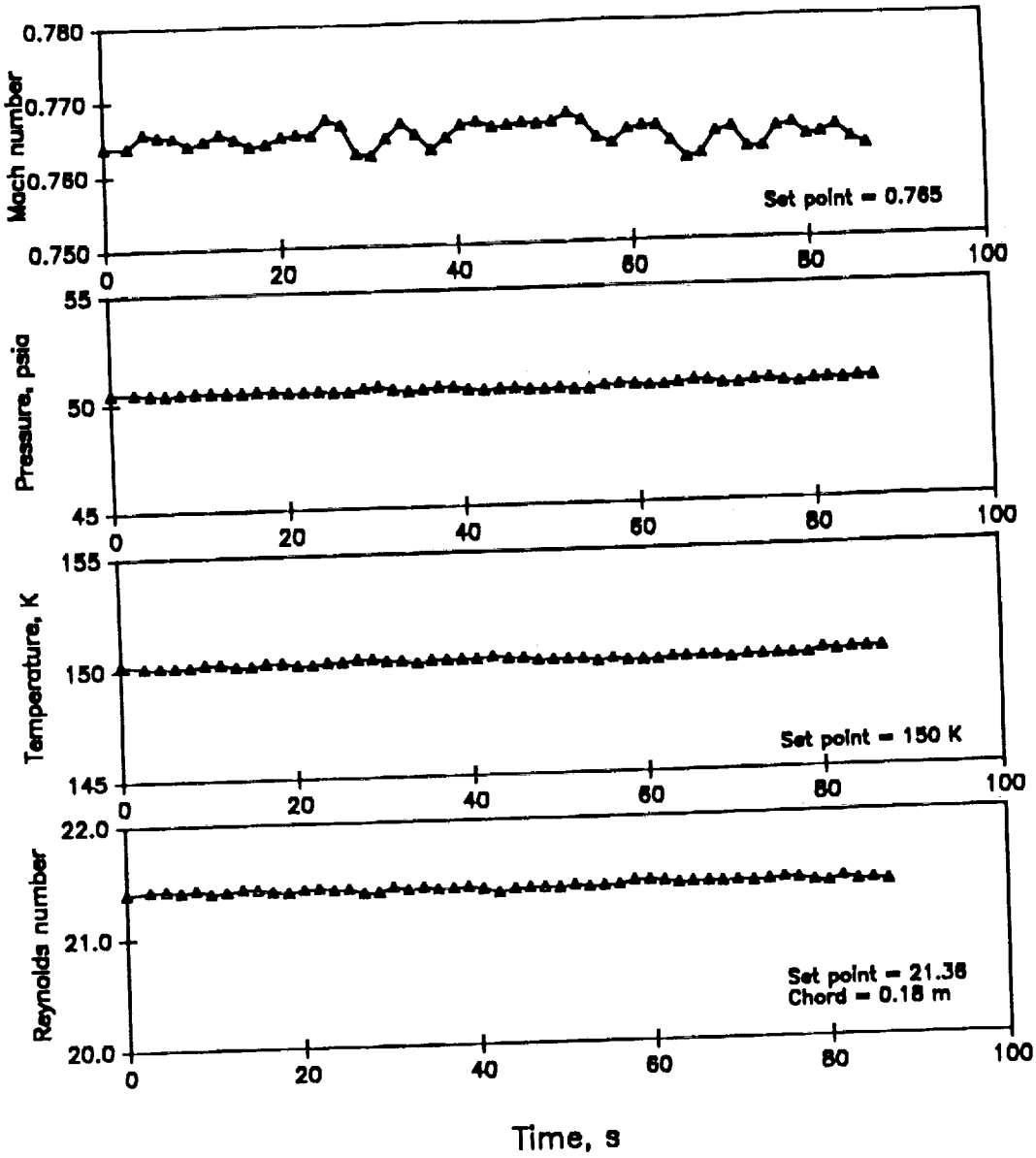

Figure 35.– Tunnel condition regulation under closed loop control.
Drag rake traverse. (3 to −2 inches)
CAST 10, α=0°.

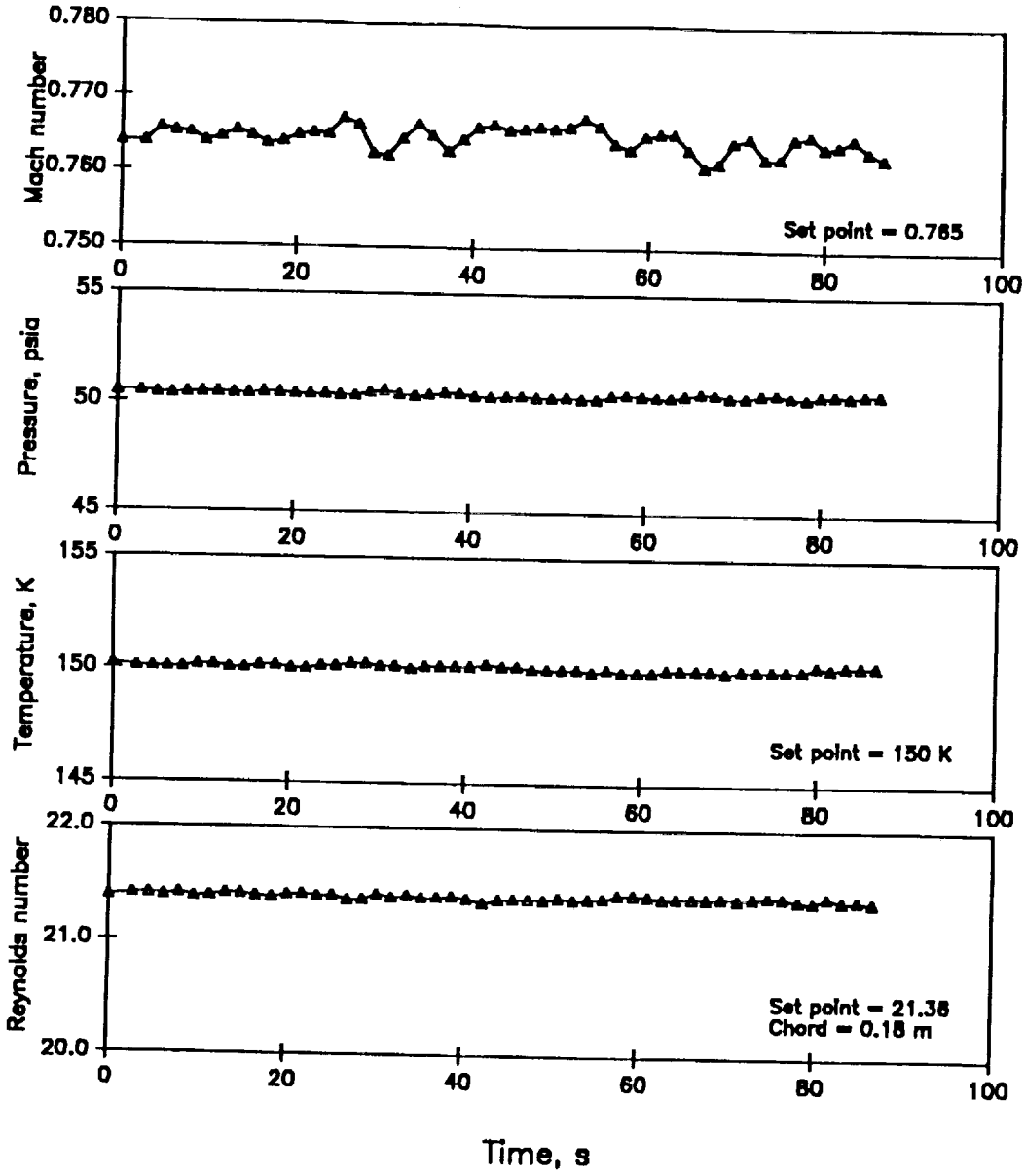

Figure 36.– Tunnel condition regulation under closed loop control.
Drag rake traverse. (3 to −2 inches)
CAST 10, α=0.25°.

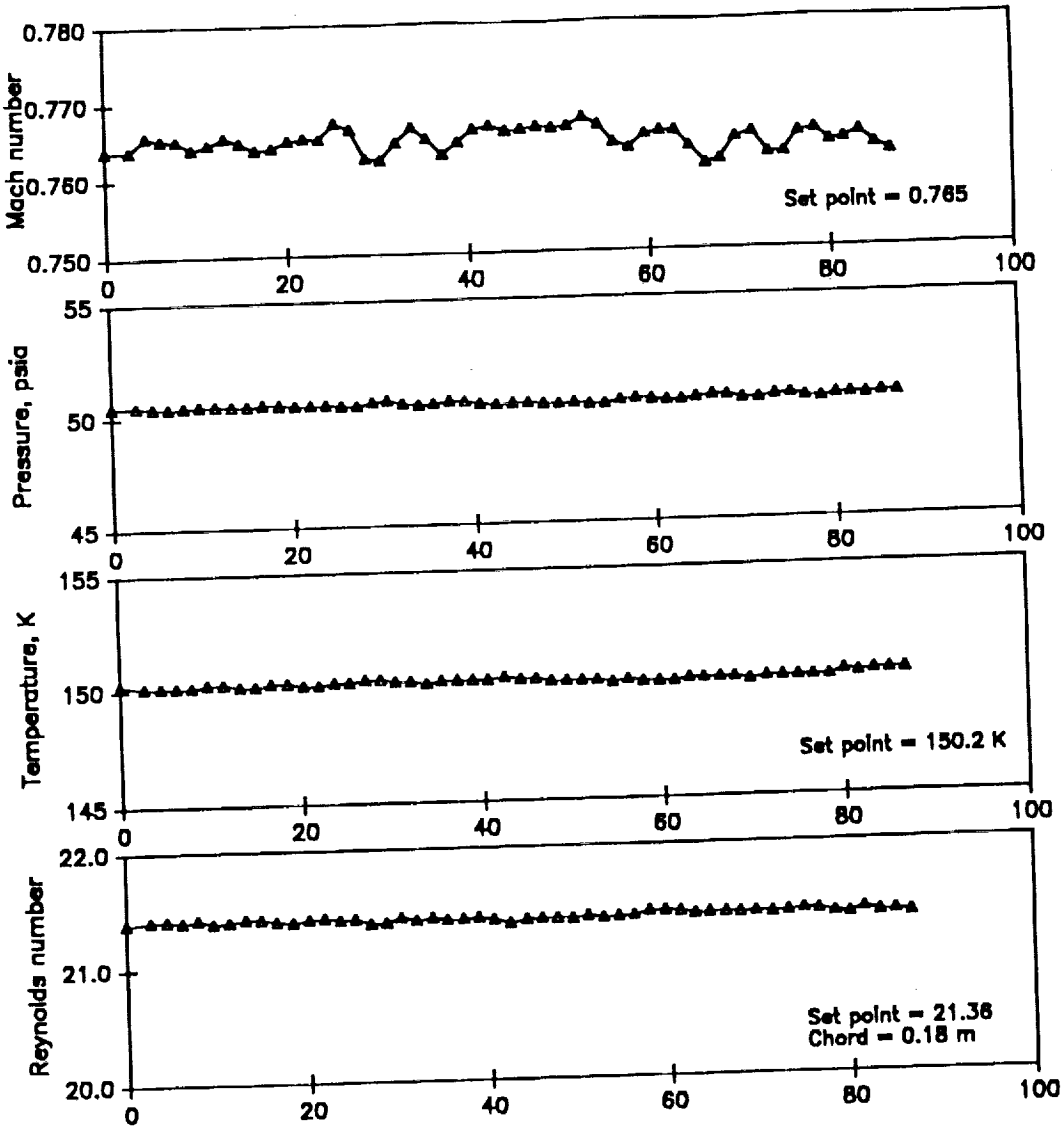

Figure 37.– Tunnel condition regulation under closed loop control.
Drag rake traverse. (3 to −2 inches)
CAST 10, α=2°.

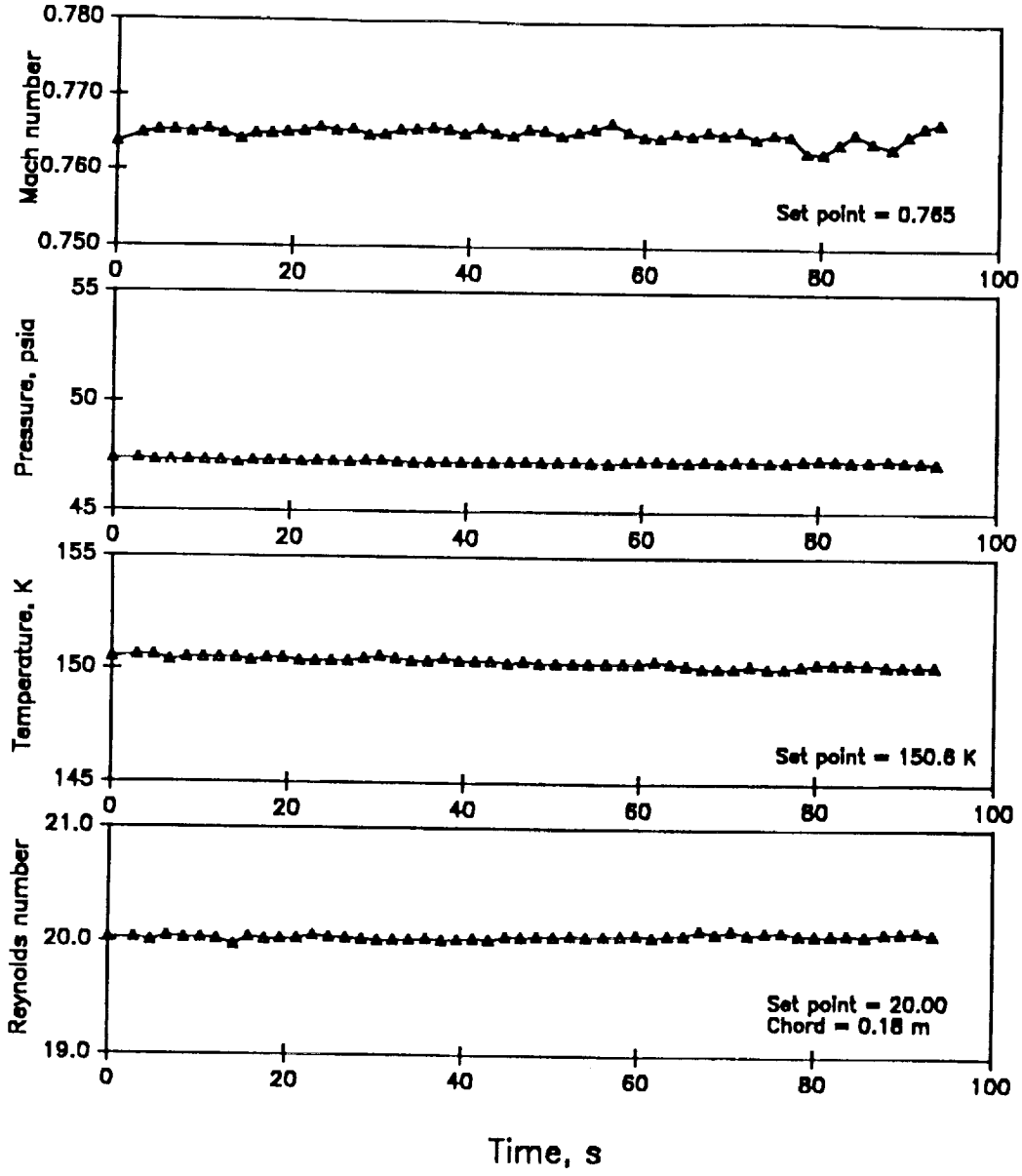

Figure 38.– Tunnel condition regulation under closed loop control.
Drag rake traverse. (3 to −2 inches)
CAST 10, α=2°.

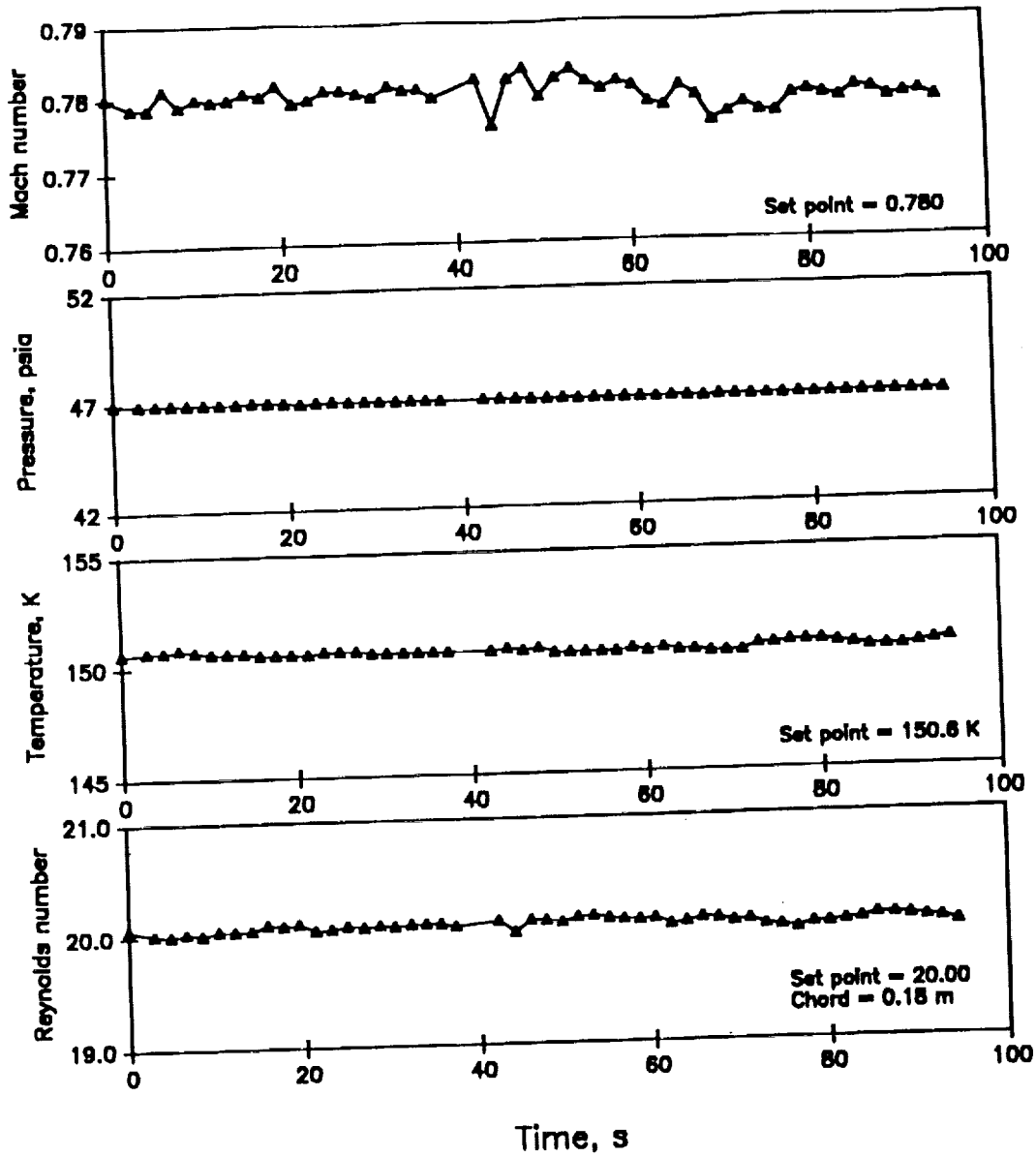

Figure 39.– Tunnel condition regulation under closed loop control. Drag rake traverse. (3.5 to −2.5 inches) CAST 10, α=2.5°.

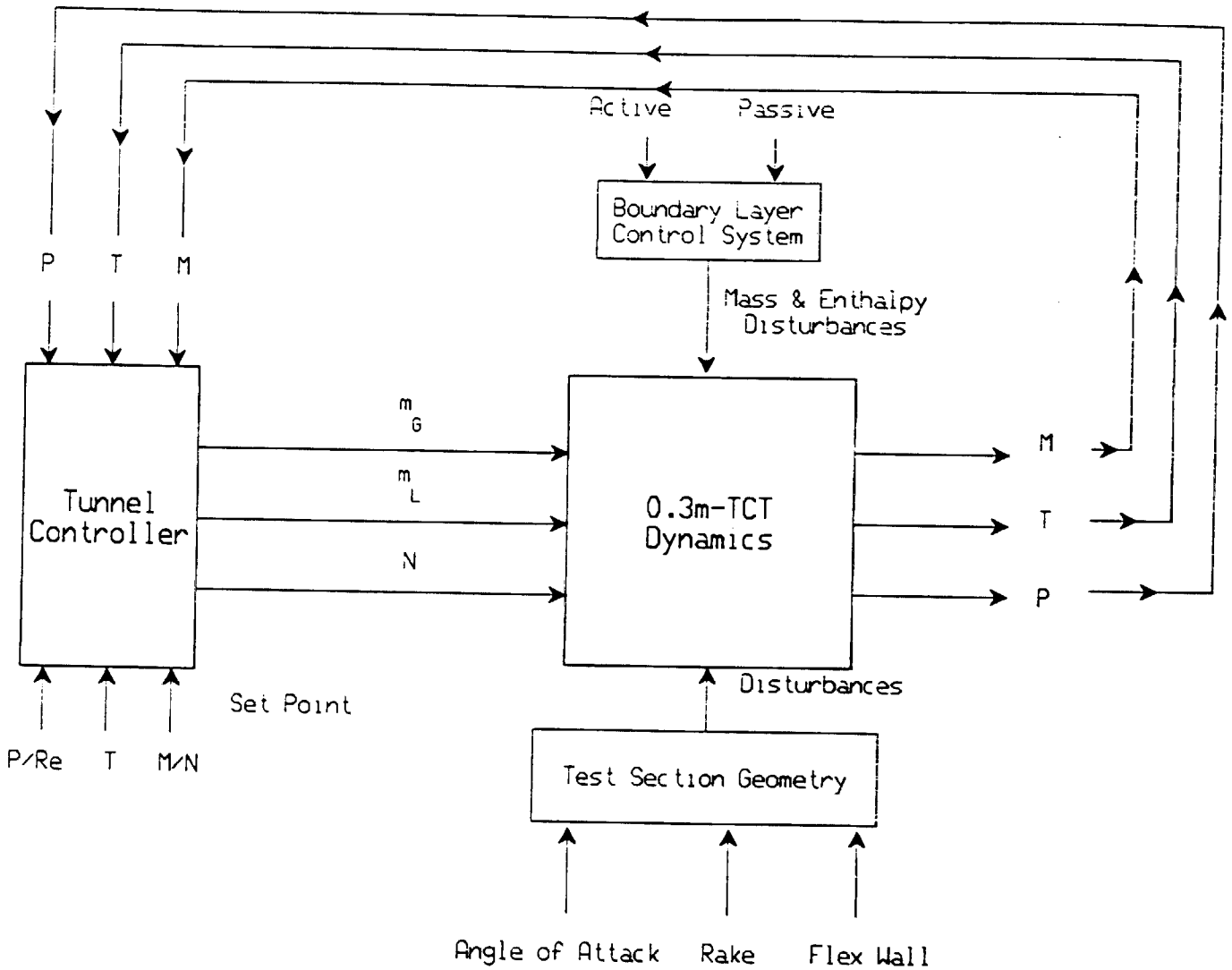

Figure 40.- 0.3-m TCT control scheme and intrusive disturbances during model data acquisition.

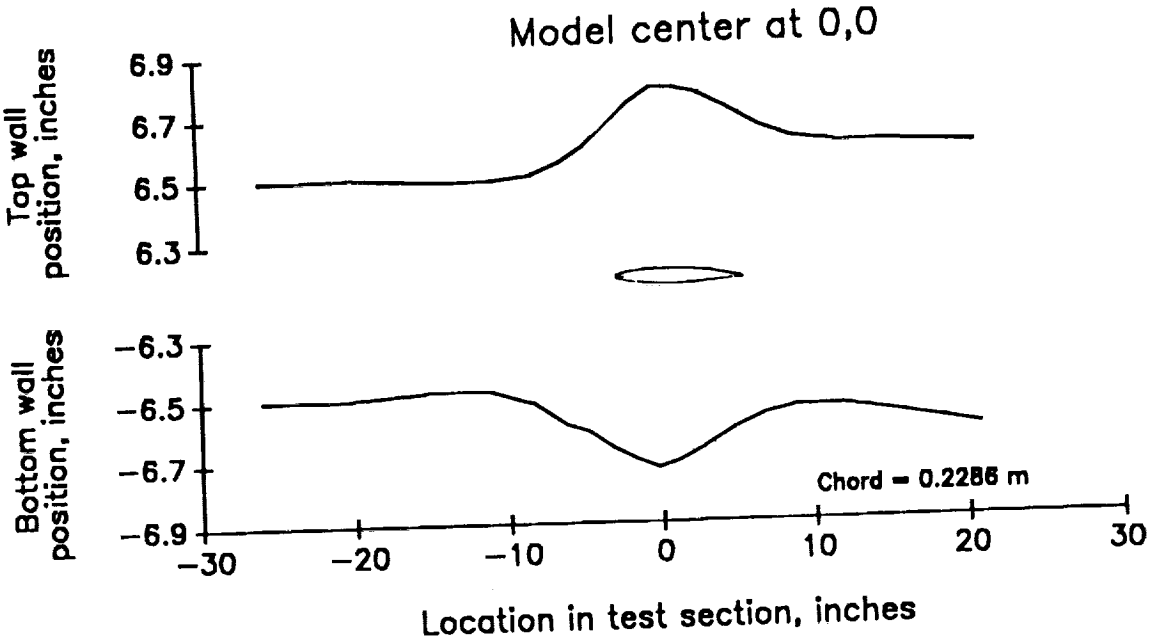

Figure 41.– Wall shape 1 corresponding to streamline condition along the wall at $\alpha=0°$ and Mach number=0.765. CAST 10 model

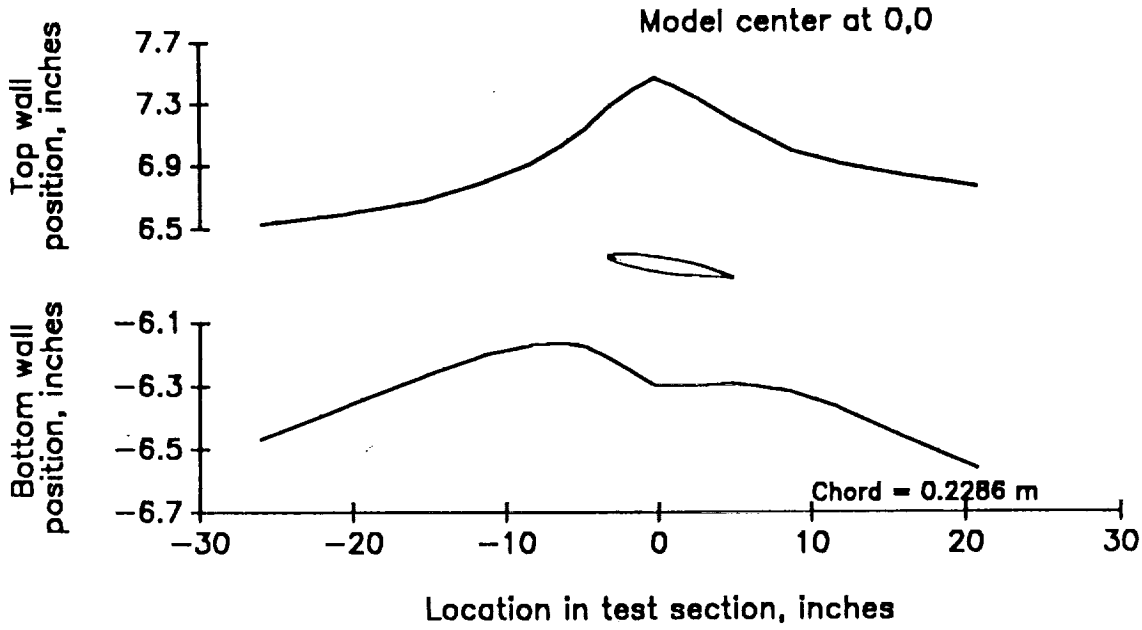

Figure 42.– Wall shape 2 corresponding to streamline condition along the wall at α=2° and Mach number=0.765. CAST 10 model.

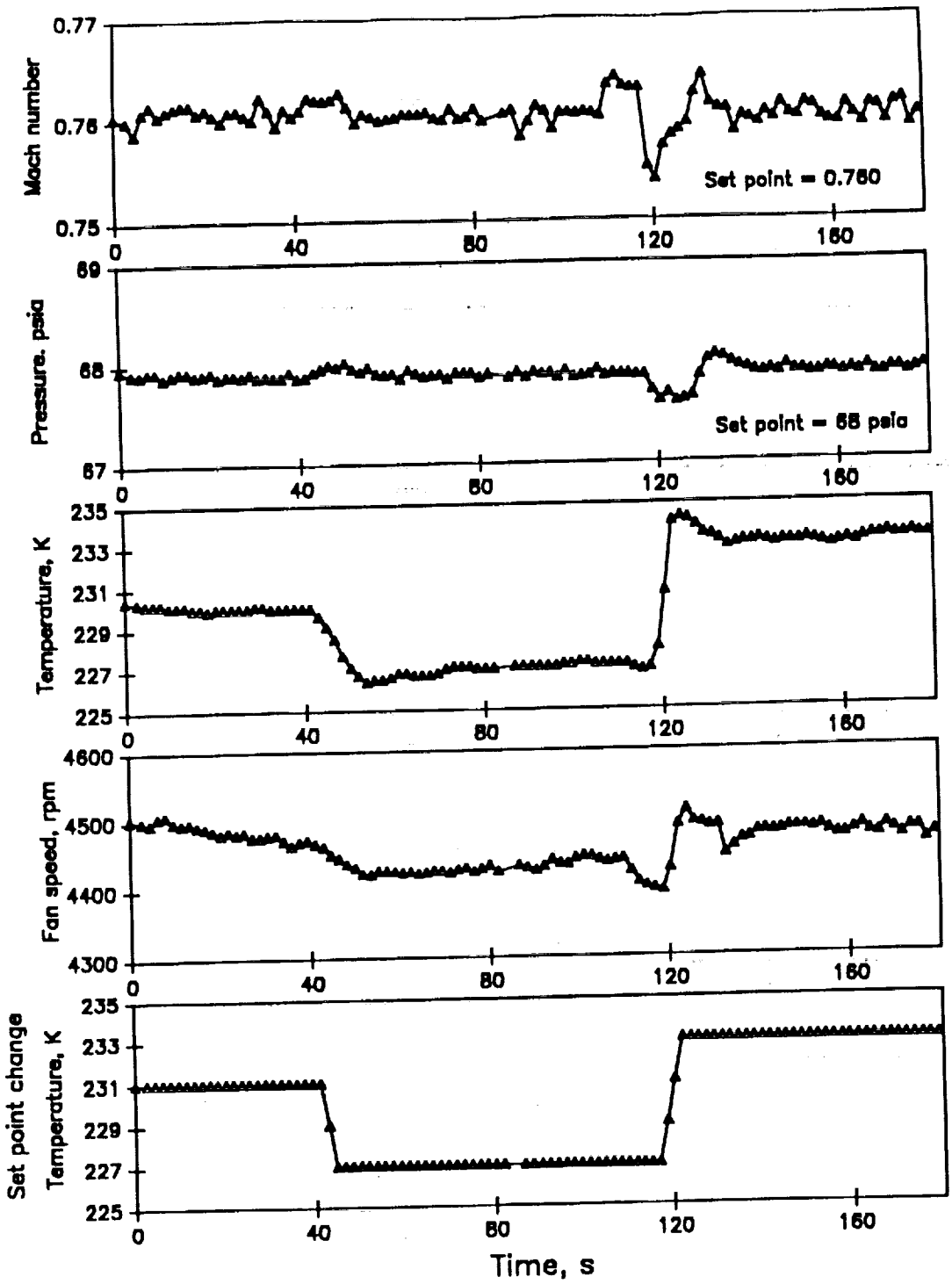

Figure 43.– Tunnel response while in closed loop control to temperature set point command change. Drag rake traverse. (4.4 to −2.8 inches) CAST 10 model, α=0°.

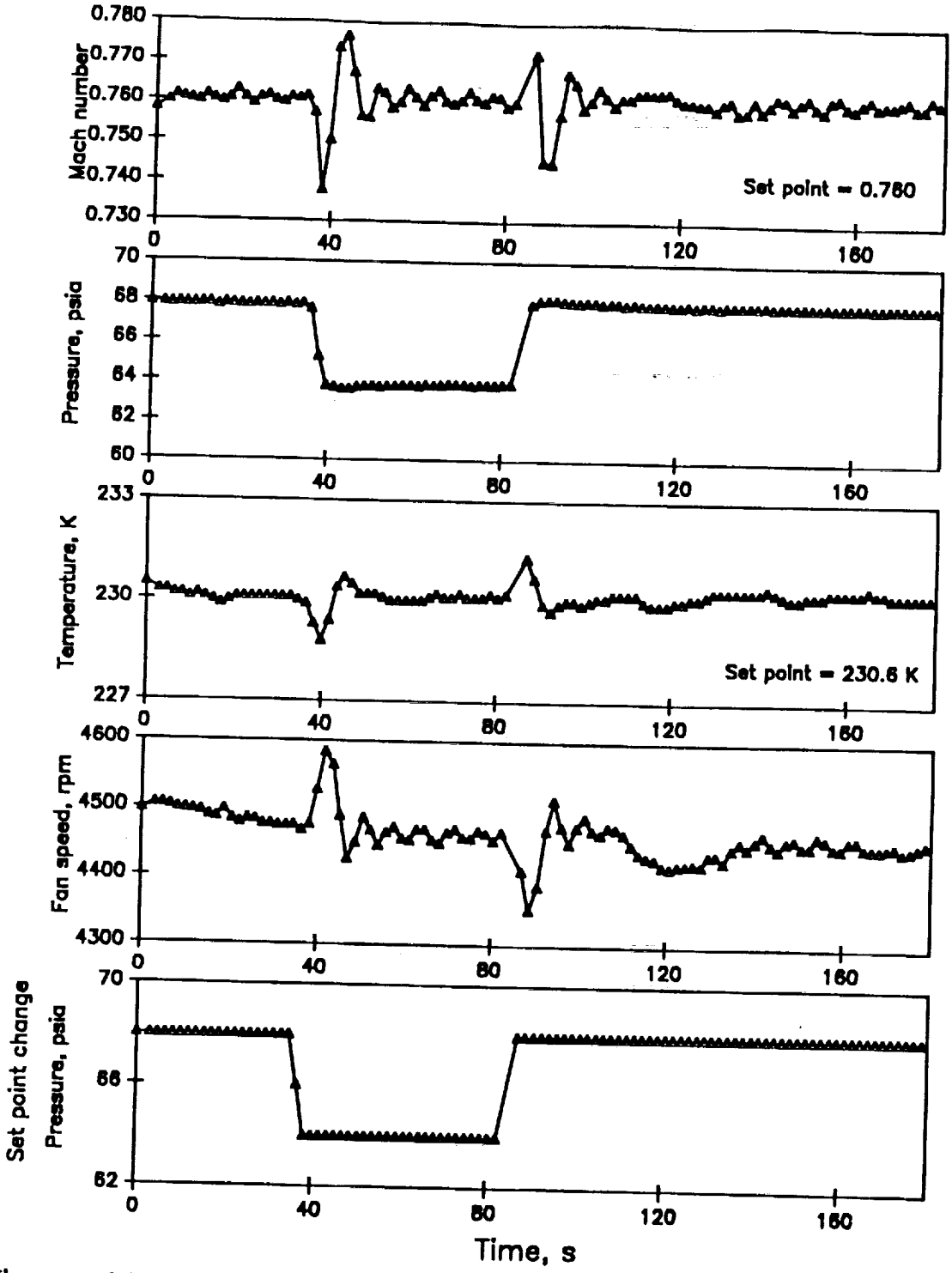

Figure 44.– Tunnel response while in closed loop control to pressure set point command change. Drag rake traverse. (4.4 to −2.8 inches) CAST 10 model, α=0°.

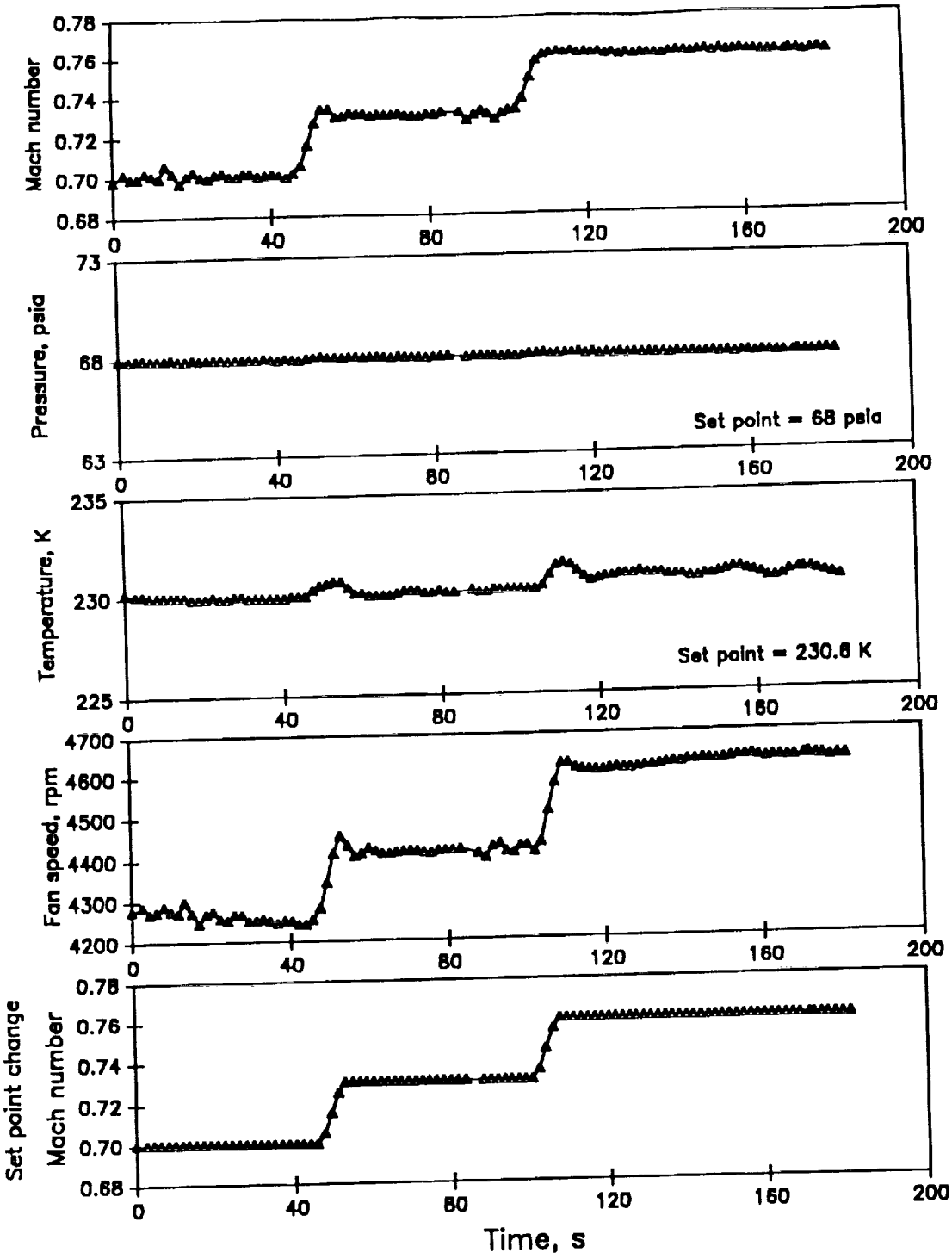

Figure 45.– Tunnel responses while in closed loop control to Mach number set point command change. Drag rake traverse. (4.4 to −2.8 inches) CAST 10 model, α=0°.

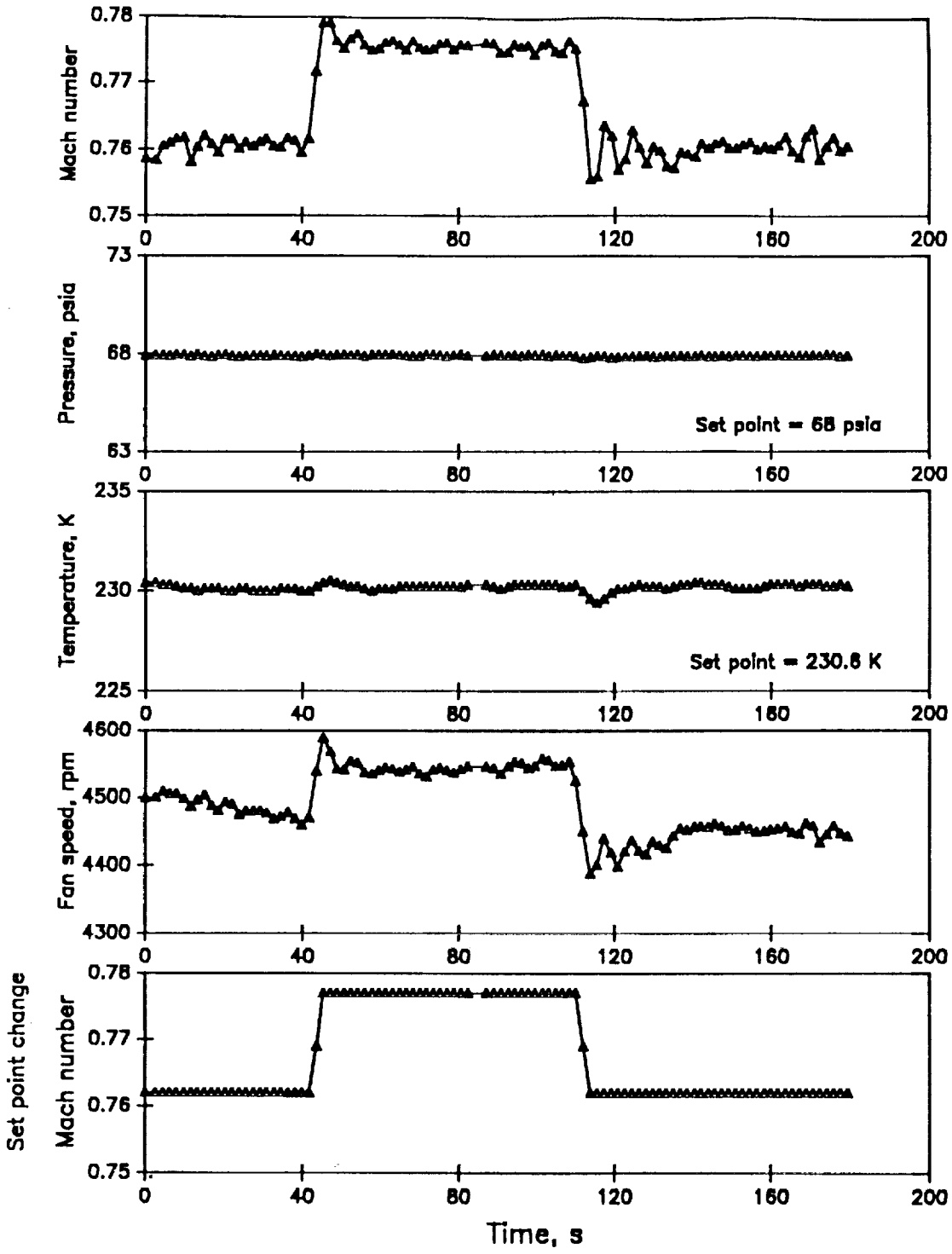

Figure 46.— Tunnel response while in close loop control to Mach number set point command change. Drag rake traverse. (4.4 to −2.8 inches) CAST 10 model, α=0°.

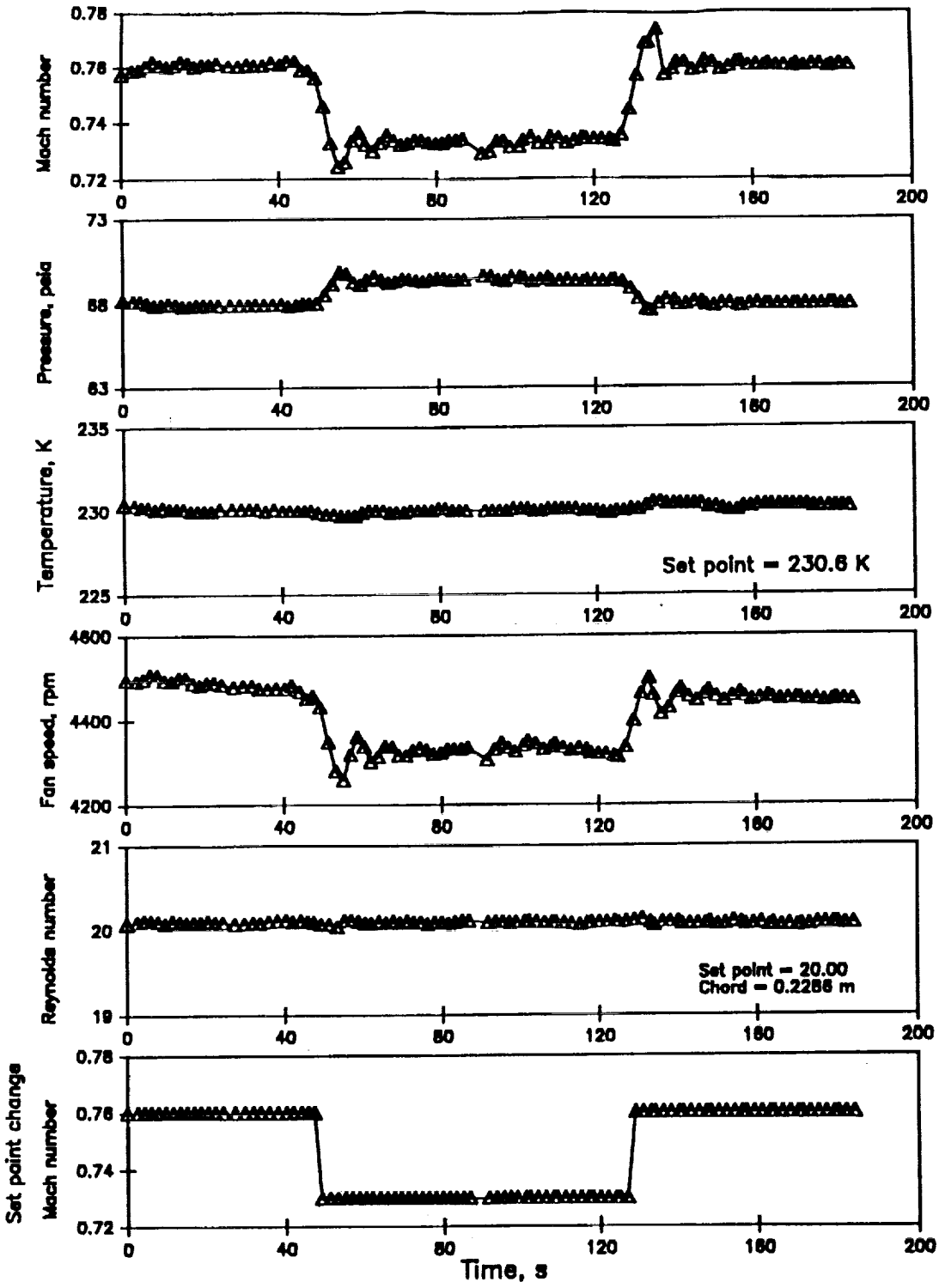

Figure 47.– Tunnel response while in closed loop control to Mach number set point change. Drag rake traverse. (4.4 to −2.8 inches) CAST 10 model, α=0°.

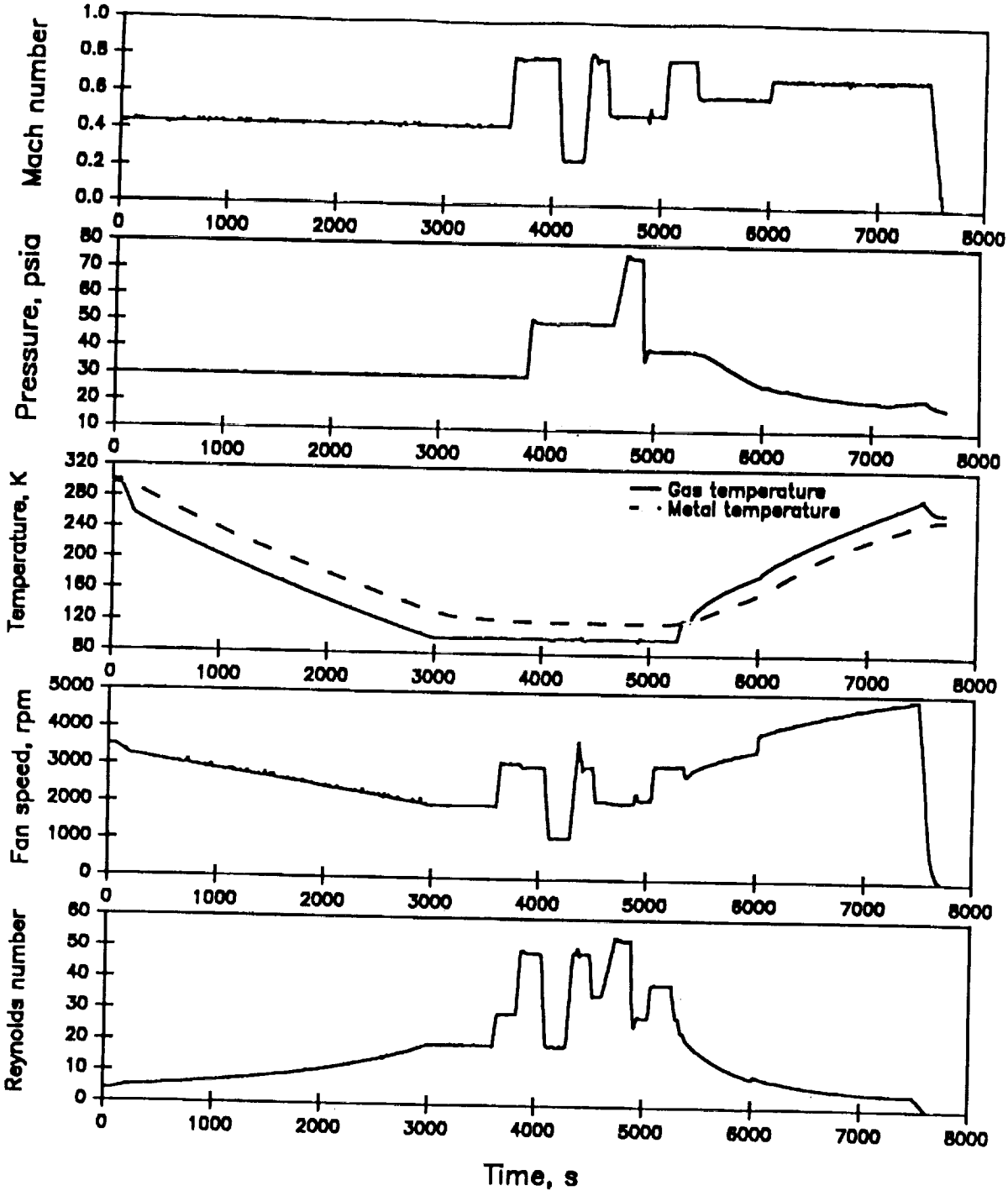

Figure 48.– Response to large set point changes during tunnel cooldown and warmup at constant Mach number conditions.

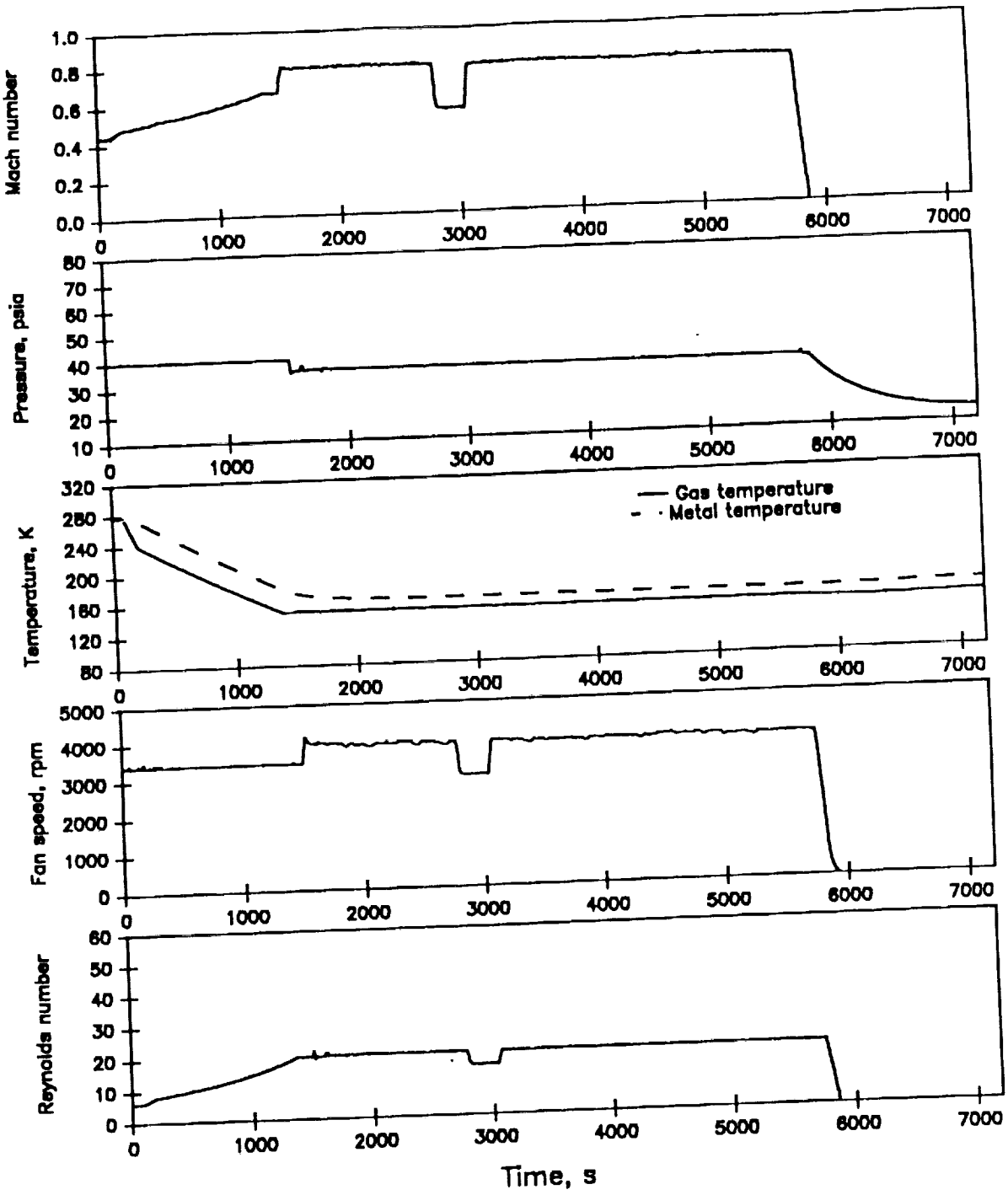

Figure 49.– Response to large set point changes during tunnel cooldown at constant fan speed.

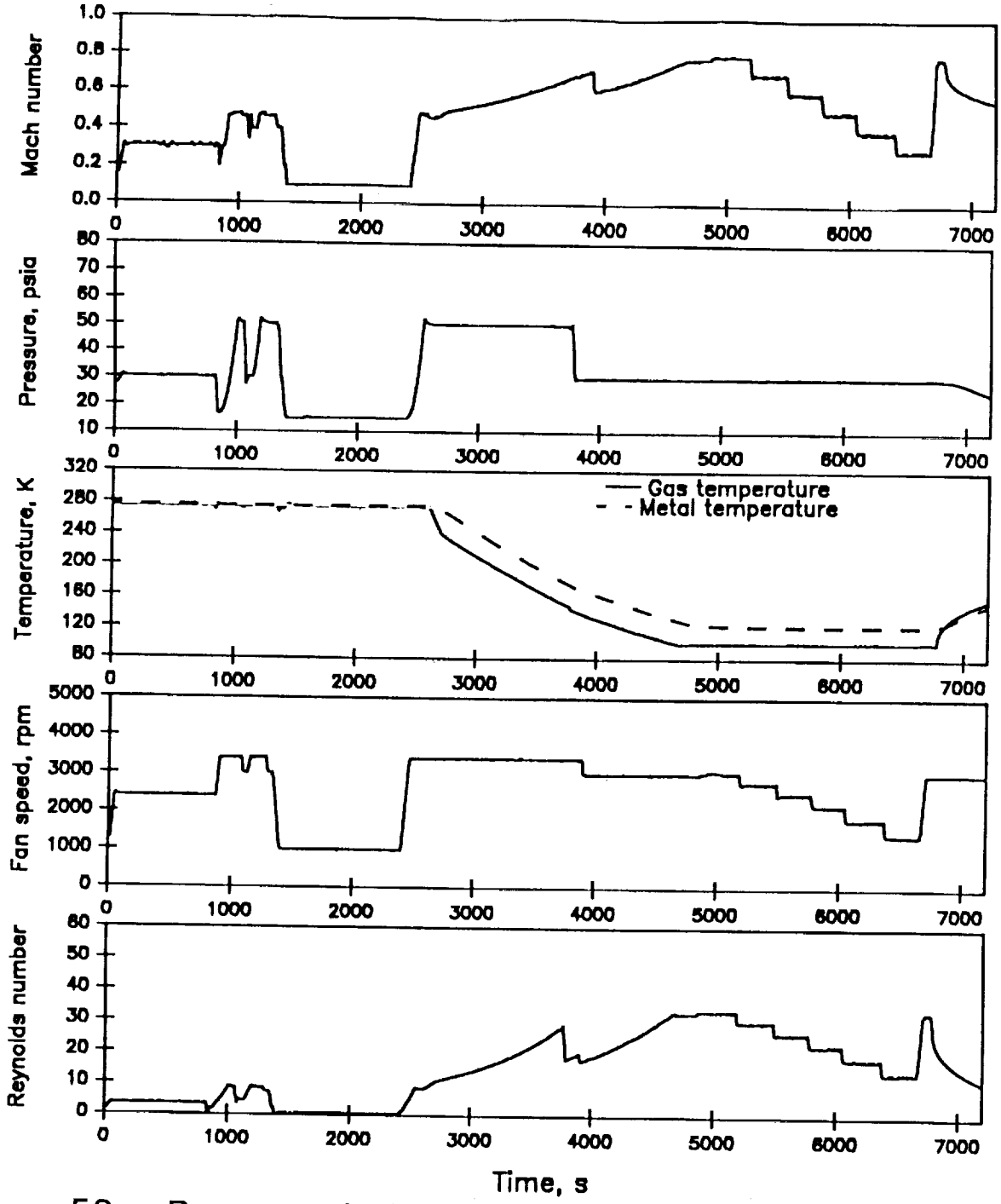

Figure 50.– Response to large set point changes during cooldowr and boundary layer system mass–enthaply disturbances.

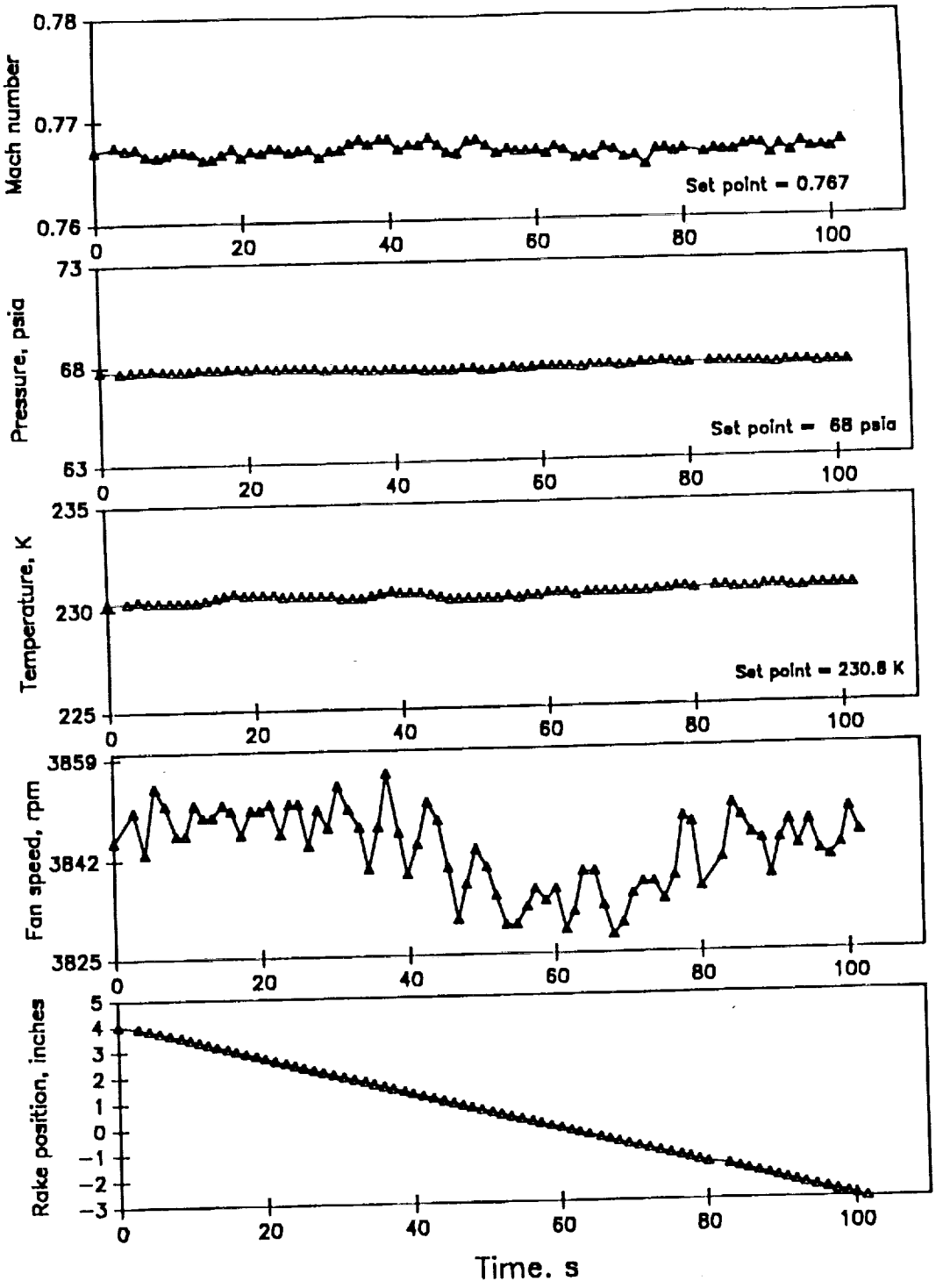

Figure 51.– Tunnel response while in closed loop control to disturbances caused by drag rake traverse. CAST 10 model, α=1.8°, walls streamlined.

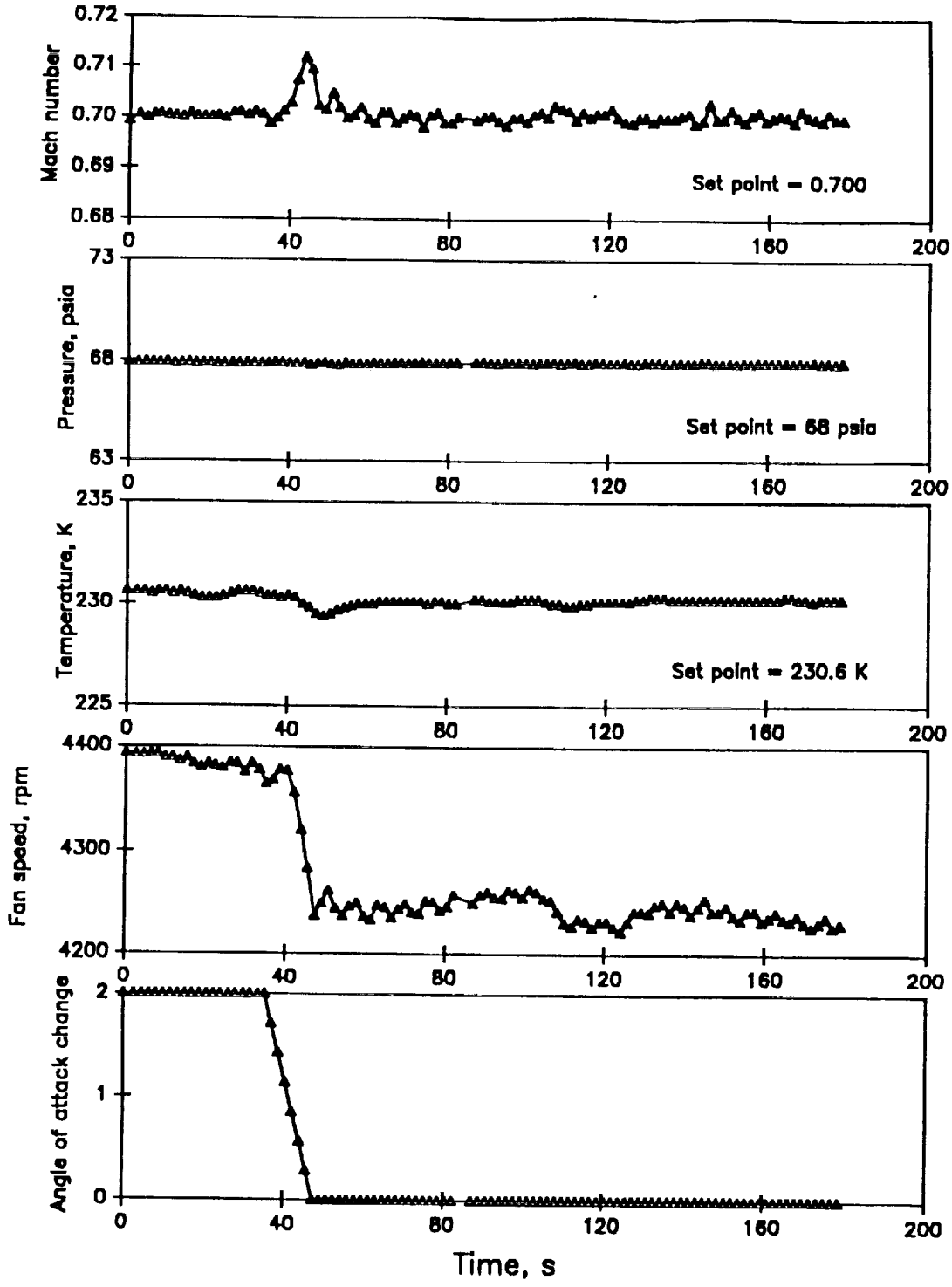

Figure 52.– Tunnel response while in closed loop control to changes in angle of attack. Drag rake traverse. (4.4 to −2.8 inches) CAST 10 model.

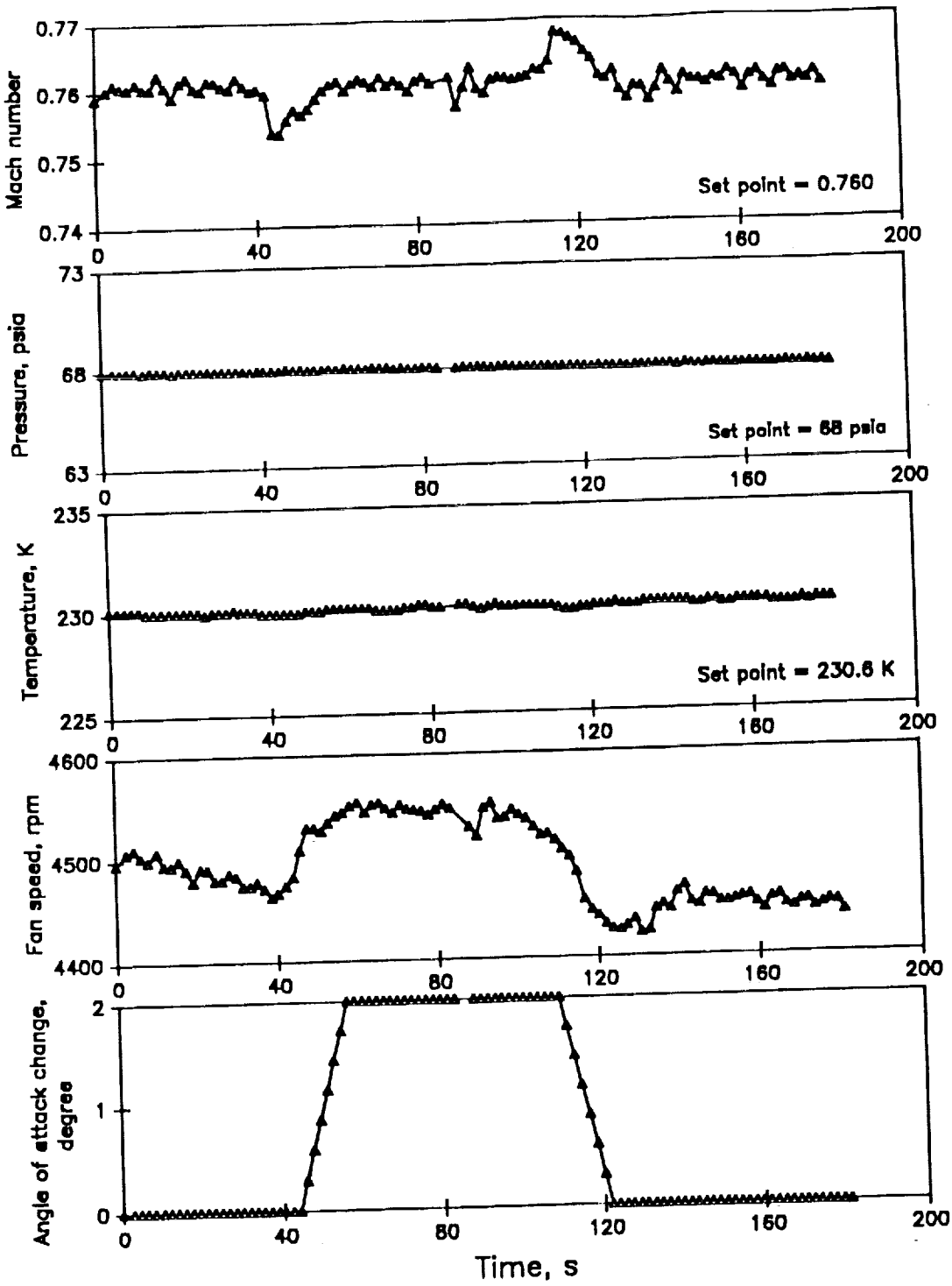

Figure 53.– Tunnel response while in closed loop control to changes in angle of attack. Drag rake traverse. (4.4 to −2.8 inches) CAST 10 model.

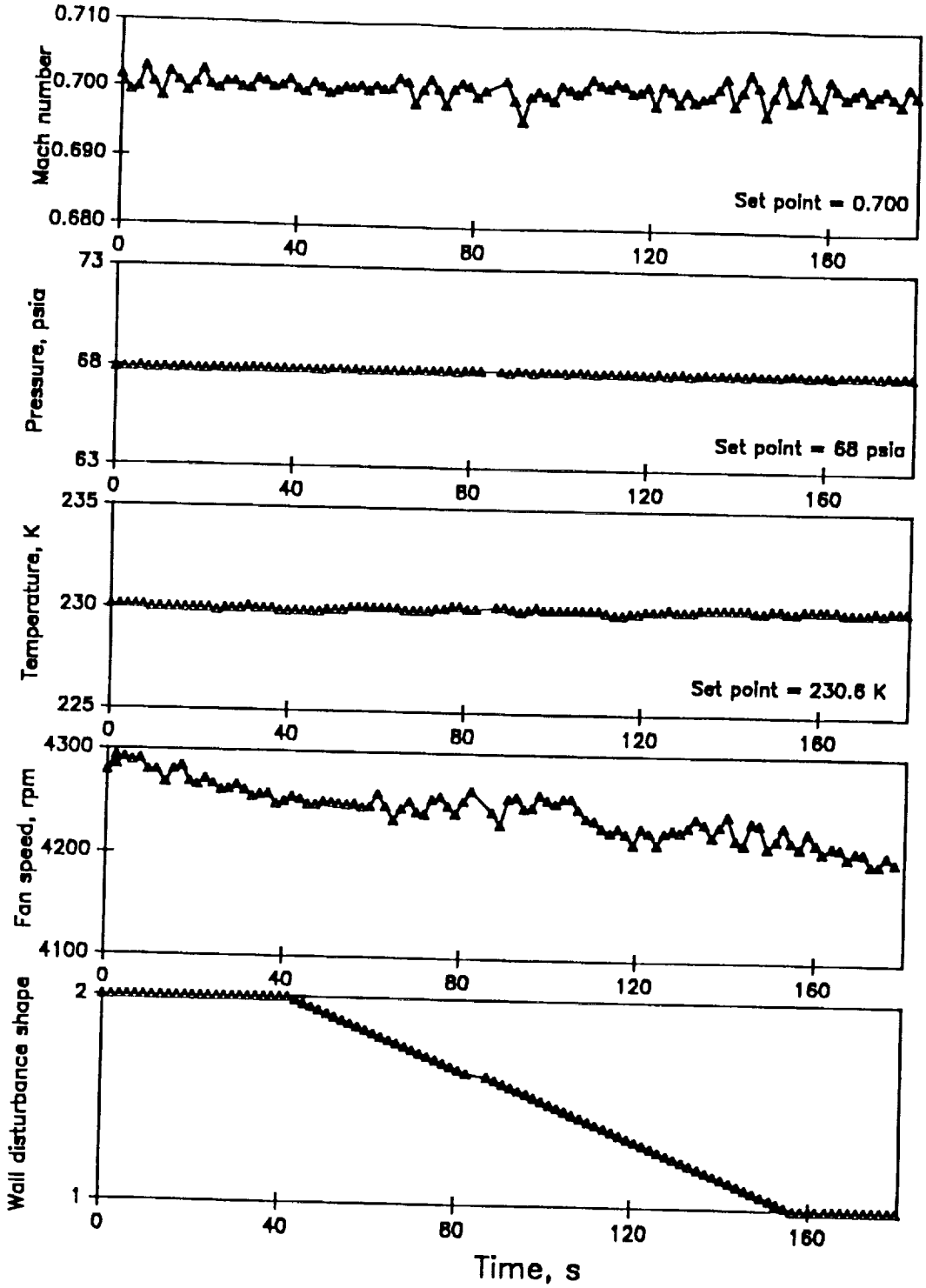

Figure 54.– Tunnel response while in closed loop control to disturbances caused by wall shape change. Drag rake traverse. (4.4 to −2.8 inches) CAST 10 model, α=0°.

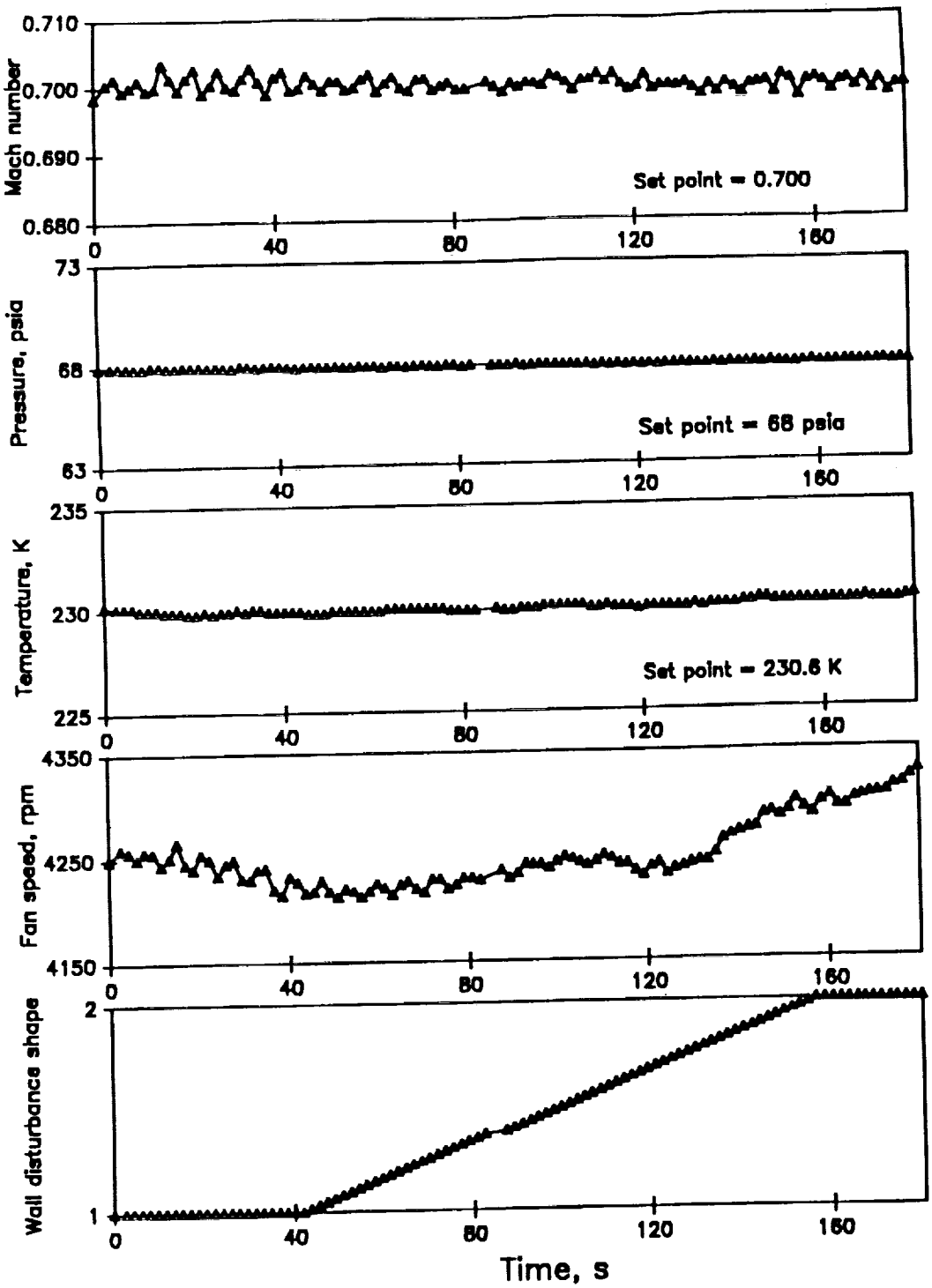

Figure 55.– Tunnel respones while in closed loop control to disturbances caused by wall shape change. Drag rake traverse. (4.4 to −2.8 inches) CAST 10 model, α=2°.

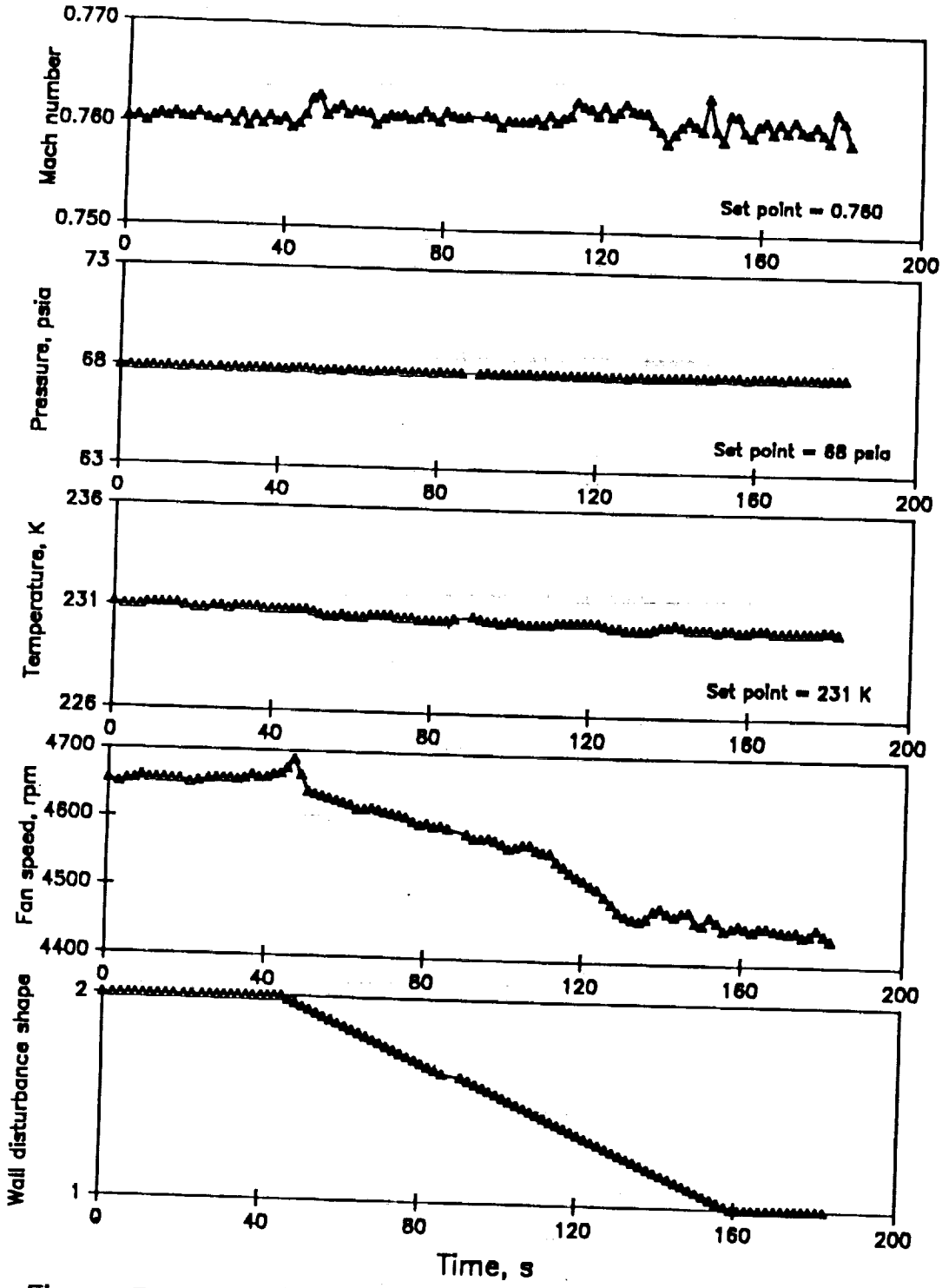

Figure 56.– Tunnel while in close loop control to disturbances caused by wall shape change. Drag rake traverse. (4.4 to −2.8 inches) CAST 10 model, α=0°.

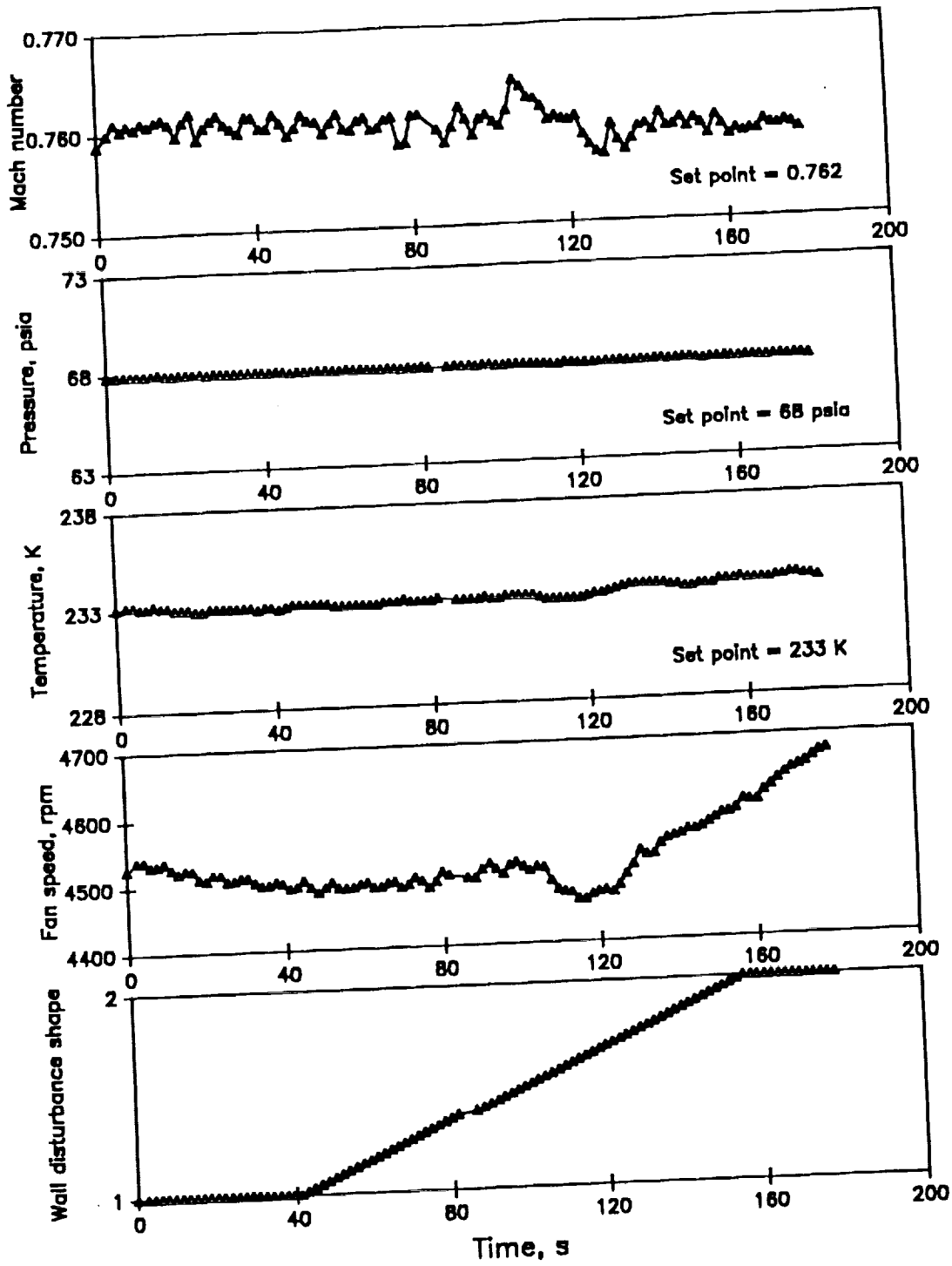

Figure 57.– Tunnel response while in closed loop control to disturbances caused by wall shape change. Drag rake traverse. (4.4 to −2.8 inches) CAST 10 model, $\alpha=0°$.

☆U.S. GOVERNMENT PRINTING OFFICE:1989-627-064/ 86031

0.3-m TUNNEL T-P/R-M CONTROLLER

	LN PUMP W1	TEMP LOOP W2	Pt/Re LOOP W3	RPM/MACH LOOP W4
SET POINT	W5 ,psia	W6 ,K(Final) W7 ,K(Use)	W8 ,Psia W9 ,Miln/Chrd	W10 ,Mach W11 ,RPM
PROCESS	FLAG 1 W12 ,psia	FLAG 2 W13 ,K-GN2 W14 ,K-WALL	FLAG 3 W15 ,Psia W16 ,Miln/ChRD	FLAG 4 W17 ,Mach W18 ,RPM
COMMAND	W19 ,%opn	W20 ,%opn	W21 ,% opn V1 W22 ,% opn V2	W23 ,% RhsT W24
INPUTS Delete	B= W25 ,psi	Temp= W26 ,K ALQ%= W27 ,opn	Pres= W28 ,psia Ryno= W29 ,miln AGv%= W30 ,opn Chrd= W31 ,m	Mach= W32 ,Mach Nrpm= W33 ,rpm
STATUS		GRAD= W34 ,K/mt SAT= W35 ,K	CHORD= W36 ,m P st= W37 ,psia Del P= W38 ,psi	W39 W40

Figure 58.- Display format for the controller monitor.

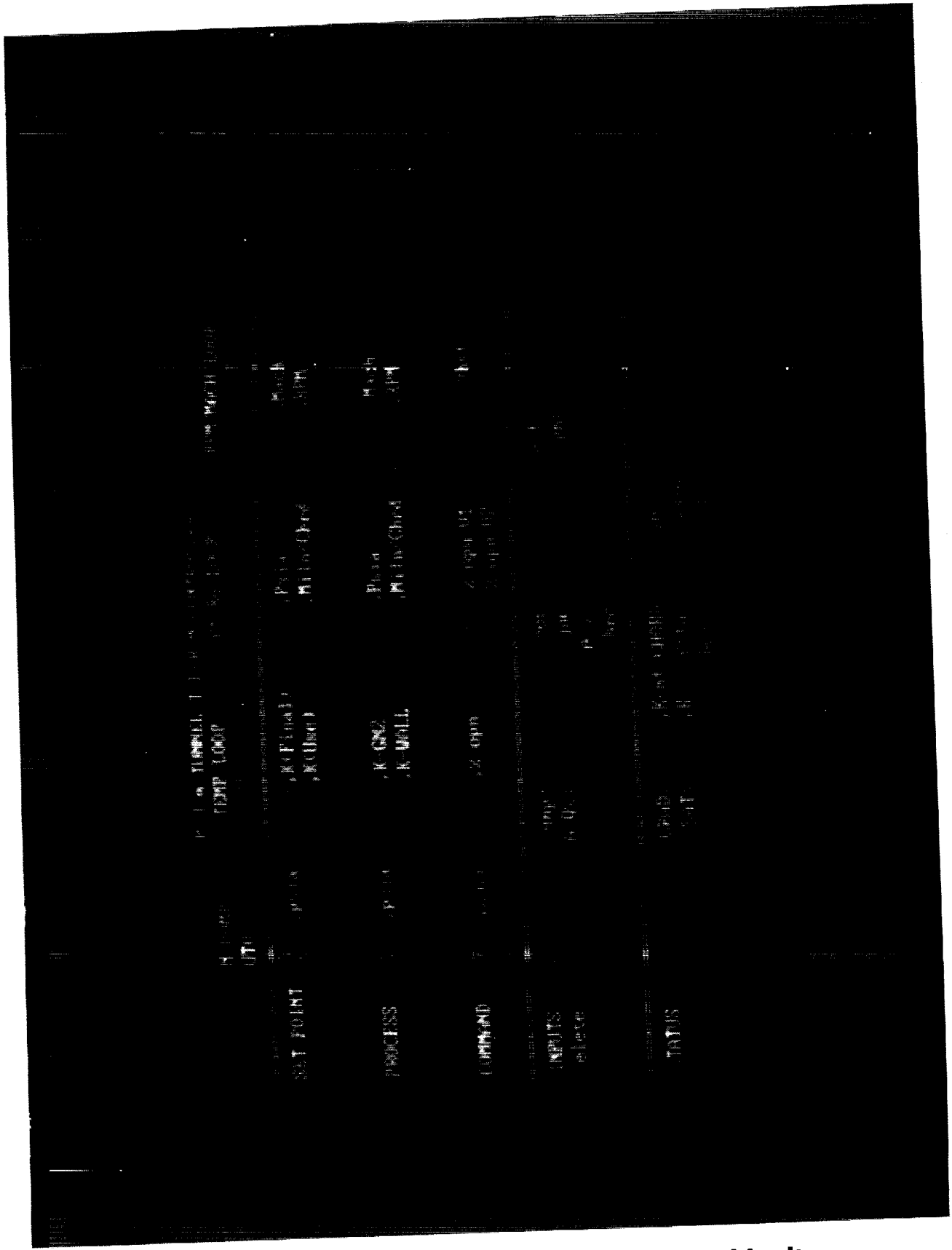

L-88-11,127

NASA

Figure 59.- Typical Tunnel Control display on the Monitor.

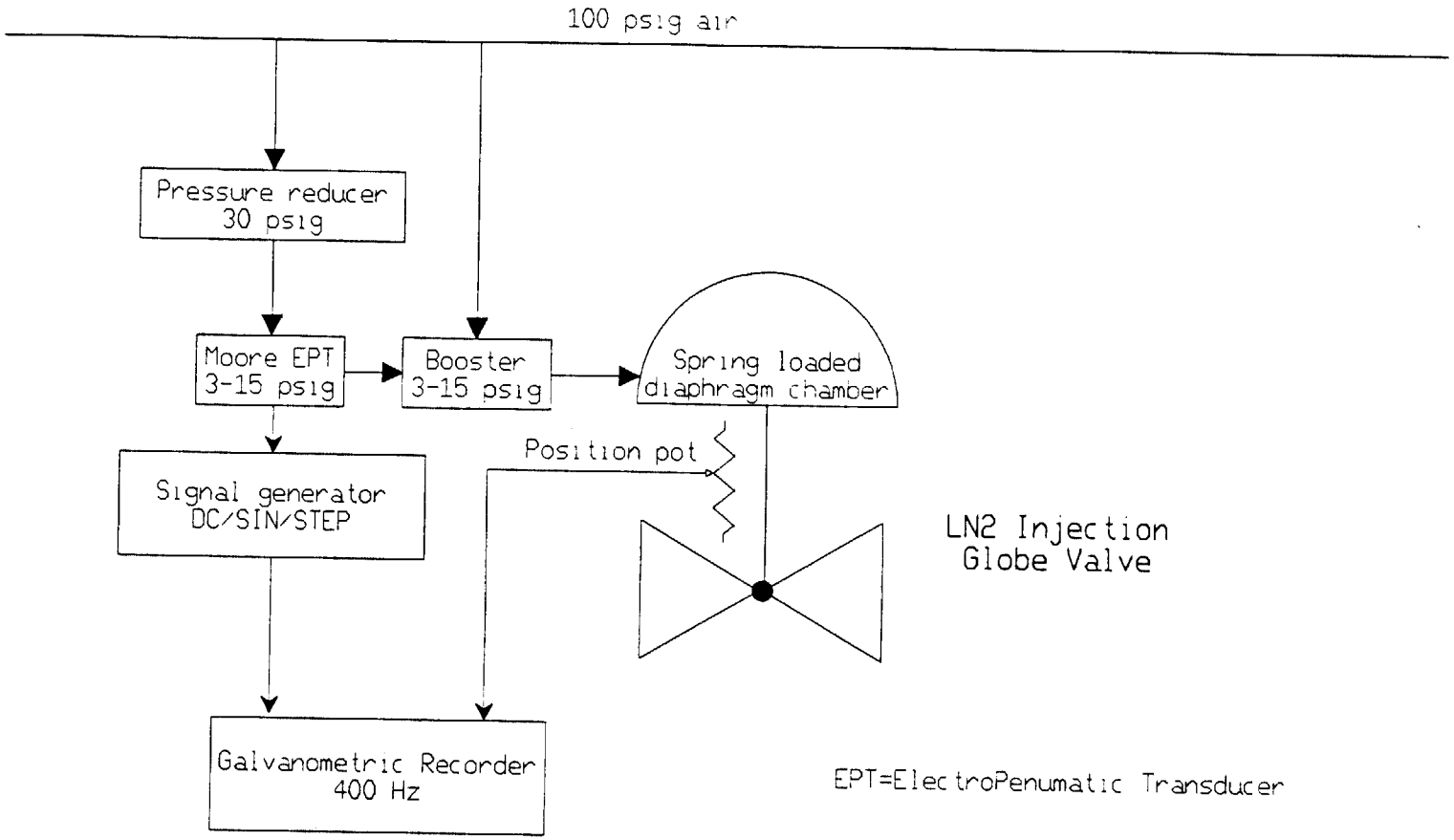

Figure 60.-Schematic for performance test on LN2 injection valve.

NASA National Aeronautics and Space Administration

Report Documentation Page

1. Report No.	2. Government Accession No.	3. Recipient's Catalog No.
NASA CR-181808		

4. Title and Subtitle	5. Report Date
Microcomputer Based Controller for the Langley 0.3-M Transonic Cryogenic Tunnel	March 1989
	6. Performing Organization Code

7. Author(s)	8. Performing Organization Report No.
S. Balakrishna and W. Allen Kilgore	10. Work Unit No. 505-61-01-09

9. Performing Organization Name and Address	11. Contract or Grant No.
Vigyan Research Associates, Inc. 30 Research Drive Hampton, VA 23665-1325	NAS1-17919
	13. Type of Report and Period Covered
12. Sponsoring Agency Name and Address National Aeronautics and Space Administration Langley Research Center Hampton, VA 23665-5225	Contractor Report
	14. Sponsoring Agency Code

15. Supplementary Notes

Langley Technical Monitor: Edward J. Ray

16. Abstract

Flow control of the Langley 0.3-meter Transonic Cryogenic Tunnel (TCT) is a multivariable nonlinear control problem. In this work, globally stable control laws have been generated to hold tunnel conditions in the presence of geometrical disturbances in the test section and precisely control the tunnel states for small and large set point changes. The control laws are mechanized as four inner control loops for tunnel pressure, temperature, fan speed, and liquid nitrogen supply pressure, and two outer loops for Mach number and Reynolds number. These integrated control laws have been mechanized on a 16-bit microcomputer working on DOS. This document details the model of the 0.3-m TCT, control laws, microcomputer realization, and its performance. The tunnel closed loop responses to small and large set point changes are presented. The controller incorporates safe thermal management of the tunnel cooldown based on thermal restrictions. The controller is shown to provide control of temperature to ±0.2K, pressure to ±0.07 psia, and Mach number to ±0.002 of a given set point during aerodynamic data acquisition in the presence of intrusive geometrical changes like flexwall movement, angle-of-attack changes, and drag rake traverse. The controller also provides a new feature of Reynolds number control. The controller provides a safe, reliable, and economical control of the 0.3-m TCT.

17. Key Words (Suggested by Author(s))

Cryogenic Wind Tunnel
Microcomputer Control
Pressure Control
Temperature Control
Mach Number Control
Reynolds Number Control

18. Distribution Statement

Unclassified - Unlimited

Subject Category: 09

19. Security Classif. (of this report)	20. Security Classif. (of this page)	21. No. of pages	22. Price
Unclassified	Unclassified	148	A07